Chemical Science

ROYAL SOCIETY OF CHEMISTRY

REVIEW

View Article Online
View Journal | View Issue

Cite this: *Chem. Sci.*, 2021, **12**, 13613

Recent developments in chemical conjugation strategies targeting native amino acids in proteins and their applications in antibody–drug conjugates

Min Sun Kang, Theresa Wai See Kong, Joycelyn Yi Xin Khoo and Teck-Peng Loh *

Received 1st June 2021
Accepted 27th September 2021

DOI: 10.1039/d1sc02973h

rsc.li/chemical-science

Many fields in chemical biology and synthetic biology require effective bioconjugation methods to achieve their desired functions and activities. Among such biomolecule conjugates, antibody–drug conjugates (ADCs) need a linker that provides a stable linkage between cytotoxic drugs and antibodies, whilst conjugating in a biologically benign, fast and selective fashion. This review focuses on how the development of novel organic synthesis can solve the problems of traditional linker technology. The review shall introduce and analyse the current developments in the modification of native amino acids on peptides or proteins and their applicability to ADC linker. Thereafter, the review shall discuss in detail each endogenous amino acid's intrinsic reactivity and selectivity aspects, and address the research effort to construct an ADC using each conjugation method.

1. Introduction

1.1. Bioconjugation and its applications

Bioconjugation, combining biomolecules such as proteins or cells with exogenous moieties, leads to enhanced therapeutic efficacy and a wider range of functions.[1] Among the conjugated molecules, one prominent example that is rising as a promising therapeutic modality in oncology is antibody–drug-conjugate (ADC) (Fig. 1). The ability of the antibody to deliver the payload to specific targets to kill the cancer cells with fewer side effects makes this class of compounds an attractive target for new therapeutics development.

With such exciting applications of bioconjugates, the development of a suitable linker, which connects biomolecules with payloads in a selective and efficient fashion, is increasingly garnering attention from the biomedical field. In this review, we will be focusing on the ADC chemical conjugation technology.

1.2. Antibody–drug-conjugate (ADC)

The synergy of a target-specific antibody and cytotoxic chemical led to the United States Food and Drug Administration (US FDA) approval of eleven ADCs, and 302 clinical studies, as of the second quartile of 2021. The first FDA-approved ADC is gemtuzumab ozogamicin (GO, Mylotarg™), developed by Pfizer to

Division of Chemistry & Biological Chemistry, School of Physical & Mathematical Sciences, Nanyang Technological University, 21 Nanyang Link, 637371, Singapore. E-mail: esther.kang@ntu.edu.sg; teckpeng@ntu.edu.sg

Min Sun Kang, born in South Korea, received her BSc (2018) in chemistry from Imperial College London. She then worked as an Investor Relations representative at SillaJen (South Korea). She is presently working as a research officer with Professor Teck Peng Loh. Her work focuses on protein functionalization, antibody–drug conjugate research and water-based synthetic methodology.

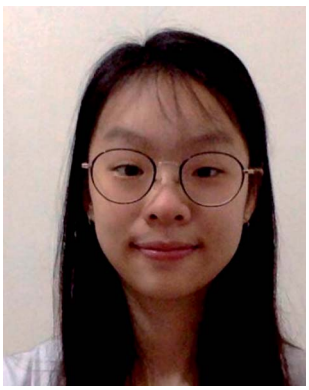

Kong Wai See, Theresa received her BSc in chemistry and biological chemistry from Nanyang Technological University, Singapore in 2021.

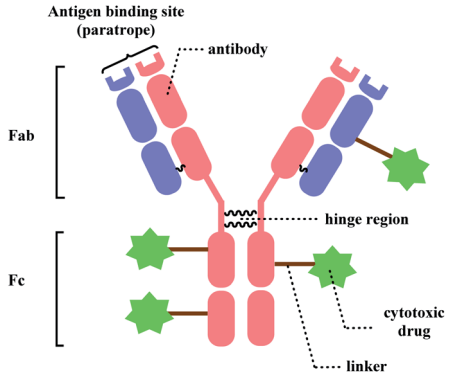

Fig. 1 General structure of antibody–drug conjugate.

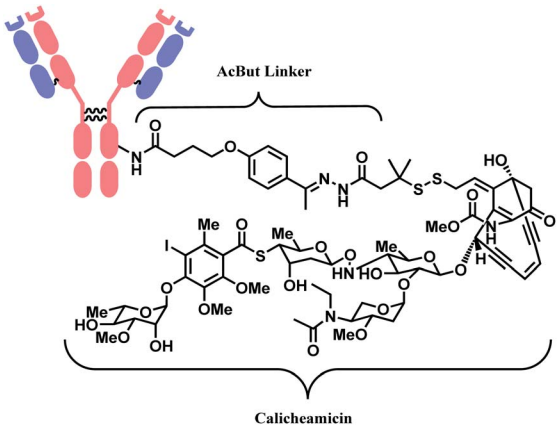

Fig. 2 | Structure of Mylotarg™ (antibody: CD33-targeting IgG_4 mAb) and Besponsa™ (antibody: CD22-targeting IgG_4 mAb).

treat patients with acute myeloid leukemia (AML) who first relapsed.[2] It is a conjugate of an engineered humanized monoclonal IgG_4 antibody directed against the CD33 antigen present on leukemic myeloblasts, and a potent DNA-binding cytotoxic antibiotic, calicheamicin derivative (*N*-acetyl-γ-calicheamicin 1,2-dimethyl hydrazine dichloride).[3] A bifunctional linker, 4-(4-acetylphenoxy)butanoic acid (AcBut) connects the CD33 targeting antibody and a calicheamicin derivative (Fig. 2).[3] Pfizer conjugated the same AcBut linker-calicheamicin derivative payload to G544, an IgG_4 isotype that specifically recognizes human CD22, to synthesize inotuzumab ozogamicin (InO, Besponsa™). It was approved in 2017 for the treatment of acute lymphoblastic leukemia (ALL).[4]

In 2011, brentuximab vedotin (BV, Adcetris™), developed by Seattle Genetics, received a FDA approval to treat relapsed Hodgkin lymphoma (HL) and relapsed systemic anaplastic large-cell lymphoma (sALCL).[5] BV is generated by conjugating synthetic antitubulin agent monomethyl auristatin E (MMAE) to CD30-targeting mAb, *via* a maleimidocapryl L-valine-citrulline *p*-aminobenzyl alcohol (mc-vc-PABC) linker (Fig. 3).[6] Seattle Genetics conjugated the same linker-payload to Nectin-4 targeting mAb to produce enfortumab vedotin (EV, Padcev™),[7] which is approved in 2019 to treat urothelial cancer.[8] The MC-VC-PABC linker–MMAE payload is also employed by

Khoo Yi Xin, Joycelyn received her BSc in chemistry and biological chemistry from Nanyang Technological University, Singapore in 2021. She is currently pursuing her PhD at the same institution under the supervision of Professor Teck-Peng Loh. Her research interests are in the area of antibody–drug conjugates and the green synthesis of natural products.

Teck-Peng Loh is a distinguished university professor of chemistry at Nanyang Technological University, Singapore. Under the tutelage of Professor E. J. Corey, he obtained his PhD (1994) from Harvard University. He has published 422 international refereed papers in reputable chemistry journals bearing high impact factor and 10 patents. He has been invited to give more than 100 lectures in many institutions in the world and plenary and keynote talks in conferences such as the ICOS, OMCOS, Asian European Symposium, etc. He has also served as chairman of many of these conferences. He has been awarded outstanding researcher awards from both National University of Singapore and Nanyang Technological University. In 2017 he received the Yoshida Prize (Japan) and the prestigious President's Science Award (individual) Singapore. He has been elected Fellow, Academia of Sciences, Singapore (2018) and Fellow of Academia of Sciences, Malaysia since 2010. His research work mainly focuses on the development of new synthetic methodology, green chemistry, and synthesis of natural and unnatural products.

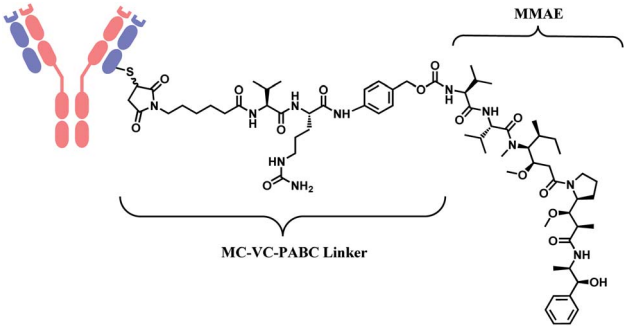

Fig. 3 Structure of Adcetris™ (antibody: CD30-targeting IgG_1 mAb), Padcev™ (antibody: Nectin-4-targeting IgG_1 mAb), and Polivy™ (antibody: CD79b-targeting IgG_1 mAb).

polatuzumab vedotin (PV, Polivy™), and it is conjugated to monoclonal antibody against CD79b, which is a B cell receptor component. PV is developed by Roche and it is approved for the third-line treatment of adults with relapsed/refractory diffuse large B-cell lymphoma (DLBCL).[9]

In 2013, trastuzumab emtansine (T-DM1, Kadcyla™), developed by Roche, received a FDA approval to treat human epidermal growth factor receptor-2 (HER2) expressing metastatic breast cancer and to improve patient prognosis.[10] T-DM1 conjugates HER2 targeting monoclonal IgG_1 antibody trastuzumab with potent microtubule-disrupting agent DM1 *via* a linker, succinimidyl-4-(*N*-maleimidomethyl)-cyclohexane-1-carboxylate (SMCC) (Fig. 4).[11]

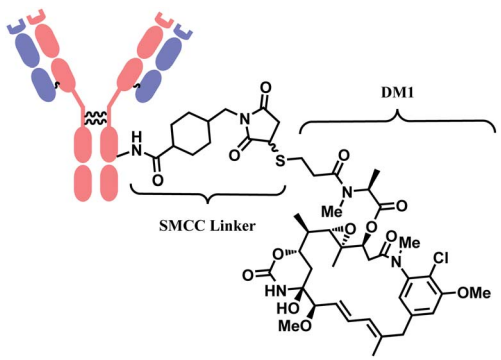

Fig. 4 Structure of Kadcyla™ (antibody: trastuzumab).

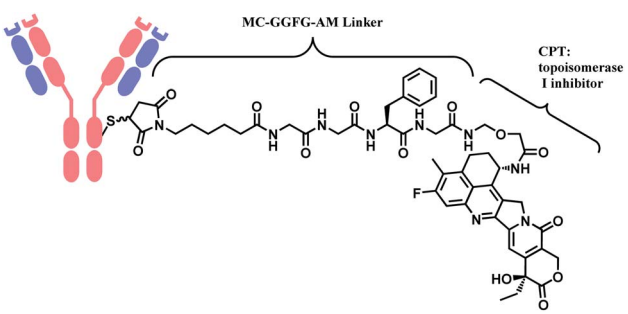

Fig. 5 Structure of Enhertu™ (antibody: trastuzumab).

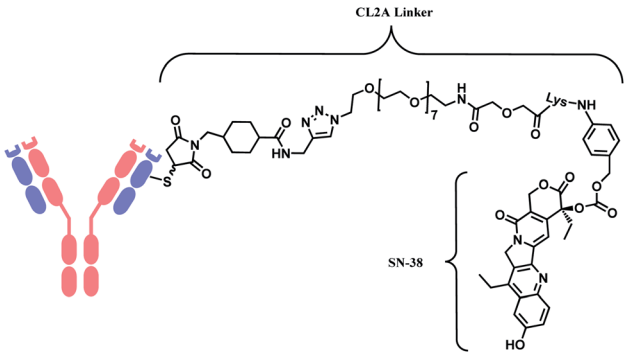

Fig. 6 Structure of Trodelvy™ (antibody: TROP-2 targeting IgG_1 mAb).

In 2019, trastuzumab deruxtecan (T-Dxd, Enhertu™) developed by AstraZeneca was approved as an unresectable or metastatic HER2+ breast cancer therapy.[12] Trastuzumab and the payload, a camptothecin (CPT) derivative, were linked *via* MC-glycyl glycyl phenylalanyl glycine (GGFG)–aminomethyl (AM) linker. The CPT forms a stable complex with human DNA topoisomerase I (Topo I) and DNA, which induces DNA damage and cell apoptosis.[13] Its structure is shown in Fig. 5.

In 2020, sacituzumab govitecan (SG, Trodelvy™), developed by Immunomedics was approved as a second-line therapy for triple-negative breast cancer.[14] It is a conjugate of mAb targeting trophoblast cell-surface antigen 2 (TROP-2) and topoisomerase inhibitor, SN-38 (irinotecan metabolite). The linker is known as CL2A, containing polyethylene glycol (PEG) groups (Fig. 6).

Belantamab mafodotin (Belamaf, Blenrep™) is developed by GlaxoSmithKline, for the treatment of multiple myeloma. It couples an IgG_1 mAb targeting B-cell maturation antigen (BCMA) and a microtubule-disrupting agent, monomethyl auristatin F (MMAF) *via* a MC linker (Fig. 7).[15]

In 2021, loncastuximab tesirine (LT, Zynlonta™), developed by ADC Therapeutics was approved as a treatment for relapsed/refractory diffuse large B cell lymphoma (DLBCL).[16] A CD19-targeting mAb and a pyrrolobenzodiazepine (PBD) DNA-alkylating warhead are connected *via* the linker consisted of maleimide group that binds to the antibody, polyethylene glycols (PEGs), protease-cleavable valine–alanine (VA) and PABC (Fig. 8).

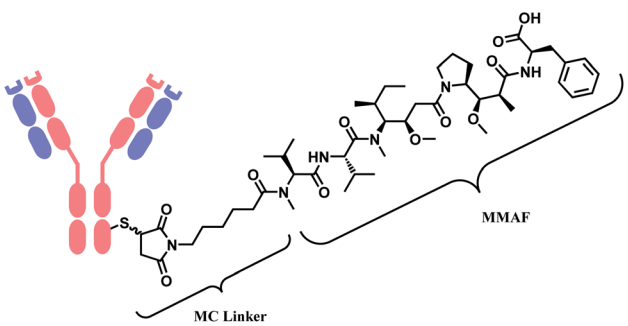

Fig. 7 Structure of Blenrep™ (antibody: BCMA-targeting IgG_1 mAb).

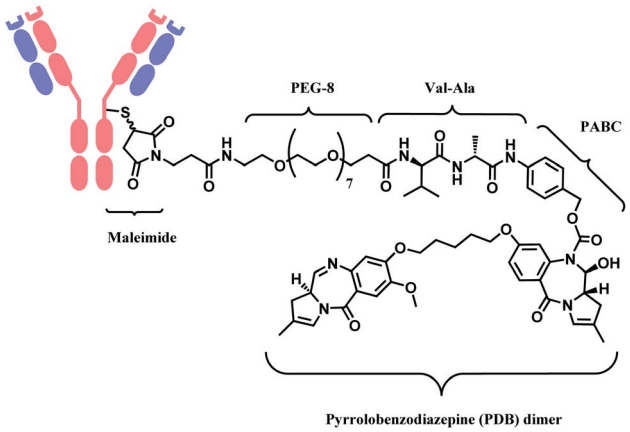

Fig. 8 Structure of Zynlonta™ (antibody: CD19-targeting IgG1 mAb).

Moxetumomab Pasudotox (MP, Lumoxiti™) is a conjugate of CD22-targeting mAb and a truncated form of Pseudomonas exotoxin (PE38).[17] PE38 is connected to the V_H chains of the mAb *via* a ASGGPE peptide bond, which is achieved by recombinant technology.[18] MP was approved to treat hairy cell leukaemia.[19]

1.3. Benefits of ADC over antibody

Proteins alone serve as therapeutic agents, and they have increased dramatically in number and frequency of use since the introduction of the first recombinant protein therapeutic, human insulin, 25 years ago.[20] Antibodies, especially, have become the predominant class of new drugs in chronic diseases, arthritis, and cancer.[21] As oncological drugs, they trigger immune system response by exploiting antigenic differences between malignant cells and healthy cells.[22] 79 therapeutic monoclonal antibodies (mAbs) have been approved by the US FDA, including 30 mAbs in cancer.[21] While they show significant advantages over traditional chemotherapies, a number of limitations can be addressed; (1) ineffectiveness in tumour cells with low expression of target antigens,[23] (2) insufficient antitumor response after binding to antigen,[24] and (3) significantly higher production cost compared to chemical drugs.[25,26] Conjugating mAbs with cytotoxins has a potential to overcome such limitations and lead to great synergy. The following paragraphs introduce clinical or pre-clinical results of ADC which show such potential.

In a phase III clinical trial on HER2 positive breast cancer which compared T-DM1 and trastuzumab head-to-head, T-DM1 was shown to significantly reduce the risk of invasive breast cancer recurrence or death from any cause by 50% compared to the antibody trastuzumab alone.[27] A stable SMCC linker in the T-DM1 construct has enabled the incorporation of a highly potent drug DM1 (*in vitro* $IC_{50} = 0.030$ nM), which is unable to be safely dosed on its own, thereby achieving improved anti-cancer effects.[11]

On top of the enhanced therapeutic efficacy, ADC requires fewer doses as compared to monoclonal antibodies alone. The required dosage of T-DM1 is 3.6 mg per kilogram of body weight, whereas trastuzumab is administered 6 mg per kilogram of body weight.[27] Another ADC of trastuzumab and cytotoxin, T-Dxd (Enhertu™) is administered 5.4 mg per kilogram of body weight.[12] ADCs, with their chemical drugs, drive down the amount of expensive mAbs needed for the therapeutic dose.

The mechanism of ADC involves 'bystander effect', depending on the linker type,[28] and it enables this mAb-based therapeutic to be efficacious in tumours with low or heterogenous expression of antigens as well. The bystander effect refers to the killing of proximal antigen-negative tissues by cytotoxic payloads which diffuse out from the cell.[29] In the preclinical study, the ADC of *anti*-CanAg mAb and cytotoxin, DM1 or the DNA alkylator DC1, eradicated tumors containing both antigen-positive and antigen-negative cells.[29]

1.4. ADC linker technology

As demonstrated in the structures of FDA-approved ADCs in the above section, the linkers connecting 'A' and 'D' can consist of different groups. (1) chemical conjugation moiety that binds to the antibody, (2) protease- or acid-cleavable group with self-elimination spacer, and (3) hydrophilic poly(ethylene glycol). The approved ADCs selectively have different combinations of each. Depending on the existence of protease- or acid-cleavable group with self-elimination spacer, the linker is classified as either cleavable or non-cleavable. 2 out of 11 FDA-approved ADCs, T-DM1 (Fig. 4) and Belamaf (Fig. 7) use non-cleavable linkers, as they only have chemical conjugation moiety. In T-DM1, trastuzumab (T) and DM1 are linked *via* a succinimidyl 4-(*N*-maleimidomethyl)cyclohexane-1-carboxylate (SMCC), a heterobifunctional linker with NHS ester group and a maleimide reactive group at each end of a cyclohexyl spacer. In Belamaf, MMAF is attached to the antibody *via* maleimide with a hexyl spacer. It is believed that the drugs DM1 and MMAF are released with an amino acid appendage from the antibody in tumour cells *via* the catabolism of antibody itself.[28]

In contrast, the other 9 FDA-approved ADCs utilise cleavable linkers that contain peptide- or acid-cleavable groups to release drugs in the lysosomes by exploiting the tumour-associated intracellular conditions. GO and InO (Fig. 2) have a hydrazone moiety that is stable at neutral pH in blood, but becomes more susceptible to hydrolysis inside tumour cells.[30] The disulfide adjacent to the hydrazone undergoes thiol–disulfide exchange with abundant intracellular glutathiones (GSH) to release the payloads.[31] SG (Fig. 6) also contains pH-sensitive benzyl carbonate bond.[32] Alongside, it has a lysine unit, which undergoes cleavage by cysteine protease cathepsin B,[33,34] which is overexpressed in invasive and metastatic cancers.[35]

In cases of SG and LT, polyethylene glycol (PEG) groups were inserted to increase solubility and reduce aggregation of hydrophobic cytotoxic drugs in blood plasma.[36] BV, EV and PV (Fig. 3) and LT (Fig. 8) have a dipeptide valine–citrulline and valine–alanine linked with *p*-aminobenzyl oxycarbonyl (PABC) electronic cascade spacer. Upon the cleavage by cathepsin B, the PABC undergoes 1,6-elimination to release the free drug with the expulsion of carbon dioxide.[37] T-Dxd, on the other hand, has

a tetrapeptide Gly–Gly–Phe–Gly as a lysozyme-cleavable group linked with self-immolative amino methylene (AM) spacer.[38]

While a variety of protease cleavable groups and self-elimination spacer are employed in the FDA-approved ADCs, the chemical conjugation strategies are limited to only two kinds; *N*-hydroxysuccinimidyl ester and maleimide.

2. Bioconjugation methods for ADC linker

In this review, recent advancements in native amino acid conjugation methods will be analysed in light of the applicability as ADC linker. With aforementioned aspects of ADC and general rules of bioconjugation taken into consideration, criteria for ADC linker molecules can be summarized as follows: (1) they must bind to proteins in a highly site-selective manner, so that the number of payloads conjugated to antibody is well-controlled with no side products (2) they must efficiently bind to antibodies under biocompatible conditions (aqueous medium, pH neutral, no transition-metal catalyst, room temperature), without perturbing the ternary structure of proteins (3) the chemistry of resulting protein–linker conjugate should be highly stable in blood plasma, with no retro-reaction (4) it should be synthetically easy to attach functional payloads on the linker.

Site-selectivity comes in two categories: chemoselectivity and regioselectivity. Chemoselectivity can be achieved by exploiting the intrinsic reactivity of a certain functional group in mAbs. Of 20 kinds of canonical amino acids constructing a mAb, the cysteine thiol (–SH) group and the lysine amino (ε-NH_2) are the most common targets as conjugation sites, due to their nucleophilicities and availabilities in solvent-accessible regions.[30] Three of FDA-approved ADCs link cytotoxic drugs to lysine residues, and the rest, including the most recently approved ADCs, use cysteine modifications. While being widely used in these clinical ADCs, the issue of regioselectivity (*i.e.* conjugating to a specific cysteine or lysine residue among many) remains unsolved and research efforts to address and resolve it will be analysed in this review. Along with this, recent developments and selectivity aspects of bioconjugation to other amino acids including tyrosine (Tyr), tryptophan (Trp), and methionine (Met) will be explored. Last but not least, the conjugation should ideally avoid generating a new stereocentre. The stereochemical heterogeneity of the conjugation linker complicates the product analysis.

Linker molecules must be reactive enough to bind to mAb rapidly under biocompatible conditions, because mAbs are highly sensitive to reaction conditions. Transition-metal ions are reported to perturb a strictly defined 3-dimensional structure of mAb by cleaving the hinge region (shown in Fig. 1), forming highly stable pluridentate with nucleophilic amino acids, or by catalysing redox reactions of amino acid side chains.[39,40] Hence, bioconjugation methods involving transition-metal catalysts will not be reviewed. Moreover, the mechanical stress caused by stirring is reported to lead to the aggregation of mAbs.[41] For one example, the percentage of aggregation of anticancer mAb cetuximab after 24 h stirring-period was about 25%.[42] Therefore, the reaction duration of each bioconjugation method will be addressed in details. As summarised in Scheme 1, ADC linker molecules should bind to mAb in pH neutral aqueous system at room temperature with the minimal mechanical stress. The detailed effects of organic solvent, pH variance, and light (ultraviolet or fluorescence) on monoclonal antibodies are discussed in the related reviews.[43,44]

Recently, many methods to achieve site-selective linker conjugation for homogenous ADC production were reported. One is an enzymatic conjugation strategy, such as transglutaminase-driven glutamine modification.[45] Another approach involves engineered carbohydrates or engineered amino acids to provide an orthogonal handle for conjugation. One of the most advanced approaches is the THIOMAB® technology,[46] which involves mutating amino acid residues at particular sites in the constant domains of the antibody to Cys residues that can then be selectively conjugated *via* their thiol groups. An excellent summary on such methods are recently published.[47]

Although these newly developed chemical conjugation technologies have shown clear advantages in DAR control, an important consideration is that these strategies introduce mutations to antibodies and these can be potentially problematic in immunocompetent patients.[48] Furthermore, a full replacement or introduction of an unnatural amino acid into proteins is not straightforward, where a new tRNA, new tRNA-amino acids transferase, and genetic codon modifications are needed to cheat the ribosome complexes.[49] The mutation site can have drastic effects on the stability of resulting antibodies.[50] In spite of the fact that recent advances have addressed stability issues, early-stage clinical ADCs rely on mutations or inefficient conjugation chemistries often requiring extensive engineering or multiple steps.

This review will focus on how establishing new organic synthesis principles can solve the existing challenge of ADC chemical conjugation technology. Protein engineering methods or enzymatic ligation methods will not be discussed. Rather, this review will highlight novel and relatively obscure conjugation chemistries which use native amino acids. In addition, the review will cover in-depth the problems of traditional methods. A wider choice of suitable conjugation linkers with different synthetic scopes will provide an orthogonal and complementary approach to preparing the desired protein conjugates.

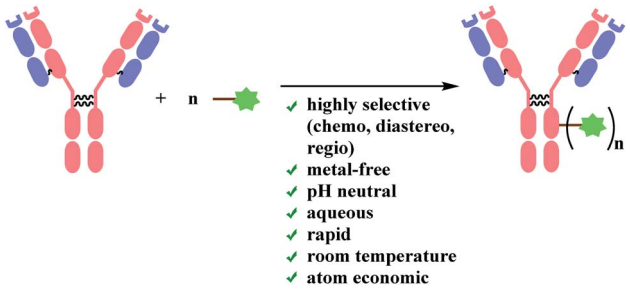

Scheme 1 Requirements for bioconjugation strategies for ADC chemical conjugation technology.

2.1. Lysine functionalisation

Lysine modification is used to produce three of eleven FDA-approved ADCs, GO,[2,3] T-DM1,[51] and InO.[52] A typical immunoglobulin G1 (IgG1) antibody has roughly 90 lysine residues, meaning that non-selective conjugation strategies have the potential to give up to 10^6 distinct species statistically possible when targeting the DAR value of 2 to 4.[53] In industry, the process condition is optimized that the conjugation occurs at 8–10 kinetically preferred lysine sites out of 90.[54]

50% of anti-CD33 mAbs are reported to be unconjugated in GO, with the remainder being a mixture ranging from 4 to 6 drugs per mAb.[2] Such heterogenicity was further studied by its developer with size-exclusion chromatography – the species with higher average drug loading were found to be responsible for forming aggregates.[55] Physical instability such as aggregation is a stability limiting parameter for ADC; the product was voluntarily withdrawn from the US market in 2010 due to safety concerns.[56] InO has an average DAR of 6, and the drug load distribution varies from 0 to 9.[54]

T-DM1 has an average 3.5 DM-1 molecules conjugated to every trastuzumab molecule, and at least 70 lysine sites are partially conjugated with the drug.[57] The statistical study demonstrated that the drug load distribution varies from 0 to 8 and fits to a Poisson distribution.[57] For a DAR of 3.48 this leads to a relatively large variance (λ) of about 3.28 in the Poisson model, demonstrating a drug load with high heterogeneity.

Another noteworthy aspect of lysine modification strategy is a potential conjugation of an electrophilic linker to the N-termini of mAb. In other words, lysine conjugation strategy does not display good levels of chemoselectivity. The pK_a of the N-terminus α-amino group of the protein is lower (p$K_a \sim 8$) than the pK_a of ε-amino group of the lysine side chain (p$K_a \sim 10$–11). At the conjugation pH 7.5–8, the α-amino groups of the N-termini of the mAb molecules are more likely to be deprotonated compared to the ε-amino groups of the lysine side chains. The higher reactivity of the N-terminal amines at the conjugation pH along with other factors such as better accessibility to the electrophilic linker leads to some conjugation at the N-termini of the mAb molecules. While it is unclear whether the conjugation of the drug to the N-termini of the mAb directly leads to the formation of aggregates, the structural characterization studies have shown that the level of conjugation to the N-termini of the mAb was higher in aggregates than in the monomeric ADC.[55]

However, it is debatable whether they directly lead to inferior therapeutic profiles. It is worth introducing a preclinical study on cervical cancer, where a lysine conjugated ADC afforded a greater efficacy on a molar payload basis than a site-specific engineered cysteine conjugated ADC.[58] Establishing a general rule about ADC chemical conjugation technology is not as simple, due to the complexity of cellular mechanisms of cancer and the mode of action of ADC. Hence, a more meticulous study is required to further investigate the causal relationship between the linker conjugation selectivity and therapeutic efficacy.

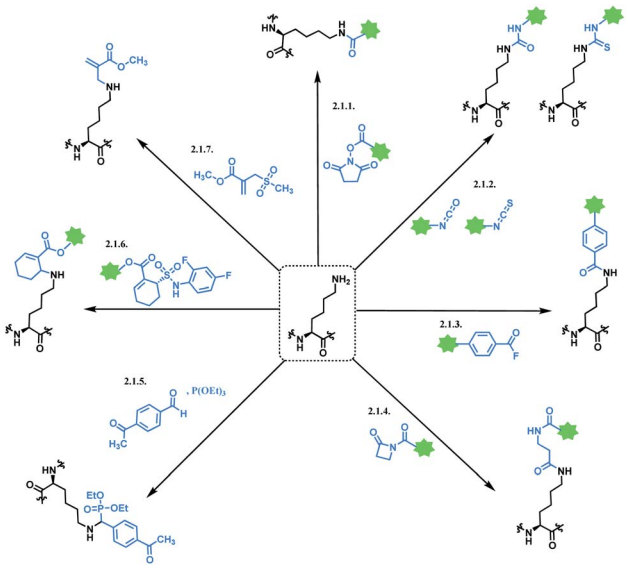

Scheme 2 Lysine conjugation methods.

Moreover, there have been recent developments in a regioselective approach for lysine conjugation, suggesting novel synthetic methodologies can overcome the existing drawbacks of lysine conjugation. Scheme 2 shows an overall summary of reported lysine conjugation methods. While not covered explicitly in the following section, the research work by Kelly and co-workers is also worth noting, as they have demonstrated that a stilbene derivative molecule can selectively label 1 of the 8 lysine ε-amino groups displayed on the surface of the plasma protein transthyretin.[59]

2.1.1. Lysine conjugation (1): *N*-hydroxysuccinimide (NHS) ester. In most cases, lysine-conjugated ADCs (GO, InO, T-DM1) used *N*-hydroxysuccinimide (NHS) ester as a conjugation linker. To our knowledge, NHS ester was first developed in 1963, by Callahan and co-workers.[60] They especially emphasized NHS ester's excellent water solubility, which facilitates protein conjugation under aqueous conditions. The NHS ester conjugates to the lysine ε-amino group *via* the covalent attachment of an acyl group to the nitrogen atom of ε-amino group, followed by the displacement of an NHS leaving group (pK_a = 6.0 (ref. 61)), thereby producing a stable amide bond.[62] The NHS ester's high reactivity towards aliphatic amines is exploited in the modification of DNA[63] and gaseous protein[62] as well.

In the production of GO and InO, succinimidyl-activated calicheamicin derivative (linker-payload) is synthesized prior to conjugation to mAb (Scheme 3).

The NHS ester moiety in activated calicheamicin derivative is susceptible to hydrolysis under aqueous conditions, so the pH of the aqueous medium is well-controlled in the purification step.[54] The conjugation reaction reaches completion within 2 min, at 10 mg mL^{-1} mAb concentration, demonstrating a high reactivity of the NHS ester towards lysine.

The resulting 4-(4-acetylphenoxy)butanoic acid (AcBut) linker is stable in physiologic buffers (pH 7.4) and the acid-labile hydrazone moiety releases calicheamicin in an acidic

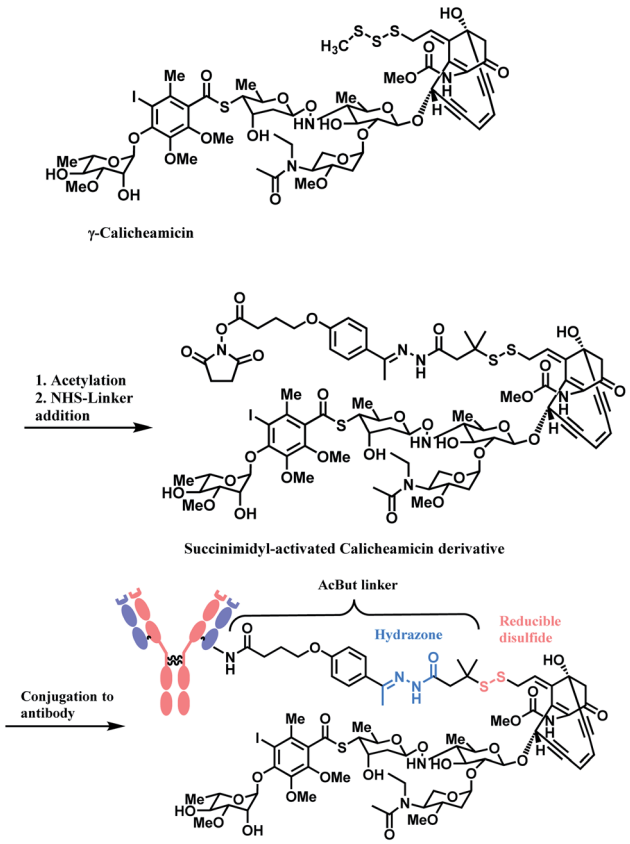

Scheme 3 Synthesis of NHS linker-Calicheamicin derivative payload and conjugation to antibody.

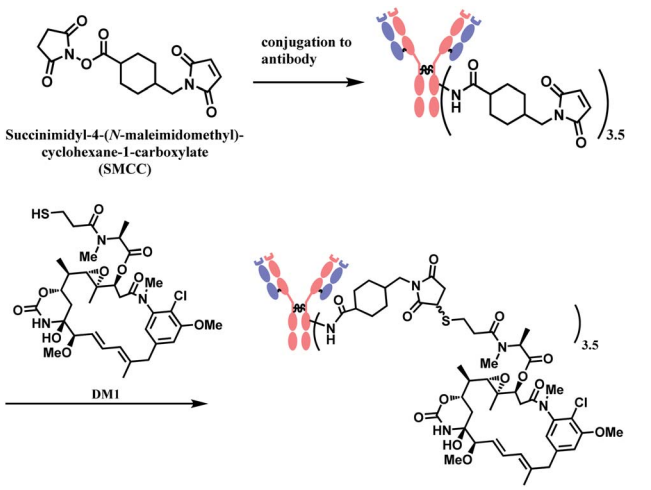

Scheme 4 Conjugation of SMCC linker to antibody followed by DM1 attachment.

pH environment such as found in lysosomes and endosomes (pH 4–6).[64,65] However, it is reported that even in human plasma, the hydrazone hydrolyses at a rate of 1.5–2% per day.[66] The premature release of ozogamicin resulting from the instability of hydrazone[67,68] is hypothesized to be a primary reason for the poor efficacy of Mylotarg, which was withdrawn from the market in 2010.

Whilst also employing an acid-sensitive *N*-acyl hydrazone linkage, the linker contains a reducible disulfide that is stable at physiologic pH but susceptible to nucleophilic attack from thiols. This disulfide linkage has been stabilized by two methyl groups to prevent premature release of calicheamicin.[28] It breaks down selectively in tumour cells *via* a thiol–disulfide exchange reaction with thiol-containing glutathiones (GSH), which are elevated in cancer tissues (up to 1000-fold higher) due to stress conditions such as hypoxia.[31] With these chemically labile groups, the AcBut linker is classified as cleavable.

In the production of T-DM1, the NHS-based linker is conjugated to the antibody first, and the DM1 covalently attaches to maleimide on the other side of the linker *via* a thioether bond formation (Scheme 4).[11] The resulting conjugate exists in diastereomers, as two stereochemical configurations are possible with the C–S bond formed.

NHS esters are observed to react with cysteines, serines, tyrosines, and threonines, not just lysines.[69] The mass spectra analysis showed that they also carry out methionine oxidation, and deamidation at asparagine and glutamine residues.[69] Not just the lack of chemoselectivity, their inherent issue is low regioselectivity. Therefore, research attempts on enhancing its regioselectivity are worth introducing. Weil and co-workers have achieved a more selective lysine by using a substoichiometric amount of NHS. With 0.5 equiv. of NHS relative to RNase A, only a mono-adduct was yielded, as only the most reactive and accessible residue reacted. However, such approach decreases the conjugation yield, and an optimal equiv. with each mAb should be first found out to efficiently use such approach.[70]

In 2019, Yamada and co-workers have developed a platform termed 'AJICAP' to achieve the regioselective modification of antibody even with NHS ester, through the use of Fc affinity peptide.[71,72] A trastuzumab–DM1 conjugate was generated with an average DAR of 1.9.

2.1.2. Lysine conjugation (2): isocyanates and isothiocyanates. Isocyanate reacts readily with an amino group to yield a stable urea linkage, and this reaction is widely exploited in the elastomer industry, not just in bioconjugation.[73] Isocyanate's high reactivity towards proteins is confirmed with its reaction with albumins or keratins in the airway, which is known to be a cause of allergic respiratory diseases.[74] However, despite its high reactivity, isocyanate holds the following limitations as a bioconjugation agent. Firstly, it reacts promiscuously with many nucleophilic amino acid residues. In 1965, Stark found that the rate of reaction of isocyanates with amino groups is related linearly to pK_a,[75] meaning that at pH 7 or below, the N-terminus of peptides and proteins react ~100 times faster than the ε-NH_2 group of lysine. An analytical study with tandem mass spectrometry by Siegel and co-workers in 2009 has confirmed this, and it was also shown that a side-chain amine of arginine reacted with the isocyanate as well.[76] Secondly, it is highly sensitive towards moisture and in fact, the reaction between an isocyanate and a hydroxyl-containing compound is widely used in the manufacture of polyurethanes.[77] Therefore, isocyanate linkers are unstable upon long-term storage and most importantly, are not suitable for use

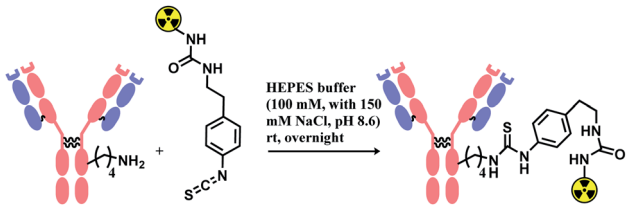

Scheme 5 Construction of antibody–radionuclide conjugate using isothiocyanate linker.

in aqueous medium required for protein conjugation. No research attempt on using an isocyanate as a linker molecule for ADC was carried out, to our knowledge.

Isothiocyanate is reported to be more stable than isocyanate in many literatures,[78,79] and hence was used in constructing an antibody–radionuclide conjugate of ^{211}At and CA12.10C12, an IgG_1 isotype mAb.[80] The conjugation was carried out in HEPES buffer (100 mM with 150 mM NaCl, pH 8.6) and required overnight stirring (Scheme 5). It has provided high labelling yields ranging from 72 to 92%. The isothiocyanato-conjugate was reported to have a lower renal toxicity as compared to its maleimido-conjugate analogue.

However, it should be noted that benzyl isothiocyanate has been recently reported as a cysteine-selective conjugation molecule.[81] Keserü and co-workers have exploited the effect of reaction pH on the protonation states of amino acid residues; at pH 7.4–9.1, amino groups of lysine residues are protonated ($-NH_2 \rightarrow -NH_3^+$), and thus, thiol reactivity is higher.

2.1.3. Lysine conjugation (3): 4-azidobenzoyl fluoride (ABF). Wagner and co-workers presented a plug-and-play strategy in 2017 by utilizing 4-azidobenzoyl fluoride (ABF) to achieve lysine conjugation.[82] The antibody first undergoes a 'plug' stage to install an azide handle for a subsequent 'play' step *via* a copper-free strain-promoted azide–alkyne cycloaddition (SPAAC), which enables the functionalisation of the antibody with one or a combination of payloads (Scheme 6).

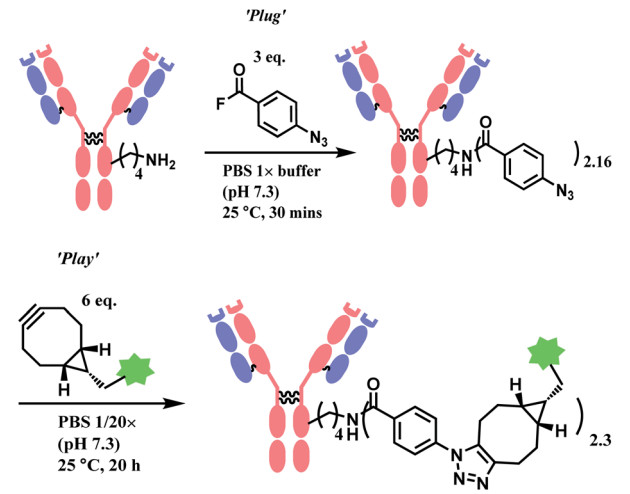

Scheme 6 'Plug' and 'Play' strategy for antibody conjugation with 4-azidobenzoyl fluoroide linker.

AFB-antibody conjugation studies were performed on Trastuzumab monoclonal antibody with varying equivalence of ABF in PBS 1× M buffer (pH 7.3) at 25 °C for 18 h to conclude a 72% efficacy of this technique. This method displays superior efficiency to an NHS ester of 4-azidobenzoic acid (ABNHS) of 49% efficacy. This could be attributed to the better reactivity of ABF with the amine groups of lysine residue. Evidence of their relative kinetics suggest that the bioconjugation with benzoyl fluoride is faster than the electrophile hydrolysis, as shown by the second-order rate constant for benzylamine acylation with ABF and ABNHS to be $k_2 = 87.9\ M^{-1}\ s^{-1}$ ($t_{1/2} = 1.9$ min) and $k_2 = 2.72\ M^{-1}\ s^{-1}$ ($t_{1/2} = 62$ min) respectively. The efficiency of the conjugation with trastuzumab was further tested starting with the experiment of trastuzumab (1 mg mL^{-1}) with ABF (4 equiv.) in PBS buffer 1× (pH 7.3). The trastuzumab–ABF (T–N_3) conjugate then undergoes SPAAC conjugation with TAMRA-BCN (1.5 equiv. for every azide group). At a room temperature of 25 °C, it was demonstrated to have a rapid and near complete conversion of ABF. The completion of reaction was reported to be after 15 min with a degree of conjugation (DoC) of 2.9 (72% efficacy).

Later in the study, this conjugation strategy was performed on the drug monomethyl auristatin BCN derivative (MMAE-BCN) linked with a valine–citrulline linker. This SPAAC modification was done with T–N_3 conjugate (DoC = 2.16) starting with 3 equiv. of ABF, which produced the following trastuzumab–MMAE conjugates with a maintained DoC of 2.10.

2.1.4. Lysine conjugation (4): β-lactams. β-Lactam as a lysine linker was developed by Barbas and co-workers.[83] When compared to β-diketone or acetone aldol adduct of a vinylketone, β-lactam is more applicable for bioconjugation due to the synthetic ease to attach functional molecules in the R position. The research group has demonstrated that β-lactam selectively conjugates to the catalytic site lysine (LysH93) of mAb 38C2. Being located at the bottom of the 11 Å deep active site, this specific lysine residue on the heavy chain has an unusually low pK_a of ~6.0, and this property enabled such selective labelling. The research group has conjugated the β-lactam equipped-cyclic RGD peptide (cyclo(Arg–Gly–Asp–D-Phe–Lys)) to 38C2. The RGD moiety allows the conjugate to bind to human integrins $\alpha_v\beta_3$ and $\alpha_v\beta_5$, expressed on human melanoma M21 cells.

Besides RGD, the research group has attached zanamivir (Relenza™), a neuraminidase inhibitor, to the β-lactam moiety.[84] They successfully formed a 38C2–zanamivir conjugate (DAR = 2) by incubating 4 equiv. of the functionalised linker with the mAb for 2 h in PBS buffer at room temperature (Scheme 7). The conjugate showed inhibitory activity (IC_{50} = 26.6 nM and 38.9 nM depending on x group) similar to zanamivir alone (IC_{50} = 16.6 nM). It was deemed that the mAb conjugation improved the binding with neuraminidase, as each 38C2 was loaded with two molecules of zanamivir, and the target enzyme is a tetramer. In the mice study, the 38C2-zanamivir conjugate had a significantly longer half-life of 72 h as compared to the zanamivir alone (10 min).

Rader and co-workers have used the β-lactam linker to conjugate 2 MMAF moieties to a lysine residue in a dual variable

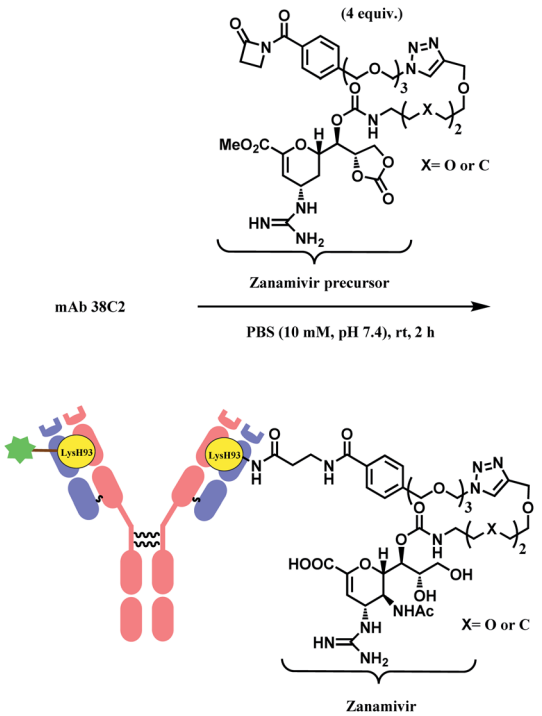

Scheme 7 Formation of 38C2–zanamivir conjugate, which targets influenza neuraminidase.

domain (DVD) format.[85] The DVDs were produced by combining the variable domains of h38C2, which is an anti-hapten mAb, and trastuzumab. Just like the LysH93 on mAb 38C2, the DVD format has two catalytic lysine residues that are located at the bottom of 11 Å deep hydrophobic pocket, that are more nucleophilic (pK_a ~6). These two lysine sites were labelled with 4 equiv. of β-lactam-MMAF (two equivalents per Lys residue) in PBS buffer within 4 h (Scheme 8). No conjugation on lysines on light chain or conjugates with higher DAR were observed.

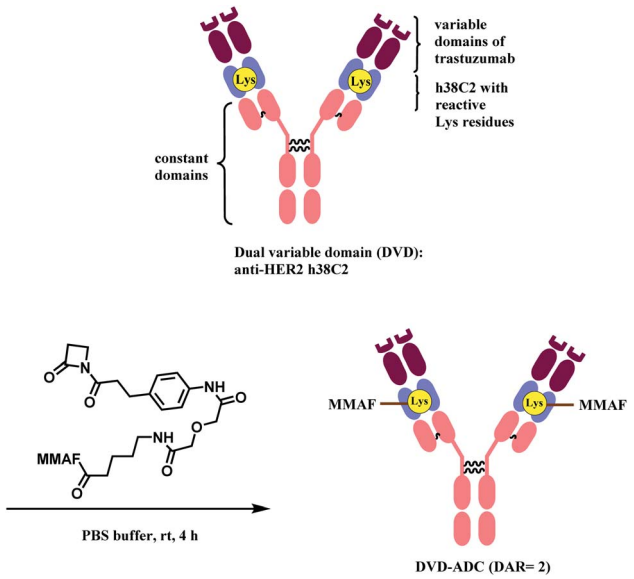

Scheme 8 Conjugation of anti-HER2 DVD-ADC with MMAF *via* the β-lactam linker.

The resulting DVD-ADC was evaluated against HER2+ (SK-BR-3) and HER2− (MDA-MB-468) breast cancer cells. It showed high potency against HER2+ cells (IC_{50} = 68 pM), with no reactivity towards HER2− cells. In addition, the cytotoxicity did not degrade even after incubation in human plasma at 37 °C for 3 days, demonstrating the high linker stability of the conjugate.

Followed by this work, Rader and co-workers expanded the use of β-lactam linker to various applications.[86–88] In one report, instead of the DVD-IgG1 format (h38C2), they have used triple variable domain Fab (TVD-Fab) format that uses a tandem inner Fv domain based on h38C2 and generated a conjugate with DAR of 2.[86] The TVD-Fab antibody carrier-MMAF conjugate had a circulatory half-life of 13.3 ± 2.5 h and deeper tumour tissue distribution as compared to the DVD-IgG1–MMAF conjugate. In another instance, with Alnylam Pharmaceuticals, they have generated a h38C2–siRNA (1 : 2) conjugate *via* the β-lactam-based linker.[89] The conjugate successfully targeted human β-catenin (CTNNB1) mRNA in multiple myeloma cells.

2.1.5. Lysine conjugation (5): Phospha–Mannich. In 2018, Rai and co-workers reported a metal-free Mannich-type reaction with benzaldehyde and triethylphosphite to selectively label a single lysine residue in protein.[90] The ε-amino group in lysine residue in enzymatic protein (1 equiv.), reacts with 300 equiv. of benzaldehyde to generate imine which subsequently reacts with 300 equiv. of triethylphosphite. The conjugation was achieved within 30 min to 1 h, depending on the protein substrate, in 0.1 M pH 7.8 phosphate buffer and DMSO (v/v 9 : 1). They confirmed that the enzymatic activity of proteins was not affected by lysine labelling through the phospha–Mannich reaction.

The phospha–Mannich reaction was applied on several proteins containing multiple lysine residues, including the Fab fragment of trastuzumab, and consistently yielded single lysine-conjugated adducts with the conversion ratio 20–42%. It is noteworthy that carbon-based nucleophiles showed poor site-selectivity, in contrast to triethylphosphite. The resulting mono-adducts could be further functionalized *via* the oxime formation of the aromatic substituent of benzaldehyde. This

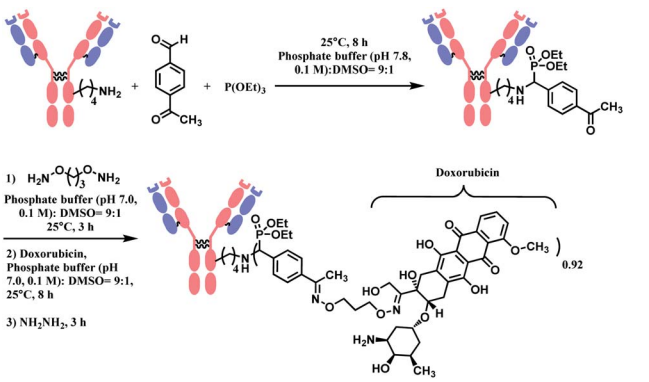

Scheme 9 Synthesis of trastuzumab–doxorubicin conjugate using Phospha–Mannich reaction.

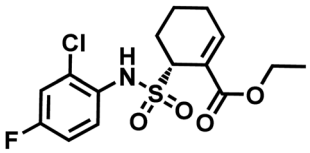

Fig. 9 Structure of TAK-242.

strategy was used to produce an ADC of trastuzumab and doxorubicin with the DAR of 0.92 (Scheme 9). However, the exact site of conjugation in the trastuzumab was not definitively given. In addition, unlike the Fab fragment conjugation, an extended reaction time of 8 h was required to modify the lysine residues of the full antibody. An additional 14 h was further needed for the post-functionalization.

2.1.6. Lysine conjugation (6): α,β-unsaturated sulfonamide. In 2014, Barbas and co-workers have demonstrated that a α,β-unsaturated sulfonamide moiety in toll-like receptor 4 (TLR4) inhibitor TAK-242 (Fig. 9) specifically conjugates to Lys64 on human serum albumin (HSA).[91]

TAK-242 contains a cyclohexene group where aza-Michael addition reaction occurs, and it features a sulfonamide moiety, which is found to be an important trigger for conjugation. Among several analogues, 2,4-difluorophenyl sulfonamide had the highest reactivity (Scheme 10). In human plasma, 2 equiv. of TAK-242 derivative (50 μM) was reacted with a recombinant HSA at 37 °C within 2 h.

TAK-242 derivative was incubated with lysine-blocked HSA, and showed no reaction with cysteines, further establishing a high chemoselectivity towards lysine. Barbas and co-workers later used this conjugation strategy to establish a synthetic method for homogenous antibody conjugate production.[92] A fusion protein of trastuzumab and HSAdIC34S, the domain I of HSA, was generated using a $(GlySer)_3$ spacer. Then, a TAK-242 derivative (R = rhodamine dye) was reacted with the Lys64 of the HSA. No reaction between TAK-242 derivative and lysine or N-termini on trastuzumab was observed, but a longer reaction time was required than previously reported for HSA alone.[91]

Although this strategy was only limited to HSA, not antibodies, this work is highly noteworthy since it is the first reported regioselective and chemoselective lysine labelling, to our knowledge. A linker molecule that is only reactive towards a certain lysine residue among many opens a new approach in selectivity control for the ADC chemical conjugation technology.

2.1.7. Lysine conjugation (7): sulfonyl acrylate. Bernardes and co-workers developed computer-assisted design of sulfonyl acrylate reagents as the aza-Michael acceptor of a single lysine residue on native protein.[93] This regioselectivity was achieved due to the differences in the local microenvironments, and hence the reactivity, of each ε-amino side chain on lysine. Chemoselectivity was also established despite the presence of other significant nucleophilic amino acid residues such as cysteine, as the ε-NH_2 group of lysine was exclusively able to form a hydrogen bond with the sulfone moiety of the Michael acceptor, during the transition state. Such hydrogen bonding thermodynamically accelerates the conjugation by several million-fold, and promotes the leaving of the methanesulfinate, favouring the reaction with entropy increase.

This conjugation reaction occurs rapidly within 1–2 h and, with only 1 equiv. of the designed sulfonyl acrylate reagent at near physiological conditions of 37 °C and pH 8.0. At this pH, the proportion of neutral, nucleophilic lysines was minimal. This was done without having to alter the proteins genetically preceding lysine conjugation or targeting specific residues located in a hydrophobic pocket. Post-functionalisation to the resulting methyl acrylate moiety on the conjugate was easily achieved *via* aza-Michael reactions, while preserving their original secondary structures and functionalities.

Lysine conjugation studies were performed on rHSA, C2Am, Lysozyme, Annexin-V, and Trastuzumab. Remarkably, all the proteins were singly modified on the lysine with the lower pK_a. Further modification of the conjugated trastuzumab–acrylate conjugate (10 μM) with crizotinib anticancer drug in 1000 equivalence (10 mM) to completely generate the respective antibody–drug conjugate (Scheme 11). Cell-line studies with the trastuzumab–crizotinib conjugate on both SKBR3 cells and HEK293 cells indicated a conserved functionality of its antigen binding properties. This is as observed of its specificity for SKBR3 cells with high Her2 antigen expression, and unlike HEK293 cells with low expression of HER2 antigen.

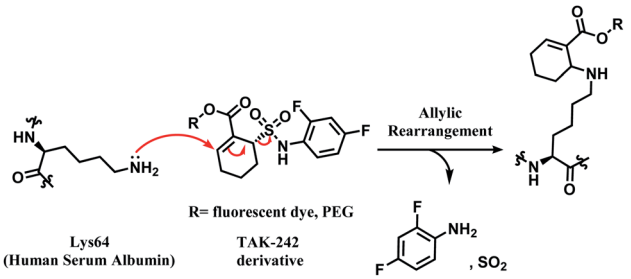

Scheme 10 Proposed mechanism of the conjugation reaction between HSA Lys64 and TAK-242 derivative.

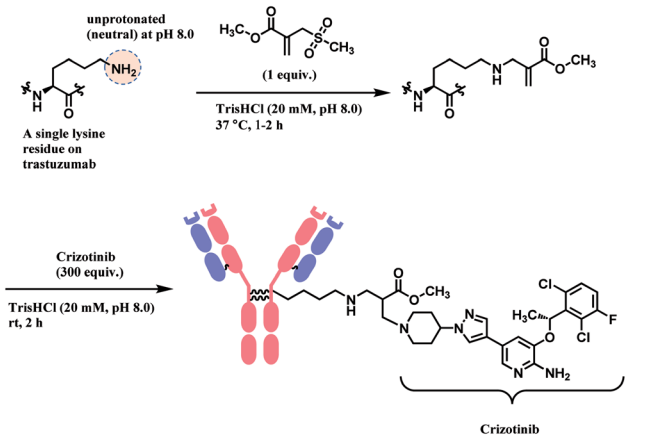

Scheme 11 Preparation of trastuzumab–crizotinib conjugate using sulfonyl acrylate linker.

2.2. Cysteine: single thiol functionalisation

Cysteine is the most commonly targeted amino acid in current ADC clinical developments. 7 out of 11 FDA-approved ADCs exploit a cysteine conjugation strategy. The following aspects make cysteine an attractive target. Firstly, its nucleophilicity is distinguished from other amino acids, which facilitates a chemoselective conjugation. Hard and Soft, Acids and Bases (HSAB) principles by Pearson classify sulfur-based nucleophiles as soft, relative to the nitrogen-based nucleophiles in ε-amine of lysine or N-terminus with higher charge density.[94] The theory suggests that soft nucleophiles thermodynamically prefer to associate with soft electrophiles, and so are hard nucleophiles and hard electrophiles. Indeed, a range of Michael acceptors (soft electrophiles) have shown to selectively conjugate to cysteine residues of protein. Furthermore, under neutral conditions, the thiol group of cysteine ($pK_a = 8$) is more acidic than other common nucleophiles in proteins, such as the ε-amine of lysine ($pK_a = 10$). Secondly, its relative rarity compared to lysine allows a better control of DAR in the ADC production. In practice, interchain disulfide bonds of antibodies are reduced by agents such as TCEP or DTT.[95] Both IgG_1 and IgG_4 mAbs have four interchain disulfide bonds in total, so reducing them generates 8 thiol moieties in each mAb.[96]

However, the issue of regioselectivity (selectively targeting one –SH among 8 thiols) still remains, and there seems to be mixed conclusions around the effect of disulfide reduction on the ADC stability.[97] An overall summary of the reported cysteine bioconjugation methods is shown in Scheme 12.

2.2.1. Cysteine conjugation (1): maleimide. A single thiol modification is used to produce BV, EV, PV, T-Dxd, SG, Belamaf and LT. All of these cysteine-conjugated ADCs in the market use maleimide-based linkers, and these linkers are summarized in Fig. 10.

In a large-scale preparation of anti-Notch 3 ADC and BV (Adcetris™),[98,99] 6 equiv. of maleimide linker-payload is reacted with mAb (anti-Notch3 mAb or brentuximab) within 1 h, in DMSO (11% v/v) and pH 7.0 buffer to afford a yield of 85–88% with an average DAR of 3.6. Maleimide is able to react with a cysteine thiol in mAb in a neutral aqueous solution rapidly with a good yield, in large-scale production.

However, the maleimide–thiol reaction generates two diastereomers, not a single product (Fig. 11). The resulting diastereomers make the profile of their chromatograms complicated,[100] and readily undergo isomerisation to each other.[101]

In addition, the resulting thiosuccinimide adduct is reported to be prone to deconjugation *via* a retro-Michael reaction,[102] or

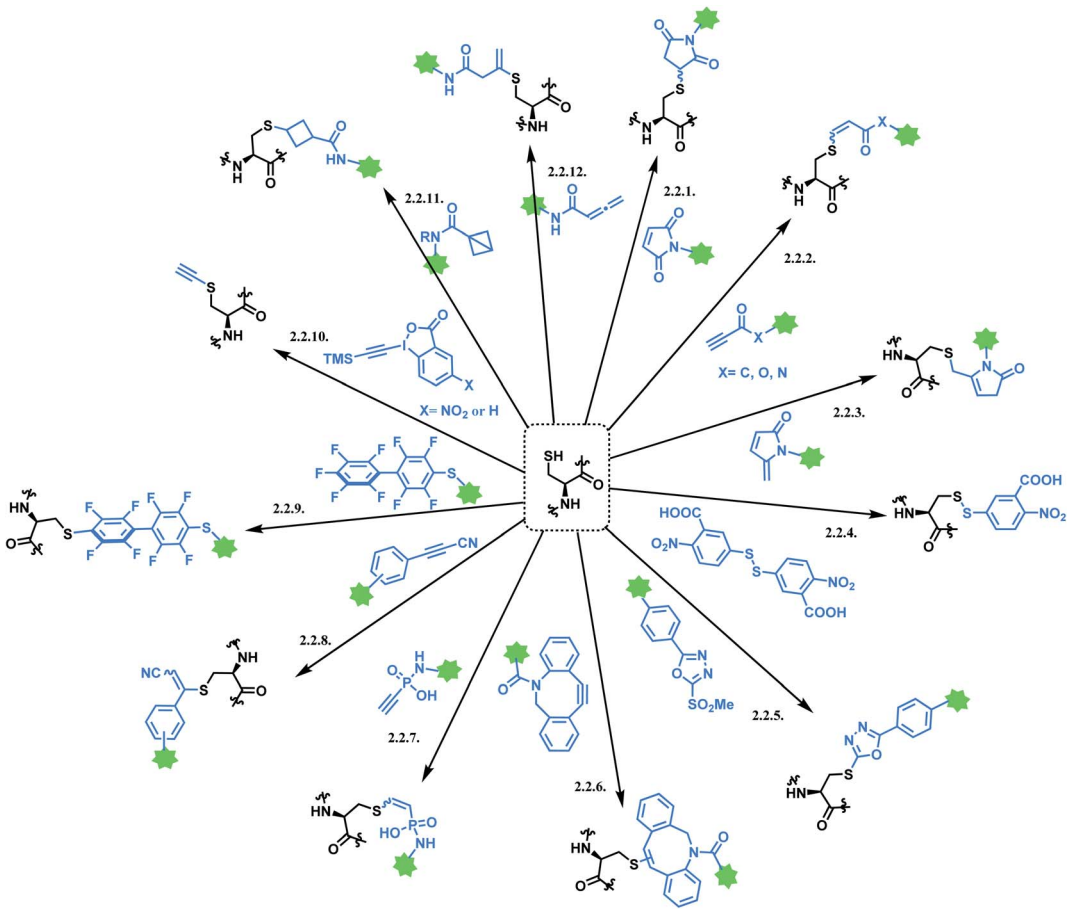

Scheme 12 Cysteine conjugation methods.

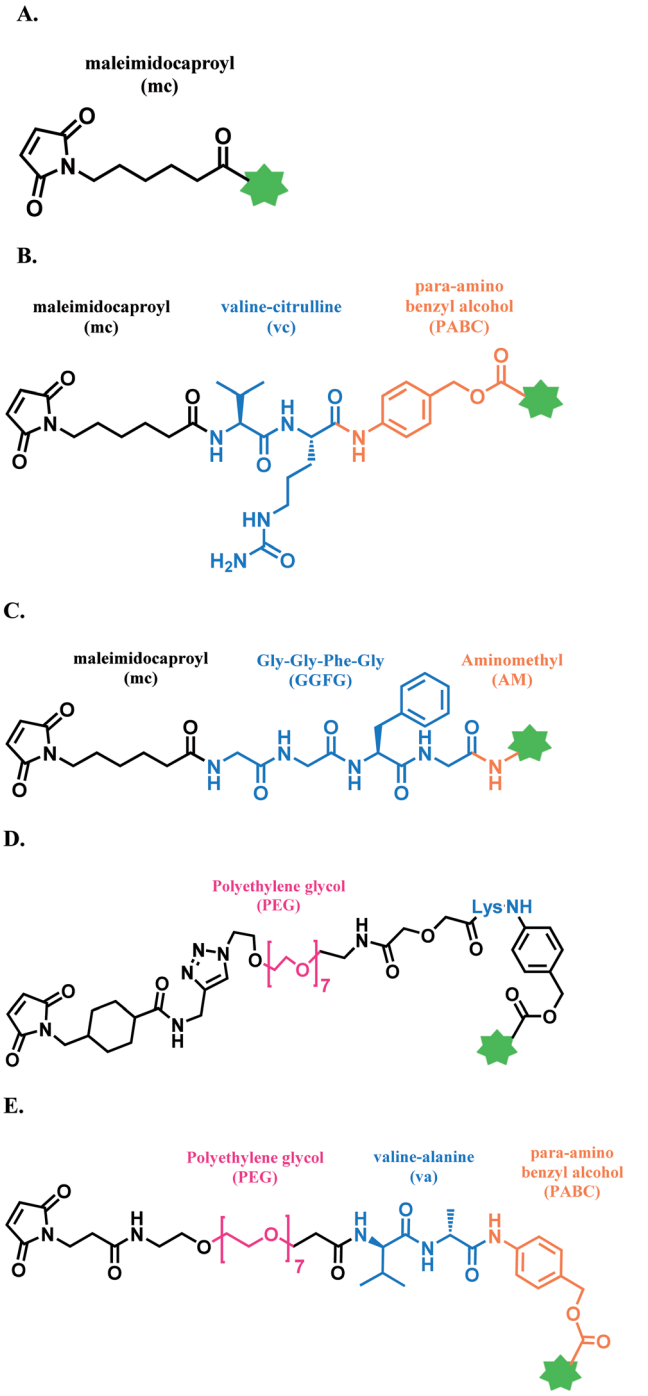

Fig. 10 Maleimide-based linkers in FDA-approved ADCs; (A) MC linker used in Belamaf; (B) MC-VC-PABC linker used in BV, EV, and PV; (C) MC-GGFG-AM linker used in T-Dxd; (D) CL2A linker in SG; and (E) maleimide-VA-PABC linker in LT.

to undergo ring-opening by hydrolysis.[103] The retro-Michael reaction leads to premature drug release in blood plasma. Regenerated maleimide linker-payload then can rapidly react with other thiol groups in blood, such as human serum albumin (HSA) or glutathione (Scheme 13).[50] The characterization study conducted by Pfizer further supports this *in vitro* study; trastuzumab–mc-vc-PABC-drug was incubated with

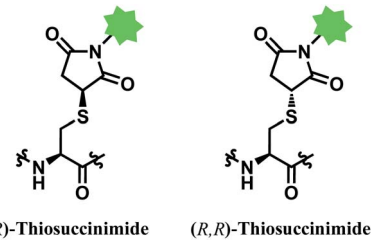

Fig. 11 Two diastereomers of the thiosuccinimide adduct.

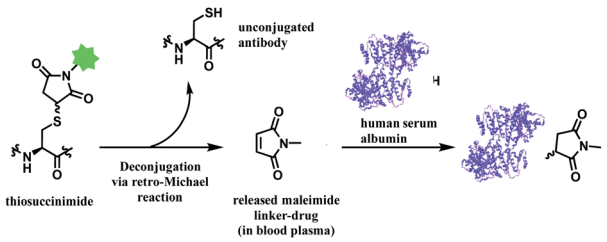

Scheme 13 Deconjugation of thiosuccinimide *via* retro-Michael process and subsequent attachment of maleimide on human serum albumin (pdb: 1AO6).

human plasma for 144 h, and almost 100% of the DAR loss happened.[104] Intact protein mass analysis showed that at the 144 h time point, the mass of albumin in human plasma had an additional 1347 Da over the native albumin extracted from human plasma, exactly matching the mass of the maleimide linker-payload. Such deconjugation and exchange reaction results in off-target toxicity, and reduced therapeutic efficacy, as less than desired amounts of cytotoxins get delivered to tumour cells.

Although the hydrolysis of maleimides was shown to improve conjugate stability and generates ADCs with increased *in vivo* potency, the occurrence of incomplete hydrolysis of many maleimides may limit this approach.

Deconjugation can be attenuated by hydrolysis of the thiosuccinimide ring to the succinamic acid derivatives. Hydrolysis leads to heterogenous mixtures of two succinamic acids, each existing in diastereomers (Scheme 14). Once the ring-opening by hydrolysis occurs, exchange reactions with HSA or glutathione no longer takes place,[105] stabilising the conjugate and thus avoiding drug loss. Companies such as Roche attempted to promote hydrolysis by using engineered antibodies with

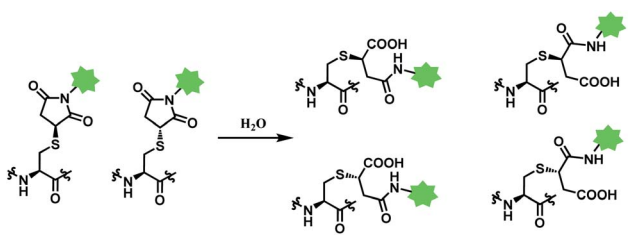

Scheme 14 Hydrolysis of thiosuccinimide conjugate.

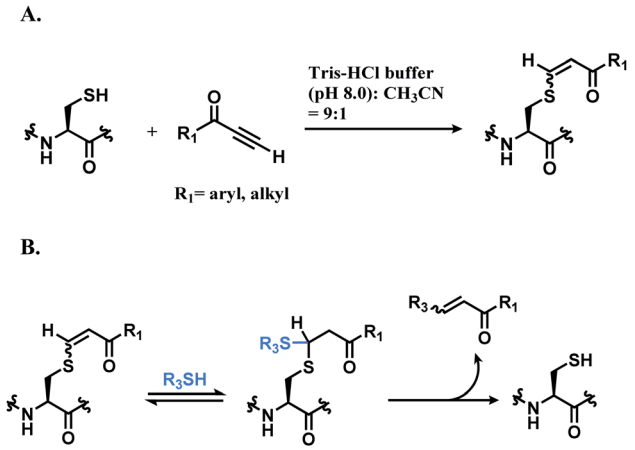

Scheme 15 Conjugation of alkynone linker with cysteine; (A) formation of regioisomeric mixtures of vinyl sulfide; (B) secondary addition of another thiol group followed by deconjugation.

unnatural conjugation site[50] or by incorporation of an amine group on the *N*-alkyl spacer.[106]

Promoting hydrolysis, however, does not solve the fundamental issue of having heterogenous mixtures *in vivo*. Maleimide-based ADCs administered to patients therefore consist of both less potent low drug-loaded species and high drug-loaded species with hydrolysed linkers, resulting in suboptimal therapeutic indexes.

A side reactivity of maleimide with the imidazole group of histidine is observed.[107] In addition, maleimide undergoes an irreversible reaction with the reducing agent TCEP to form an ylene adduct.[108]

2.2.2. Cysteine conjugation (2): alkynyl carboxylic acid derivatives. Che and co-workers have reported cysteine specific conjugation using alkynone.[109] The electrophilicity of alkynoic amides, alkynoic esters, internal and terminal alkynones towards cysteine thiol were assessed and terminal alkynone had the highest reaction rate. It conjugated to a cysteine-containing decapeptide within 5 min, with over 90% conversion in Tris–HCl buffer (pH 8.0) with 10% (v/v) of CH_3CN as co-solvent. The resulting vinyl sulfide is a mixture of regioisomers, as shown in Scheme 15A, and the *Z* stereoisomers, which are formed from the *trans* addition, are found to be the major coupling product (*Z*/*E* ratio 5 : 1). While alkynones have the highest reactivity, they have the least stereoselectivity; the *Z*/*E* ratios of alkynoic amides, alkynoic esters, and alkynones are 22 : 1, 8 : 1, and 5 : 1 respectively. The electron-withdrawing ability of the activating group leads to the isomerisation of the carbon–carbon double bond of the vinyl sulfide *via* intermediate such as allenol and ketene hemiacetal. The resulting vinyl sulfide conjugate is susceptible to the nucleophilic attack of other thiol groups (Scheme 15B).

In 2019, Vilarrasa and co-workers have reported *N*-substituted propynamide as a stereoselective, cysteine-selective linker (Scheme 16).[110] With the co-solvent system of H_2O and ^{t}BuOH (1 : 1 v/v), the resulting vinyl sulfide was mostly *Z*-isomer (*Z*/*E* = >99 : 1). The conjugate was more resistant towards hydrolysis or secondary thiol addition, than the counterpart formed with alkynoic ester linker.

The alkynoic amide linker selectively labelled cysteines on reduced oxytocin and glutathione, at concentrations of the reactants of ≤0.1 M. The linker was inert towards amino groups, even at pH 10.0 or pH 12.0. With glutathione, around an equimolar amount of the propynamide linker afforded the adduct with the yield >95% within 2 h, at pH 7.4 and 37 °C. With oxytocin, a nonapeptide with two cysteine residues, an overnight stirring at 37 °C was required for labelling.

2.2.3. Cysteine conjugation (3): 5-methylene pyrrolone (5MP). Zhou and co-workers have switched one carbonyl moiety in maleimide with methylene and demonstrated that the resulting 5-methylene pyrrolone (5MP) is highly cysteine-selective.[111] 5MP did not react with the ε-amine of lysine between even at pH 9.5, and UPLC-MS analysis showed that 10 equiv. of 5MP yielded a cysteine adduct within 10 min at pH 6.0–8.5. The labelling was still cysteine specific at pH 9.5, but was accompanied by the peptide dimerisation. Thiol addition to 5MP did not generate a stereocenter, unlike maleimide.

The thiol–5MP conjugate does not undergo ring-opening hydrolysis, in contrast to the thiol–maleimide conjugate (shown in Scheme 17). However, the thiol–5MP conjugate underwent retro-Michael reaction at pH 9.5 or thiol-exchange at pH 7.5, just like the maleimide-modified conjugate.

The research group later found that having a bromine atom at 3-position of the 5MP molecule could also serve as a thiol modification agent.[112] The efficiency and specificity of the 3-bromo-5-methylene pyrrolone (3Br-5MP) in a single thiol modification, relative to maleimide was tested with a peptide with only one cysteine. It showed a comparable reaction efficiency to maleimide, where 2 equiv. of 3Br-5MP gave cysteine-modified products in more than 96% yield within 5 min in

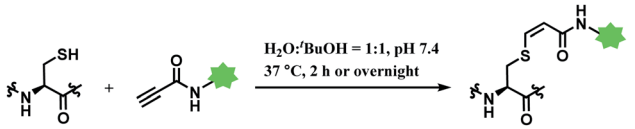

Scheme 16 Labelling cysteine residue with (*Z*)-oxopropene-1,3-diyl linker.

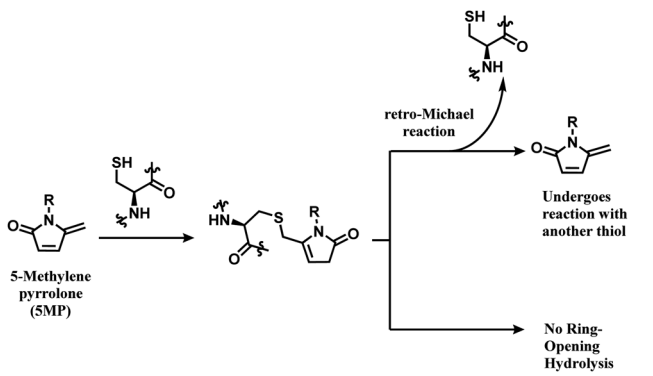

Scheme 17 5MP conjugation to cysteine and the resulting adduct's stability.

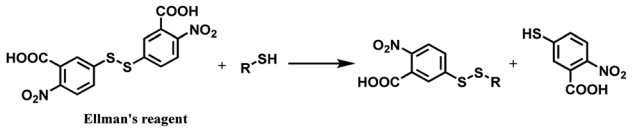

Scheme 18 Thiol–disulfide exchange of DTNB.

pH 7.5 buffer at both 37 °C and 4 °C. The 3Br-5MP showed a higher cysteine-specificity compared to maleimide. It did not show any reactivity towards N-terminal amino acids, when maleimide did. The 3Br-5MP also serves a disulfide rebridging conjugation molecule and such reactivity is explored in Section 2.3.3.

2.2.4. Cysteine conjugation (4): 5,5′-dithiobis-(2-nitrobenzoic acid) (DTNB). Ellman's reagent (5,5′-dithiobis-(2-nitrobenzoic acid) or DTNB) is a chemical that readily undergoes a thiol–disulfide exchange (Scheme 18) and hence used to measure the concentration of thiol groups in a sample.[113]

In 2012, Neri and co-workers have used the DTNB reagent as a linker to construct an ADC.[114] This ADC was designed to release the cytotoxic drug, a thiol-containing cemadotin analogue (CemCH$_2$-SH), into the extracellular region. Human antibody F8 was selected to target tumour cells and was used in a small immune protein (SIP) format. The disulfide bond between the C-terminal cysteine residues of the SIP(F8) antibodies was first reduced using TCEP before the thiol groups were activated by Ellman's reagent. After CemCH$_2$-SH was synthesized, SIP(F8)-Ellman's antibodies were incubated with CemCH$_2$-SH (10 equiv.) in PBS (pH 7.4) at room temperature for 10 min to yield the desired ADC, SIP(F8)-SS-CH$_2$Cem, with 50% yield. In addition, the ADC was stable when it was stored at −80 °C and 4 °C and was still present in mouse plasma after incubation for 72 h at 37 °C (Scheme 19).

In 2014, the research group used the Ellman's reagent to design a new immunocytokine drug conjugate (IDC) known as F8-IL2-SS-DM1, by linking a F8-IL2 fusion protein to DM1

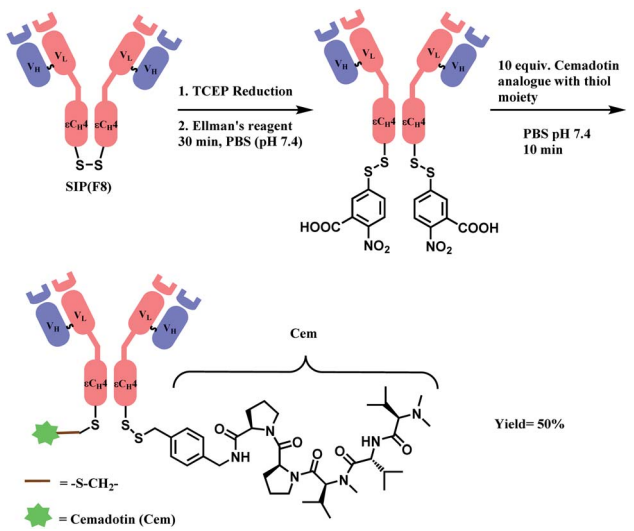

Scheme 19 Generation of ADC, SIP(F8)-SS-CH$_2$Cem.

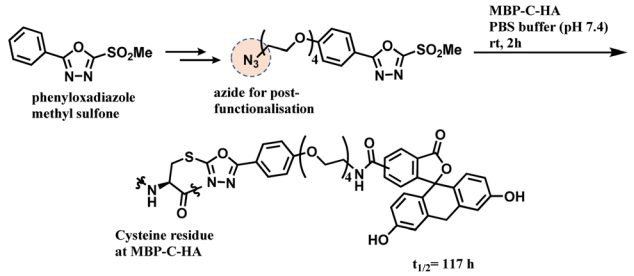

Scheme 20 Conjugation of MBP-C-HA with phenyloxadiazole sulfone (PODS) linker.

maytansinoid.[115] After this new IDC was administered to the mice that were bearing subcutaneously grafted F9 and C1498 tumours, F8-IL2-SS-DM1 was observed to selectively accumulate in the tumours and also showed stronger tumour growth inhibition than the single-payload immunocytokine F8-IL2.

2.2.5. Cysteine conjugation (5): phenyloxadiazole sulfone (PODS). Inspired by the use of methylsulfonyl benzothiazole as a thiol-blocking reagent,[116] Barbas and co-workers assessed various methylsulfonyl derivatives as cysteine-selective conjugation reagents.[117] The phenyloxadiazole sulfone (PODS) was found to be the most reactive, where it formed the thioether adducts with various cysteine derivatives within 30 min at room temperature, in tetrahydrofuran (THF) and pH 7.4200 mM PBS buffer (v/v = 1 : 1) with good yields of 78–99%. It is noteworthy that the reaction conversion was lower when pure water was used instead of the buffer. The resulting thioether conjugate was shown to have higher stability in varying pH levels as compared to a maleimide–cysteine conjugate. It did not have a thiol-exchange with glutathione.

A functional payload could be loaded on the linker as shown in the Scheme 20, and 10 equiv. of the azide-functionalised phenyloxadiazole sulfone specifically labelled Cys34 of human serum albumin (HSA), and a single cysteine on maltose-binding protein (MBP-C-HA), in pure PBS, within 2 h. A conjugate of

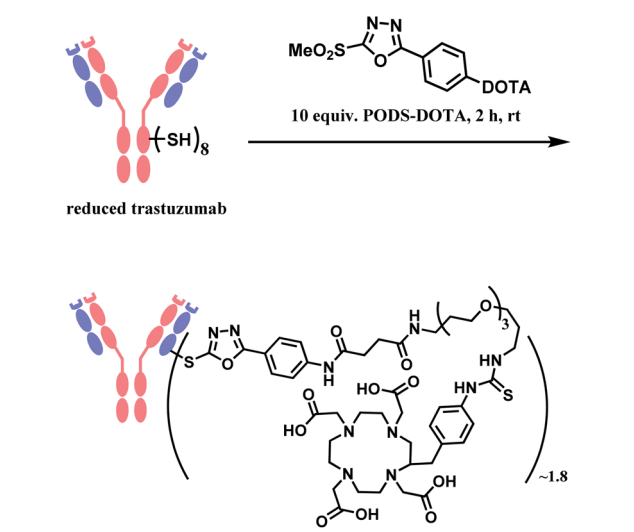

Scheme 21 Conjugation of trastuzumab with PODS–DOTA.

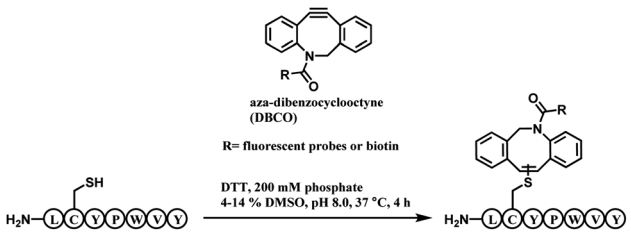

Scheme 22 DBCO-tag mediated thiol–yne reaction.

fluorescein and MBP-C-HA linked *via* PODS had a superior stability in human plasma ($t_{1/2} = 117$ h) to the maleimide-linked conjugate ($t_{1/2} = 59.9$ h).

In 2019, Zeglis and co-workers adopted this linker to generate a conjugate of trastuzumab and a radionuclide chelator 1,4,7,10-tetraazacyclododecane-1,4,7,10-tetraacetic acid (DOTA).[118] The antibody was incubated with 10 equiv. of PODS–DOTA for 2 h at room temperature and yielded the conjugate with 80% yield. The average degree of labelling was found to be ~1.8 DOTA/mAb (Scheme 21). The resulting conjugate exhibited immunoreactivities similar or better relative to the counterpart conjugate prepared by using maleimide linker.

2.2.6. Cysteine conjugation (6): cyclooctyne. The alkyne moiety in aza-dibenzocyclooctyne (DBCO) reagent, which undergoes a strain-promoted alkyne–azide cycloaddition (SPAAC), was shown to react with a cysteine residue as a side reaction.[119] Pentelute and co-workers exploited such reactivity to present DBCO as a cysteine-selective linker molecule (Scheme 22).[120]

A unique heptapeptide sequence Leu–Cys–Tyr–Pro–Trp–Val–Tyr (LCYPWVY) conjugated with cyclooctyne rapidly with a rate constant of 0.81 ± 0.02 M^{-1} s^{-1} in pH 8.0 phosphate buffer at 37 °C. Other peptide sequences do not react as rapidly or are inert to DBCO (ex. Phe–Cys–Pro–Phe), allowing a selectivity control. The researchers produced a trastuzumab–biotin conjugate by incorporating the peptide tag onto the C terminus of the heavy chains of trastuzumab and reacting it with DBCO-$(PEG)_4$-biotin. The reaction only generated 90% heavy-chain mono-adduct and no reaction between liberated thiols and cyclooctyne was observed. The resulting conjugate exists in isomers generated from addition of the thiol to either one of the two alkyne carbons.

2.2.7. Cysteine conjugation (7): phosphonamidate. Hackenberger and co-workers have reported phosphonamidate as a cysteine-selective linker molecule.[121] Diethyl ethynylphosphonite undergoes a Staudinger-phosphonite reaction with azide-functionalized molecule which induces the electron-rich triple bond of the ethynyl group to be electron-poor (*i.e.* more electrophilic), as shown in Scheme 23A. The cysteine thiol (–SH) then attacks the electrophilic alkyne in ethynylphosphonamidate, yielding regioisomeric mixture of the adduct. The full conversion was achieved at pH 8.5 within 30 min, at a concentration of 10 mM of the substrate. In aqueous systems, the Cys-phosphonamidate adduct had a high *Z* selectivity (>97%). The research group conjugated biotin-functionalised ethynylphosphonamidate (10 equiv. per thiol) to reduced thiols in

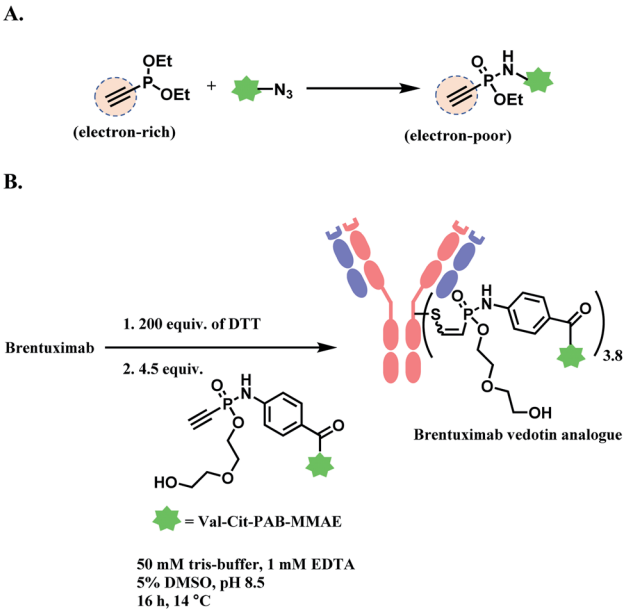

Scheme 23 Phosphonamidate electrophile for cysteine bioconjugation; (A) Staudinger-phosphonite reaction (SPhR) to generate electron-poor ethynylphosphonamidate linker; (B) generation of ADC using ethynylphosphonamidate linker *via* thiol addition.

trastuzumab. The degree of modification was 4.72 on average. The linker showed excellent selectivity towards free cysteine residues, where no modification on any amino acid was found without prior reduction. However, the reaction kinetics was 0.62 M^{-1} s^{-1}, which was significantly slower than maleimide (743 M^{-1} s^{-1}).

The linkage stability of the biotin-modified antibody was compared to the maleimide adduct in a head-to-head fashion in bovine serum albumin (BSA) solution under physiological conditions. A significant transfer of the biotin to BSA was observed for the maleimide linkage whereas the phosphonamidite linkage was stable under the tested conditions. The P–N bond hydrolysis only happened under the extreme condition of 24 h incubation at pH 0.

In 2019, the research group expanded the scope by producing a structural analogue of brentuximab vedotin (BV, Adcetris™) by substituting the maleimide linker with the phosphonamidate linker (Scheme 23B).[122] Its *in vivo* activity was tested in a Karpas 299 derived tumour xenograft model in immunodeficient female CB17-SCID mice. A superior stability of the phosphonamidate linker allowed the lower dosing of ADC to be still active, with a prolonged drug delivery in circulation.

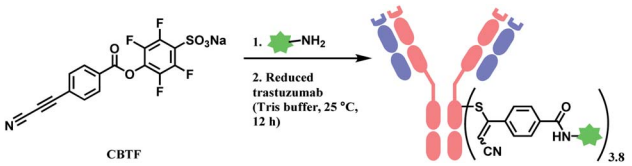

Scheme 24 Labelling cysteine residues on trastuzumab with CBTF bifunctional linker containing APN moiety.

The BV analogue with the phosphonamidate linker had a median survival of 48 days, whereas the FDA-approved BV had 21 days.[122]

2.2.8. Cysteine conjugation (8): 3-arylpropionitrile (APN). In 2014, Wagner and co-workers introduced a new class of reagents, 3-arylpropiolonitriles (APN), that could be used for cysteine conjugation in aqueous environments.[123] The reaction between 3-phenylpropiolonitrile and a cysteine derivative follows second order kinetics of 3.1 M^{-1} s^{-1}, which is higher than that of iodoacetamide, alkynoic amide and 4-vinylpyridine, but lower than that of *N*-phenylmaleimide and alkylnone. Unfortunately, 3-phenylpropiolonitrile was not completely cysteine-selective. Side reactions with other nucleophilic amino acid derivatives such as tyrosine benzamide, glycine benzamide and valine benzamide were observed within 1 h, albeit with low conversions.

In terms of the stability of the APN-cysteine adduct, no degradation was observed in aqueous medium of pH 0–14, in the presence of excess nucleophiles such as thiophenol, cysteine, thioethanol and glutathione (100–1000 equiv., 10–100 mM), as well as reducing agents that include TCEP or DTT (0.1–1 M) at pH 7.4. However, the FRET-based APN conjugate was observed to be less stable when it was incubated at 37 °C in human plasma and when it was incubated for different times in living cells. Nonetheless, the FRET-based APN conjugate displayed a higher stability compared to the FRET-based maleimide–thiol conjugate. Notably, the addition of a cysteine derivative to APN produces a stereoisomeric product mixture that contains mostly *Z*-isomers.

In the chemoselectivity assessment of APN, APN–TMPP was attached to tris(2,4,6-trimethoxymethyl)-phosphonium (TMPP), a highly responsive MS tag. The conjugation of the APN-TMPP probe to a peptide increases retention time in LC-MS. Experiments to prove the chemoselectivity of APN for cysteine were carried out by reacting APN-TMPP with tryptic digest at a 200 : 1 molar ratio of APN-TMPP to protein at 25 °C for 1 h. The peptide mixtures before and after tagging were analysed with LC-MS. It was found that all peptide mixtures with cysteine-containing peptides reacted with APN-TMPP probes since these mixtures had a higher retention time after tagging. On the other hand, mixtures that contained cysteine-free peptides did not react with APN-TMPP and thus did not exhibit any change to their retention time.

Followed by this initial discovery, Wagner and co-workers have developed a heterobifunctional linker, sodium 4-((4-(cyanoethynyl)benzoyl)oxy)-2,3,5,6-tetrafluoro benzene sulfonate (CBTF), where one end is cysteine-selective APN and the other end is amino-reactive activated ester (Scheme 24).[124] The research group reacted CBTF with TAMRA-NH_2 and later conjugated the resultant product to reduced trastuzumab. The CBTF conjugated antibodies yielded DAR values of 1.9 and 3.8 when the antibody was reduced with 1.1 and 2.2 equiv. of TCEP. For comparison, SMCC was used in place of CBTF as the bifunctional linker, the SMCC conjugates provided DAR values of 2.3 and 3.9 respectively. In addition, CBTF conjugates were observed to be more stable in human plasma compared to SMCC conjugates. The toxicity test of a CBTF model linker on HeLa and HuH-7 cell lines revealed that the linker did not show any toxicity up to 100 μM.

2.2.9. Cysteine conjugation (9): perfluoroarene. Inspired by the arylation reaction of a naturally occurring enzyme, glutathione S-transferase, Pentelute and co-workers have developed a cysteine-selective arylation method with perfluoroaromatic linker.[125] A protected cysteine derivative was labelled with hexafluorobenzene in the presence of 50 mM solution of TRIS (tris(hydroxymethyl)-aminomethane) base in an aprotic solvent, dimethylformamide (DMF) within 4.5 h.

Even when a lower equivalence of cysteine derivatives was used, disubstitution was observed, specifically at 1,4 positions. It is proposed that the stabilisation of the substituted intermediate by sulfur, favours a second thiol substitution in the *para*-position. A similar reactivity was observed with decafluorobiphenyl species. Chemoselectivity of the perfluoroaromatic linker was assessed by incubating it with model peptide systems containing various nucleophilic amino acid residues such as histidine and lysine, and was shown that no reactivity was observed between amino acids other than cysteine.

However, the reactivity of perfluoroarene is significantly lower in water, limiting its application to bioconjugation. In order to adapt the method to aqueous media, the research group has used a promiscuous enzyme, glutathione S-transferase (GST) along with the perfluoroaromatic reagents.[126] GST is a cytosolic enzyme that catalyses conjugation reactions between the Cys residue of glutathione (GSH, γ-Glu–Cys–Gly) and various electrophiles. With the presence of 5–10 mol% of GST, the quantitative labelling of cysteine in GSH with the perfluorobiphenyl moiety was

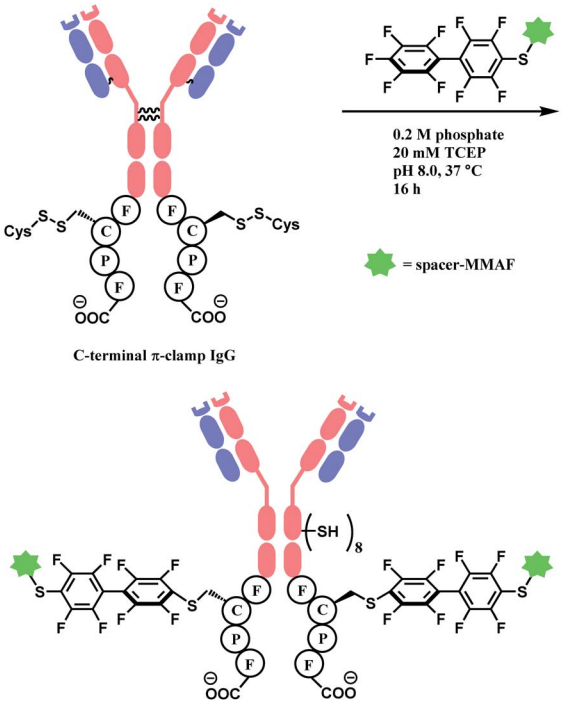

Scheme 25 Construction of ADC of trastuzumab and MMAF *via* π-clamp and decafluorobiphenyl linker.

achieved within 30 min in pH 8.0 phosphate buffer at 37 °C. No reactivity was observed in the absence of GST. Due to the nature of enzyme (GST)-substruate (GSH) interaction, this conjugation method is GSH-exclusive, where other Cys residues in different peptides or the thiol in 100-excess of 4-mercaptophenylacetate were not conjugated. Applying this strategy for the construction of ADC would therefore require an incorporation of GSH motif into antibody.

In 2016, the research group developed a specific four-amino-acid sequence (Phe–Cys–Pro–Phe), dubbed as 'π-clamp', that promotes the S_NAr reaction in water, without the aid of GST.[127] The tetrapeptide sequence was inserted into the C termini of the heavy chains of trastuzumab, C225 antibody, and the N-termini of Sortase A, and payload-perfluoroaryl compounds facily formed adducts. The MMAF loading on trastuzumab was carried out in 0.2 M phosphate with 5% DMSO, 20 mM TCEP for 16 h at 37 °C (Scheme 25). Proteins without the π-clamp showed no reactivity towards perfluoroaryl-payload, highlighting a high site-selectivity of this conjugation strategy. A conjugate of trastuzumab and MMAF connected *via* π-clamp and decafluorobiphenyl linker selectively killed BT474 cells (HER2 positive) but showed no cytotoxicity towards CHO cells (HER2 negative), demonstrating that the π-clamp conjugation does not affect the binding ability of trastuzumab.

2.2.10. Cysteine conjugation (10): ethynylbenziodoxolone (EBX). Many conjugation linkers have an alkyne moiety in the terminal end, thereby allowing the conjugate to undergo post-functionalisation *via* alkyne–azide click cycloaddition (Section 2.6.3, 2.3.2 *etc*). Waser and co-workers presented a method to directly introduce an acetylene group onto the cysteine thiol with hypervalent iodine reagent, trimethylsilyl (TMS)–ethynylbenziodoxolone (EBX).[128]

Among all the TMS–EBX reagents, the one with an electron-withdrawing NO_2 substituent showed the highest reactivity towards thiols. Many different tetrapeptide systems containing nucleophilic residues were reacted with 2 equiv. of nitro-substituted TMS–EBX in 0.2 M pH 8.2 PBS buffer at 37 °C for 15 min, in order to assess the chemoselectivity of this method (Scheme 26). Steric hindrance by branched hydrocarbon chains of isoleucine or valine did not slow down the reaction, and the TMS–EBX showed selective reactivity towards cysteine in the presence of serine, lysine, tryptophan or histidine, producing

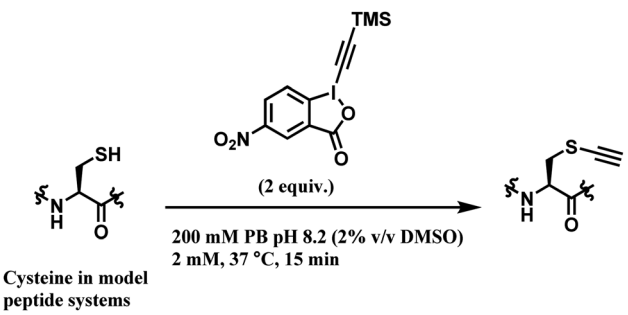

Scheme 26 Cysteine conjugation with TMS–EBX.

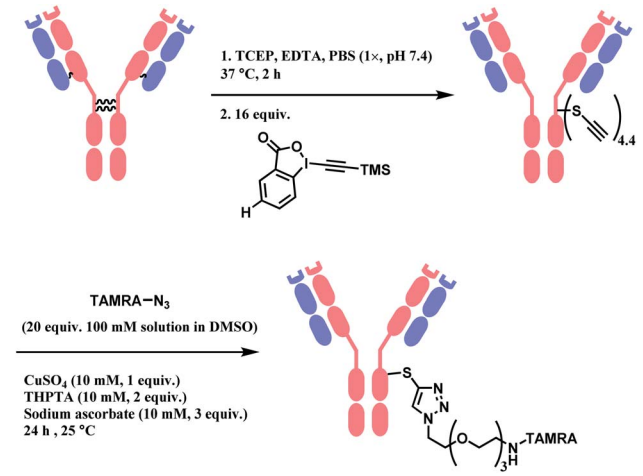

Scheme 27 Labelling trastuzumab with TAMRA with TMS–EBX reagent.

the ethynylated cysteine with >90% yields. However, undesired side-reactivity was observed with arginine and tyrosine.

When applied to disulfide-reduced trastuzumab, a complex mixture was formed after the CuAAC step, suggesting a partial degradation of the antibody or side-reactions of ethynylation or cycloaddition. When a non-reduced trastuzumab was reacted with nitro-substituted TMS–EBX, the antibody degraded even in the absence of liberated thiols and the formation of a terminal alkyne was not observed. Without the nitro-substituent, side-reactivity was decreased. 2 equiv. of TMS–EBX gave the average degree of conjugation (DoC) of 0.8, and with 16 equiv., the average DoC of 4.4 was achieved. The conversion rate and the average DoC was dependent on the pH, where pH < 7.5 led to suboptimal DoC and yield. The antibody subsequently is reacted with an azide-functionalised TAMRA probe *via* CuAAC (Scheme 27).

2.2.11. Cysteine conjugation (11): bicyclo[1.1.0]butane (BCB) carboxylic amide. In 2020, Ojida and co-workers reported bicyclo[1.1.0]butane (BCB) carboxylic amide as a new class of thiol-reactive electrophile for the application of targeted covalent inhibitors (TCIs).[129] Despite the high strain energy of the ring system (~66 kcal mol^{-1}),[130] BCB is stable under aqueous conditions,[131] facilitating its use in bioconjugation.

The thiol group undergoes strain-driven nucleophilic addition with BCB, yielding diastereomeric mixtures of 1,3-disubstituted cyclobutane (*cis* : *trans* ratio of ~7 : 3). Its reactivity towards cysteine was only studied with glutathiones (GSHs), in pH 7.2 0.1 M potassium phosphate buffer at 37 °C. The reaction rates were significantly slower than those of acrylamides, where first-order reaction kinetic analysis showed that the half-time ($t_{1/2}$) of phenyl BCB carboxyl amide was 32.7 h, whereas that of crylamide analogue (*N*-phenylacrylamide) was 1.2 h.

The chemoselectivity of BCB carboxylic amide towards cysteine was confirmed by reacting it with other nucleophilic amino acids (Lys, Ser, His, Tyr, and Trp) in 0.1 M K_2CO_3 DMF/H_2O. No reaction was observed even under such basic conditions.

2.2.12. Cysteine conjugation (12): allenamide. In 2014, Loh and co-workers reported allenamide as a highly cysteine-selective Michael acceptor linker.[132] Besides its stability at room temperature and pressure and its easy preparation, the allenamide moiety also reacts with a thiol group in a straightforward addition reaction. Importantly, allenamide moieties were found to be unreactive towards regularly encountered nucleophiles in biological systems such as hydroxyl functional groups, amines and carboxylate ions. The chemoselectivity of the allenamide moiety for cysteine was proven by reacting a benzyl allenamide with three different peptide sequences that contained both terminal and internal cysteine residues: benzyl allenamide (10 equiv.) and the peptide (250 μM) were incubated for ten minutes in ammonium carbonate buffer (pH 8.0) at room temperature. The modification of the cysteine residues was ascertained *via* LC-MS/MS analysis. Notably, conjugated products were observed to be irreversible, demonstrating the method's high applicability as ADC linker.

The reactivity of cysteine thiols in proteins with allenamide and the stability of the formed conjugates under peptic digestion conditions were also tested using bovine serum albumin (BSA) proteins by incubating the protein with benzyl allenamide at 37 °C for 30 min. The cysteine residues were successfully conjugated by the allenamide. The research group also showed that labelling probes fluorescein isothiocyanate (FITC), Cy3 and Cy5 dyes that were modified with allenamide handles were capable of labelling BSA.

The allenamide–thiol click reaction was adopted by many research groups as a robust, cysteine-targeting conjugation linker.[133–135] In 2016, Roush and co-workers have prepared a conjugate of selenocysteine-incorporated mAb (SELENOMAB) and fluorescein with allenamide and phenyloxadiazole sulfone (Section 2.2.5) linkers.[136] The reduced SELENOMAB reacted with fluorescein-allenamide within 2 h at room temperature. In human plasma at 37 °C, and SELENOMAB–allenamide–fluoroscein conjugate had the half-life of over 28 days whereas SELENOMAB–PODS–fluoroscein conjugate had a half-day of 12 h. These results demonstrate allenamide linker's high resistance against hydrolysis, thiol–disulfide exchange or deconjugation. In the *in vitro* test with SK-BR-3 breast cancer cells, it was shown that the fluoroscein conjugation with the allenamide linker did not degrade the binding ability of the antibody towards HER2 receptors.

2.3. Cysteine: disulfide functionalisation

A bis-reactive linker can undergo reactions with both thiol residues, which are produced by reducing a disulfide bond in antibody. Such method has a competitive advantage in controlling DAR near to 4 when modifying IgG_1 and IgG_4 antibodies, as they have four reducible interchain disulfides. Moreover, such bioconjugation strategy reanneals the cleaved disulfide bridges between antibody chains *via* covalent bonds. OBI-999, a clinical ADC that is currently being studied in phase I/II for advanced solid tumours, uses such disulfide rebridging linker.[137] The linker in OBI-999 is bissulfone moiety-based, and

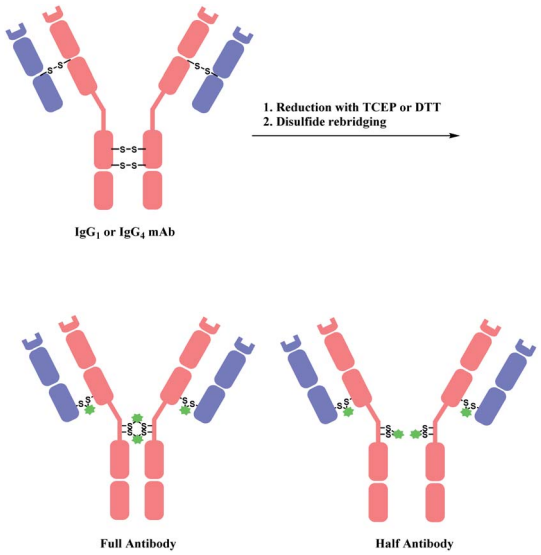

Scheme 28 Disulfide reduction followed by rebridging with linker, and the formation of undesired half-antibody.

is explored in Section 2.3.1. The DAR of OBI-999 was well-controlled to be 4 and showed good pharmacokinetic profiles.[138]

However, one drawback of disulfide rebridging linkers is the formation of 'half-antibody'. It is formed by intrachain bridging of the hinge region in heavy chain cysteines (Scheme 28).

An overview of reported disulfide rebridging linker molecules is shown in Scheme 29.

2.3.1. Disulfide rebridging (1): bis-sulfones. Godwin and co-workers at Abzena plc. have developed bis-sulfone reagent as a disulfide-rebridging linker.[139] The conjugation reconnects the reduced disulfide bonds in antibody *via* a three-carbon bridge, that is small and flexible enough not to perturb the ternary

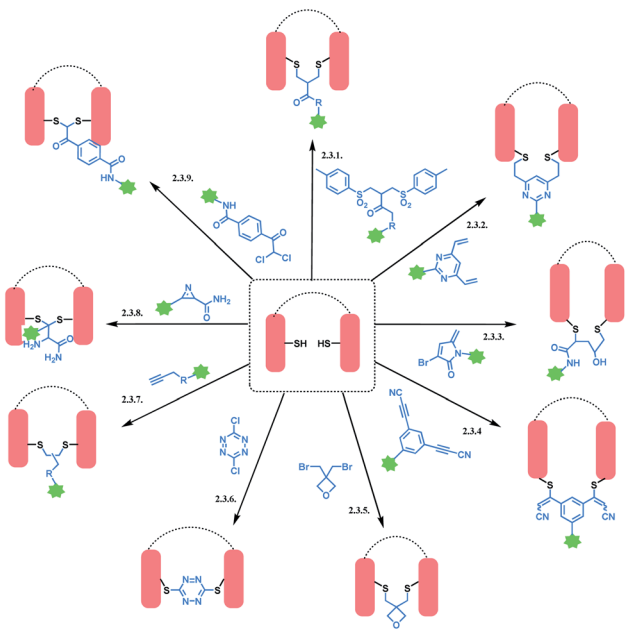

Scheme 29 Disulfide rebridging methods.

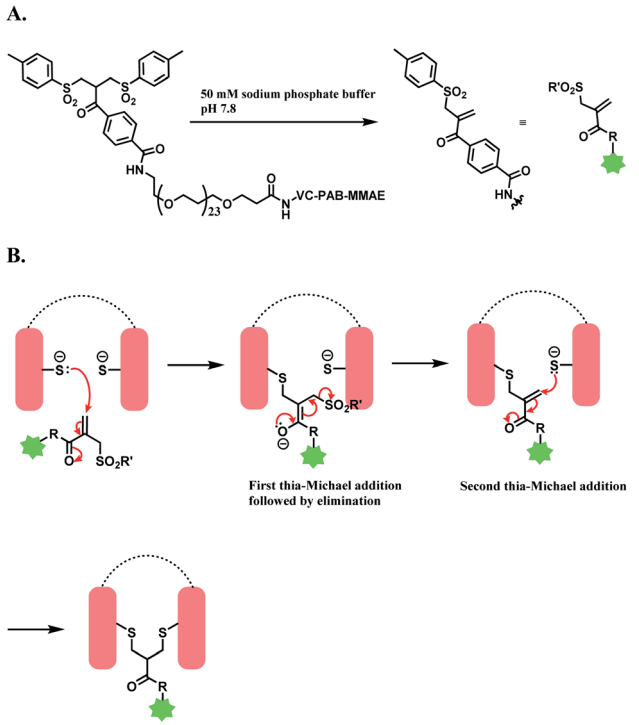

Scheme 30 Bis-sulfone reagent as a disulfide rebridging linker; (A) Formation of mono-sulfone Michael acceptor; (B) disulfide rebridging *via* a sequence of Michael addition and elimination reactions.

structure of protein. Bis-sulfone loaded with drug is produced first as a precursor, and in 50 mM sodium phosphate buffer (pH 7.8), a mono-sulfone Michael acceptor is generated to react with reduced disulfide (Scheme 30A).[140] When 6 equiv. of mono-sulfone Michael acceptor was reacted with reduced trastuzumab for 16 h at 4 °C, a 78% conversion of antibody to ADC with a MMAE loading of 4 was achieved, with no unconjugated antibody formed.

The trastuzumab–MMAE conjugate with this sulfone linker was stable in human serum containing albumin, where no DAR loss was observed after being incubated for 120 h. The ADC of trastuzumab-derived Fab and MMAE linked *via* the sulfone linker was found to have potent antiproliferative activity in both SK-BR-3 and BT-474 cell lines, which are HER2-positive.

2.3.2. Disulfide rebridging (2): divinylpyrimidine (DVP). Spring and co-workers have developed a novel divinylpyrimidine (DVP) linker platform for cysteine-bridging bioconjugation.[141] An alkyne-functionalised DVP served particularly useful for the ADC application, as the alkyne moiety could undergo copper-catalysed cycloaddition with azide-containing payloads (CuAAC).[142]

10 equiv. of alkyne-functionalised DVP per disulfide was reacted with a reduced trastuzumab for 2 h at 37 °C in pH 8 borate buffered saline (BBS), and yielded >90% re-bridging of the Fab regions. Analysis by LC-MS showed that 41% was half-antibody, and 49% was correctly bridged full-antibody. The DVP linker did not react with an unreduced trastuzumab Fab, even after 2 h at 37 °C, demonstrating an exclusive reactivity towards free thiols.

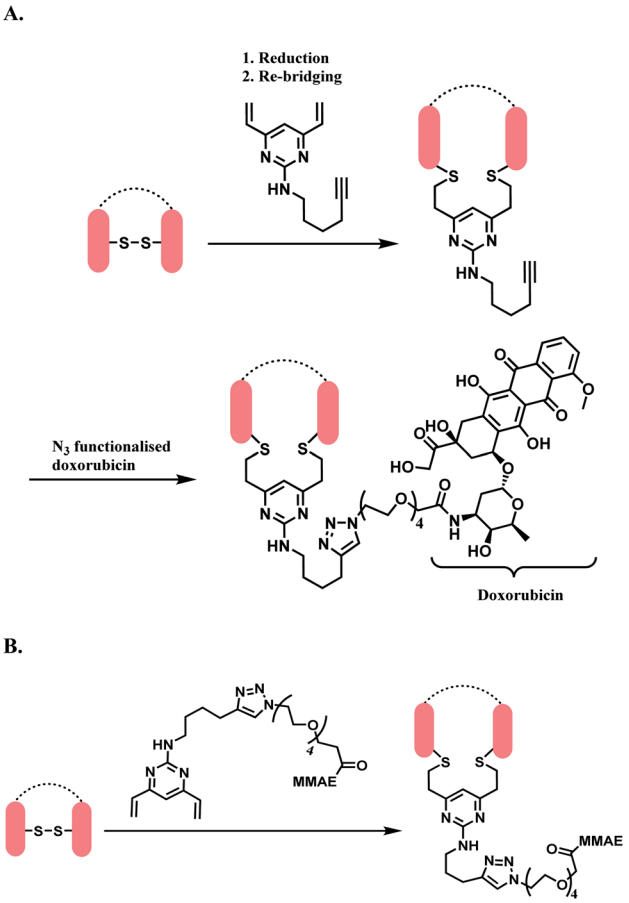

Scheme 31 DVP as a disulfide rebridging linker; (A) conjugation of linker to antibody, followed by the attachment of drug payload; (B) conjugation of DVP linker-payload moiety to antibody.

The DVP linker could either be conjugated to an antibody as a synthetic handle for post-conjugation functionalization (Scheme 31A), or form a linker-payload moiety prior to antibody conjugation (Scheme 31B).

In Scheme 31A, the trastuzumab–DVP linker conjugate was reacted with an azide-functionalized doxorubicin in the presence of $CuSO_4 \cdot 5H_2O$, (3-hydroxypropyltriazolylmethyl) amine (THPTA) and sodium ascorbate, at 37 °C for 2 h. LC-MS and UV-vis analysis revealed a high conversion to an ADC with an average DAR of 4.0. In Scheme 31B, a reduced trastuzumab was reacted with the linker-payload moiety, DVP–PEG_4–MMAE (10 equiv. per disulfide). The reaction was carried out in 0.25 M Tris buffer, at 37 °C for 3 h. LC-MS analysis demonstrated >95% conversion to a half–antibody conjugate.

The correctly bridged DVP-MMAE ADC was tested against both HER2-positive and HER2-negative breast cancer cell lines and it was shown that it only shows cytotoxicity in HER2-positive cell lines, and that the DVP linker did not affect the cell-killing ability of MMAE.

2.3.3. Disulfide rebridging (3): 3-bromo-5-methylene pyrrolones (3Br-5MP). In 2020, Zhou and co-workers have reported 3-bromo-5-methylene pyrrolones (3Br-5MPs) as a disulfide rebridging reagent.[112] The mechanism of the reaction of 3Br-

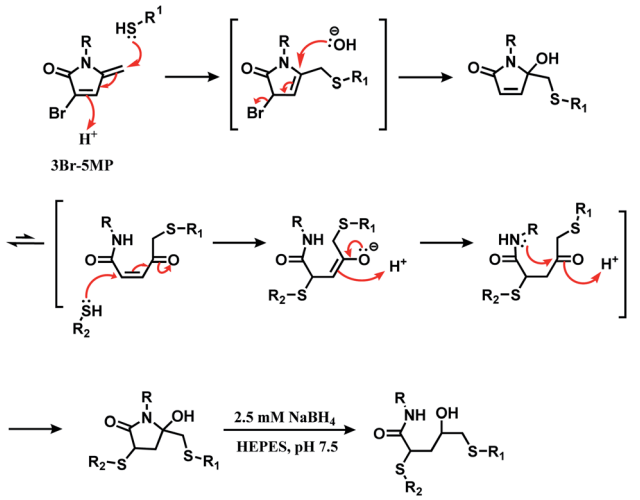

Scheme 32 Mechanism of the reaction of 3Br-5MP with two thiol groups.

5MP with two thiol groups is shown in Scheme 32. 3Br-5MPs were prepared facilely *via* a one-pot reaction from 4-bromofurfuryl acetate, and were stable in a relatively wide pH range from 6.0 to 9.5 over the course of a 5 day incubation.

Its reactivity as a disulfide rebridging agent was investigated on the endogenous hormone somatostatin (SST) and Fab fragment of goat anti-human antibody IgG. With SST, 1.3 equiv. of 3Br-5MP per reduced disulfide led to the rebridged product in a quantitative yield in HEPES buffer (pH 7.5) at 37 °C within 1 h. The rebridged product was a mixture of regioisomers, depending on which cysteine reacted first with 3Br-5MP.

The Fab fragment has one interchain disulfide bond, and 1.4 equiv. of 3Br-5MP-functionalised fluoroscein modified the reduced Fab fragment within 1 h at 37 °C. The degree of labelling determined by UV-Vis spectrum showed was 1.1 approximately. The modified fragment and the intact Fab fragment migrated to the same place on SDS-PAGE gel analysis.

2.3.4. Disulfide rebridging (4): arylenedipropiolonitrile (ADPN). Wagner and co-workers expanded their initial work on 3-arylpropiolonitrile (APN) (Section 2.2.8) to generate a disulfide rebridging linker. By having a second propiolonitrile functional group on the phenyl ring *meta*-to the first one, a bis-reactive arylenedipropiolonitrile (ADPN) was formed.[143] In a comparative study of *ortho*-, *meta*- and *para*-isomers of ADPN using reduced trastuzumab, it was demonstrated that only *meta*-ADPN yielded no free heavy or light chain fragments after it was incubated with reduced trastuzumab for 12 h. Thus, the *meta*-ADPN was chosen for the preparation of new ADCs.

Two ADCs were prepared in this study-both consist of trastuzumab (T), ADPN, a galactoside (Gal) and monomethyl auristatin E (MMAE), with one ADC containing an additional short PEG linker (PEG_4). For trastuzumab, its interchain disulfide bonds were reduced after incubation with 5 equiv. of TCEP in PBS at 37 °C. After ADPN–Gal–MMAE and ADPN–PEG_4–Gal–MMAE fragments were synthesized, the resultant products were incubated with reduced trastuzumab for 12 h at 25 °C separately. The average DAR values obtained for T–ADPN–Gal–MMAE and T–ADPN–PEG_4–Gal–MMAE were 4.5 and 4.0 respectively. An *in vitro* cytotoxicity assessment of the new ADCs on SK-BR-3 HER2-positive and MDA-MB-231 HER2-negative cancer cell-lines showed that both ADCs strong activity on HER2-positive cancer cells with IC_{50} values that are comparable to FDA-approved T-DM1. Both T–ADPN–Gal–MMAE and T–ADPN–PEG_4–Gal–MMAE were more potent towards MDA–MB–231 HER2-negative cancer cells than T-DM1.

2.3.5. Disulfide rebridging (5): 3,3-Bis(bromomethyl)oxetane. Bernardes and co-workers have grafted a four-membered oxygen ring (oxetane) into native peptides through disulfide conjugation with 3,3-bis(bromomethyl)oxetane.[144] Oxetane is a commonly found structural motif in pharmaceuticals due to its ability to influence on parameters such as lipophilicity and aqueous solubility.[145]

The disulfide rebridging with 3,3-bis(bromomethyl)oxetane was applied on somatostatin, octreotide, Fab arms of trastuzumab, DesA-Aß, and CRM_{197}. Somatostatin is a homing peptide used in Lutathera™, a peptide–drug conjugate (PDC) for the treatment of gastroenteropancreatic neuroendocrine tumours (GEP-NETs),[146] and octreotide (Sandostatin™) is used to treat acromegaly.[147] Both polypeptides contain one disulfide bond. After the reduction with TCEP, reacting the peptides with 1.2 equiv. of 3,3-bis(bromomethyl)oxetane in a 1 : 9 mixture of DMF/H_2O at 25 °C yielded the grafted cyclic peptides (yield > 70%) after 12 h. Both resulting peptides showed a similar affinity against this receptor somatostatin receptor 2 (SSTR2) to the unconjugated peptides, and the oxetane-grafted somatostatin had an improved binding property with a 4-fold increment in K_D value.

The oxetane-stapled Fab–trastuzumab was stable under reducing conditions and in human plasma, unlike the disulfide native antibody. In addition, bio-layer interferometry (BLI) experiments showed that the oxetane-stapled Fab fragment had a higher binding affinity to the HER2 receptor than the native antibody. DesAb-A$ß_{3-9}$-1, which targets the region 3–9 of human Amyloid-β (Aβ42) peptide, has a hindered intra-domain disulfide bond. By reacting the reduced antibody with 20 equiv. of 3,3-bis(bromomethyl)oxetane at 37 °C for 3 days, a complete conversion to the disulfide-rebridged antibody was achieved. The oxetane grafted antibody had a slightly increased flexibility.

CRM_{197} is used as a carrier protein for vaccines, for epitope presentation.[148] The *in vivo* study showed that the antibodies generated by the oxetane-stapled CRM_{197} had a 3-fold higher avidity (avidity index = 0.8 : 0.4 M) for the protein antigen compared to the intact CRM 197 (avidity index = 0.3 : 0.1 M).

While this work did not involve post-functionalisation or synthesis of a linker construct incorporating functionalised molecules (*e.g.* cytotoxins), the oxetane grafting was applied on a diverse range of therapeutic proteins, and the biological activity of the resulting protein–oxetane conjugates were analysed *in vivo*. Such research results provide valuable insights into the effect of covalent re-bridging of disulfide bonds on therapeutic biomolecules.

2.3.6. Disulfide rebridging (6): dichlorotetrazine. 3,6-Dichloro-1,2,4,5-tetrazine undergoes two successive

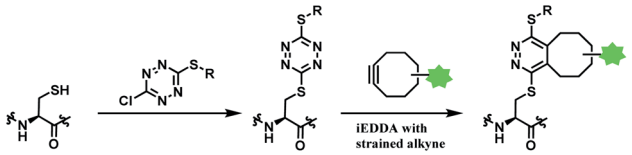

Scheme 33 Using dichlorotetrazine as a disulfide conjugation reagent, with post-functionalisation *via* iEDDA.

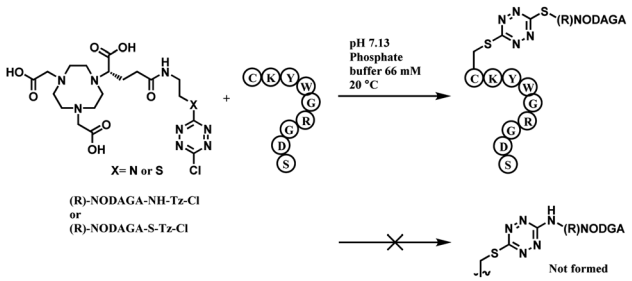

Scheme 34 Reaction between (*R*)-NODAGA–X–Cl (X = S or NH) and peptide.

nucleophilic aromatic substitutions with thiol groups.[149] Goncalves and co-workers have presented it as a dual labelling linker for cysteine residues, which is eligible for post-functionalisation through inverse-electron-demand Diels–Alder (iEDDA).[150] The overall strategy is shown in Scheme 33.

Monosubstituted chlorotetrazine, (*R*)-NODAGA–*S*-tetrazine–Cl, was reacted with two model peptides, Ac-CKYWGRGDS-NH_2, and Ac-MKYWGRGDS-NH_2 to investigate the chlorotetrazine linker's cysteine selectivity (Scheme 34). 3 equiv. of (*R*)-NODAGA–*S*-tetrazine–Cl linker conjugated to the cysteine residue of Ac-CKYWGRGDS-NH_2 (20 μM) within 1 min at room temperature in pH 7.13 phosphate buffer, leading to full conversion. The *S*-tetrazine–Cl linker did not react at all with the other peptide with no cysteine, demonstrating its high selectivity towards cysteine. (*R*)-NODAGA–NH-Tz–Cl did not lead to conjugation with both peptides at biocompatible temperature. The necessity to have a sulfur atom *para* to chloro-highlights the dichlorotetrazine's potential as a double thiol conjugation linker.

The method was only applied on bovin serum albumin (BSA), not monoclonal antibodies. Disulfide reduction was not carried out, and in a slightly acidic buffer (pH 5.15), 10 equiv. of (*R*)-NODAGA–*S*-tetrazine–Cl was used to target a free thiol of Cys34. A mono-adduct was yielded after 1 h at room temperature. Post-functionalisation attached a fluorophore Sulfo-Cyanine5 (sulfoCy5) to the adduct, *via* iEDDA with a sufloCy5-bicyclo[6.1.0] nonyne (BCN). The iEDDA with BCN took 12 h at 37 °C and the protein recovery yield was 68%. The resulting BSA–sulfoCy5 conjugate was stable in human plasma at 37 °C for 48 h.

2.3.7. Disulfide rebridging (7): thiol–yne coupling. Thiol–yne coupling is a newly rising 'click' reaction and has been used widely in material science.[151] Thiol–yne reaction either proceeds through a radical process under UV irradiation or a nucleophilic addition with electrophilic alkynes (Section 2.2.7 phosphonamidate). Due to the lack of regioselectivity as a single thiol conjugation reagent, it is more useful for disulfide-rebridging.

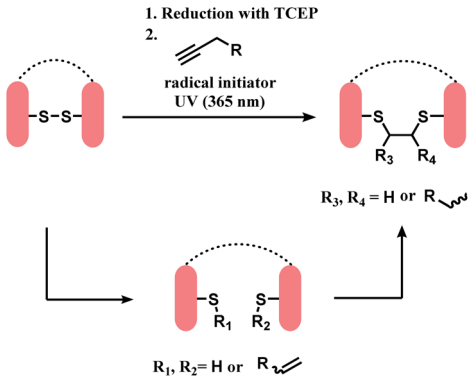

Scheme 35 Sequential steps of thiol–yne coupling to rebridge reduced disulfide.

In 2015, Bräse and co-workers have reported a direct insertion of an alkyne into a disulfide bond. After reduction of the disulfide bond with TCEP, thiol–yne reaction in a photochemical batch reactor, yielded the dithioether with 49% isolated yield as a mixture of diastereomers in about a 1 : 1 ratio. The solvent system in the reactor was water/methanol (v/v = 1 : 1).[152]

This method was applied on terlipressin and pressinoic acid, polypeptides with a single disulfide bond. After the reduction of the disulfide bond, the substrates were treated with 6-heptynoic acid, and the resulting mixture was then irradiated with UV-light (365 nm) of an LED UV-pen, in the presence of lithium phenyl-2,4,6-trimethylbenzoylphosphinate (LAP) as radical initiator. Both peptides yielded a mixture of two regioisomers, and each regioisomer existed in two diastereomers. LC/MS analyses showed that the thiol–yne reaction proceeds *via* a monoaddition of a thiyl radical on the alkyne in the first 1 h, and a subsequent intramolecular thiol–ene coupling between the alkene of the monoadduct and the second cysteine thiol group (Scheme 35). Sufficient reaction time of 3 h was needed to completely yield the desired bis-addition products.

Using this thiol–yne coupling, a disulfide bond in Fab fragment M14-G07 was successfully bridged with 6-heptynoic acid as the alkyne (1 equiv.) and LAP. The reaction was carried out over 4 h, and 20 mol% of LAP was added each hour of UV irradiation (4 × 20 mol%). However, the method was not applied on a full antibody. The concentration of the protein solution was shown to be critical, where a concentration lower than 46.1 mg mL^{-1} did not lead to the desired conjugation.

2.3.8. Disulfide rebridging (8): 2*H*-azirines-2-carboxamides. In addition to allenamide linkers for a single thiolate modification, Loh and co-workers also discovered the novel application of 2*H*-azirine-2-carboxamides as a bifunctional thiol linker under mild, metal-free conditions, while being atom-economical and possessing high selectivity.[153] The bioconjugation process of thiol-2*H*-azirine coupling occurs *via* a thiol addition onto 2*H*-azirines, with a subsequent ring opening to cleave of the C–N double bond present on 2*H*-azirine *in situ* and in a single step.

The optimal conditions for the diaddtion of thiophenol to 2*H*-azirine Ph(CNCH)CONH$_2$, forming the thiocetal products selectively over monothiol adducts, was determined to be performed with an 8.0 : 1.0 equivalence of PhSH and 2*H*-azirine respectively, in a cosolvent system of PBS and EtOH (v/v = 1 : 1) at pH 7.4 under nitrogen and 37 °C. Utilizing these conditions, various 2-substituted 2*H*-azirines, such as carboxylic acid, esters and amides showed efficient synthesis of the dithiol product. Further studies on the reactivity of 2-amide-2*H*-azirines concluded that aryls that have electron donating substituents, possesses a quaternary carbon, are heterocyclic-, napthalenyl-, or cyclohexyl-substituted yielded the desired product, except for the aryls with electron withdrawing substituents which remain unreacted. On the other hand, coupling reactions with alkyl dithiols, napthalenyl- and heterocyclic substituted thiols proceeded smoothly to yield the desired thioacetals. Similarly, thiolphenols that possess electron rich groups gave a higher yield of thiolacetals than electron deficient groups, whereas those with active hydrophilic amino and hydroxyl groups achieved complete chemoselectivity without *N*- or *O*- adducts detected.

Lastly, the reactivity of cysteine derivatives with multiple 2*H*-azirines containing MeO, Cl and CN functional groups in solely aqueous PBS solvent at room temperature was investigated, and the most reactive methoxy 2*H*-azirine was subsequently used to couple with different peptides with free thiol moieties. Single cysteine residues generate dimerized thioacetals as the linkers function in a linchpin mode, while peptides having 2 cysteine residues will result in cyclic thioacetal adduct bridges. In both situations, it is selective to only to amino acids residues of thiol groups.

In general, the thioacetalization reaction pathway for 2*H*-azirine was proposed to undergo *via* an aziridine intermediate, specific to thiol functional groups.

2.3.9. Disulfide rebridging (9): dichloroacetophenone. In order to reduce potential harmful by-products with the use of 2*H*-azrines linkers, and to improve atom efficiency and the number of synthetic steps for ADCs, Loh and co-workers presented α,α-dichloroacetophenone as a disulfide bridging linker.[154] This method was proposed to be environmentally friendly and chemoselective towards cysteine residue and can occur under physiological conditions. Even in the presence of other nucleophiles, this disulfide bridging method is highly effective in targeting functionalised thiol substrates, cysteine for instance. The optimal reaction condition for the di-thiol conjugation with dichloroacetophenone is performed under a cosolvent system of 0.2 M pH 7.6 PBS buffer and 10% aprotic solvent, such as DMSO and CH_3CN, at near room temperature of 30 °C to give the disulfide bridged product with a high yield of >90%. It was also investigated that the nature and the position of the substituents on the phenyl ring of dichloroacetophenone affected the reactivity of the coupling reaction. Electron withdrawing substituents on the *para*-position of dichloroacetophenone were concluded to be favoured. Further investigations also reported that the preferred thiol would be that with an ester group on the α-position, and one that undergoes intramolecular disulfide bridging rather than intermolecular.

The strategy was applied onto 2 different peptides, lanreotide and *N*-Ac-oxytocin. Disulfide reduction was first performed with tris[2-carboxyethyl]phosphine (TCEP, 1.1 equiv.) for 30 min to release two free thiol groups derived from cysteine residues. They are then subjected to the dichloroacetophenone substrate for 2 h at 15 °C, in NH_4HCO_3 (0.1 M) buffer solution and MeCN (10%, v/v). Both the peptides were able to successfully produce the respective disulfide bridged conjugates.

2.4. Tyrosine functionalisation

Tyrosine residues are attractive conjugation targets, as the reactivity of the phenol substituent is mostly orthogonal to that of cysteine or lysine. In addition, tyrosine residues are often partially buried in the surface of the proteins, because of the amphiphilic nature of the phenolic group[155] with the hydroxyl group being solvent exposed. Appearing relatively scarce on protein surfaces, one of several tyrosine residues could be targeted selectively through a proper linker molecule design. While this provides an attractive alternative to lysine or cysteine-targeting strategies with a higher homogeneity of resulting conjugates, it can be translated as lack of conjugation sites. This can deter the oncological application of ADCs, as the drug loading less than 4 was observed to give less potent antitumor effects.[156] However, tyrosine conjugated ADCs could be applied in non-cancer indication, such as human immunodeficiency virus (HIV) infection. This shows the wide applicability of tyrosine conjugation methods in ADC, beyond oncological drugs.

Despite its potential, only a relatively small number of biocompatible transformations have been developed, as shown in Scheme 36. Aside from the reactions covered in this section, palladium-catalysed *O*-alkylation of tyrosine by Trost allylation,[157] or metalloenzyme-catalysed tyrosine conjugations[158–160]

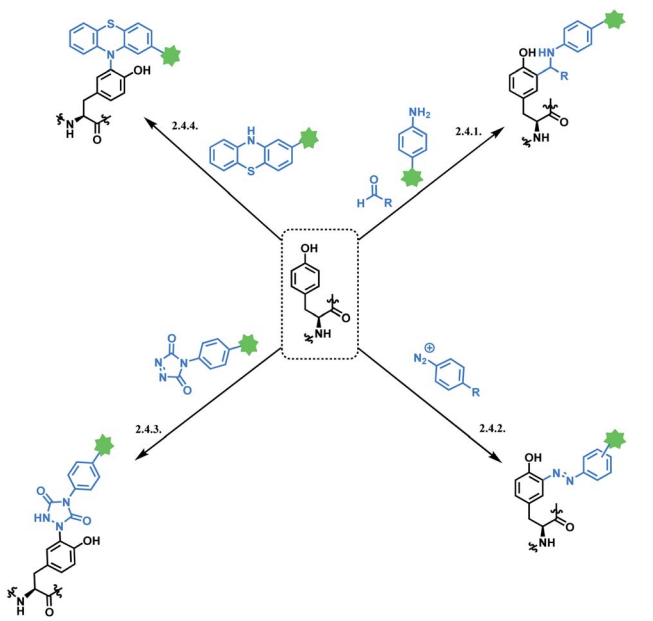

Scheme 36 Tyrosine conjugation methods.

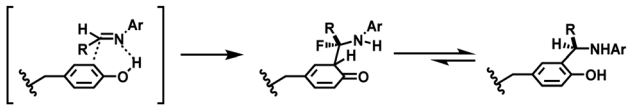

Scheme 37 Reaction between tyrosine and *in situ* generated imine.

are reported. However, they involve toxic transition-metal ions and therefore, will not be reviewed.

2.4.1. Tyrosine conjugation (1): Mannich-type three component reaction. The Mannich-type electrophilic aromatic substitution reaction reported by Francis and co-workers in 2004 has revealed the presence of a solvent-accessible tyrosine residue on the protein surface, thereby serving as a proof-of-concept for tyrosine-selective bioconjugation.[161] Tyrosine residue (1 equiv.) reacts with imine which is *in situ* generated from formaldehyde (1250 equiv.) and electron-rich aniline (1250 equiv.), and it is proposed that a cyclic transition state occurs in which the phenolic group donates a hydrogen bond to the imine nitrogen, thereby increasing the nucleophilicity of the phenol (Scheme 37).

The method selectively conjugated a fluorescent rhodamine dye with various proteins, including chymotrypsinogen A, lysosome and RNase A, within 18 h in pH 6.5 0.1 M phosphate buffer at room temperature. Chymotrypsinogen has four tyrosines in the primary sequence,[162] and it has been shown that 34% of chymotrypsinogen A molecules were unconjugated. Of the other 66%, only one tyrosine residue was conjugated to the dye. They further expanded the scope to the conjugate of chymotrypsinogen A and short peptide sequences with useful properties, such as aniline-terminated Myc, FLAG epitopes, an HIV-Tat derived peptide and sequences that bind terbium(III) ions or nucleate gallium arsenide nanocrystals.[163] The protein labelling with these peptides was carried out at physiological temperature 37 °C for 20–24 h.

The chemoselectivity of this three-component coupling was explored with isotopic labelling and nuclear magnetic resonance (NMR)-based studies.[162] It was revealed that side reactions between reactive formaldehydes and the nucleophilic indole ring of tryptophan residues occurred. Aside from this selectivity aspect, it should also be noted that no reactivity has been observed for horse heart myoglobin, a protein that has relatively low number of surface-accessible tyrosine residues. Furthermore, a relatively long reaction time (20–24 h) and the requirement of a large excess of coupling reagents make this method less attractive.

2.4.2. Tyrosine conjugation (2): diazonium salt. A tyrosine labelling strategy to use diazonium salts was done by Francis and co-workers in 2003, where tyrosine moieties in the internal shell of the MS2 bacteriophage were reacted with 4-nitrobenzenediazonium salts (Scheme 38A).[164] It should be noted that the research group has grafted the already-existing concept of diazonium salt onto novel protein conjugation strategy. An excess amount of diazonium salt (5 equiv.) was required, and the coupling was achieved within 15 min at pH 9 and 4 °C, with the conversion rate higher than 95%.

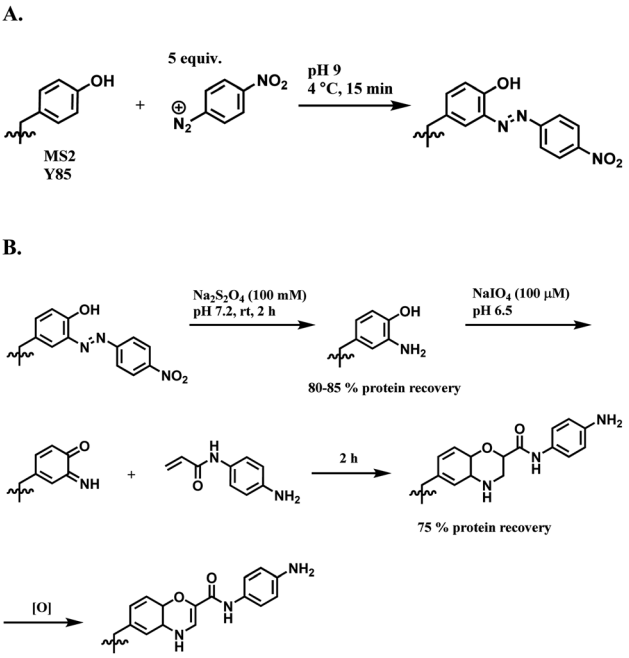

Scheme 38 (A) Reaction of 4-nitrobenzenediazonium salt with tyrosine linings of MS2 bacteriophage; (B) post-functionalisation of the resulting *o*-imino-quinone conjugate.

The nitro substituent in the diazonium salt reagent was irreplaceable in the reaction, thus limiting the substrate scope. Therefore, the reactive functional group *o*-imino-quinone was introduced by redox reactions (Scheme 38B) in order to react with another exogenous moiety, acrylamide, through a novel hetero-Diels–Alder reaction. After the reaction with acrylamide, 75% of the MS2 was recovered.

In later work, Francis and co-workers used 35 equiv. of diazonium salts to selectively label tyrosine residues in the exterior protein shell of the tobacco mosaic virus (TMV).[165] In this work, they reported a decrease in the efficiency of diazonium coupling to TMV, from >90 to ~30%, by replacing the *para*-substituent of the diazonium salt from NO_2 group to a less electron withdrawing $C(O)NH_2$ (Scheme 39).

This strategy to use diazonium salts was accommodated by many other research groups and brought significant developments in tyrosine bioconjugation. In 2012, Haddleton and co-workers selectively conjugated monomethoxy poly(ethylene glycol)s (mPEGs) to tyrosine residues of [D-ala2] leucine enkephalin (enkeph) and salmon calcitonin (sCT), by using

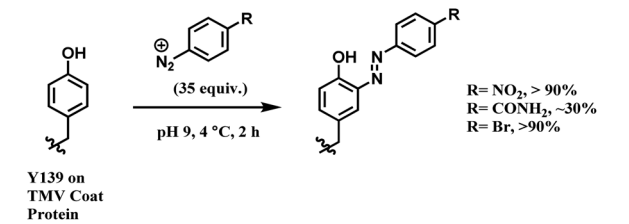

Scheme 39 Varying yields of diazonium salt labelling of tyrosine based on the *para*-substituent of the diazonium salt.

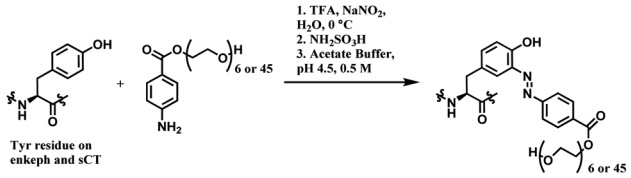

Scheme 40 Synthetic strategy to label tyrosine residue with *in situ* generated diazonium salt.

diazonium derivatives as coupling agents (Scheme 40).[166] The pH was adjusted to 4 for this PEGylation reaction, not 9. This was to prevent diazonium derivatives from reacting with other nucleophilic amino acids. Tryptophan has been reported to react efficiently with diazonium salts such as 3-diazonium-1,2,4,-triazole (3-DT) at pH lower than 3. A general trend for the N-nucleophiles (Lys, Arg, and N-terminal amine) is that with lower pH, higher proportions of the nucleophilic nitrogen centres will be in their protonated form, which is non-reactive toward electrophilic reagents such as diazonium salt derivatives. Therefore, the pH of the reaction medium was adjusted to 4, where tyrosine residues could react to diazonium salts selectively.

Instead of using diazonium salts directly, aniline-terminated polymers were generated and converted to the required diazonium derivatives *in situ*, by trifluoroacetic acid and $NaNO_2$ at 0 °C, during the peptide conjugation. The pH was then adjusted to 4.5 with 0.5 M acetate buffer, and the reaction was carried out for 24 h. With the 10 equiv. of diazonium derivatives, enkeph and sCT, both containing a single tyrosine residue, yielded mono-adducts. At pH 7, cross-reactivity with His, N-terminal amine, and Lys in sCT was observed. When the number of PEG groups in the diazonium derivative linker molecule was increased from 6 to 45, a longer reaction time of 56 h, and a higher molar equivalence (20 equiv.) were required to yield 78% conversion ratio with sCT.

In the same year, Barbas and co-workers reported that 4-formylbenzene diazonium hexafluorophosphate (FBDP) selectively reacts with tyrosine residues of trastuzumab antibody in 0.1 M phosphate buffer pH 8, within 30 minutes at room temperature (Scheme 41).[167] An excess amount of FBDP (10 equiv.) was required. With the aldehyde functionality instead of nitro group at 4-position, the introduction of payloads was easier. The aldehyde tag was then modified with 20 equiv. of biotin–oxyamine (pH 6.0, 4 °C). Each trastuzumab molecule was found to have an average of 1.8 biotin tags.

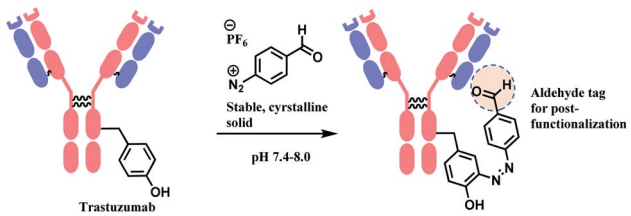

Scheme 41 Labelling tyrosine residues of trastuzumab with 4-formylbenzene diazonium hexafluorophosphate (FBDP).

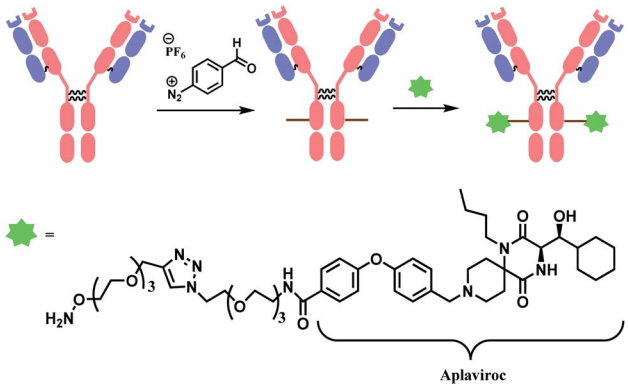

Scheme 42 Formation of mAb–aplaviroc conjugate.

In 2013, the research group used the same method to produce trastuzumab–aplaviroc conjugates, as well as conjugates with broadly neutralizing antibodies (Scheme 42), and tested them in HIV cell line.[168] Aplaviroc is CCR5 antagonist developed for the treatment of HIV infection.[169] It was found that 1 aplaviroc moiety was loaded per trastuzumab molecule on average. With broadly neutralising monoclonal antibodies (BNmAbs b12, 2G12, PG9, PG16) and CD4-IgG, a relatively homogenous DAR value of 0.5 to 2 was observed. The PG9–aplaviroc conjugate was tested against a panel of 117 HIV-1 strains and was found to neutralise 100% of the viruses.

2.4.3. Tyrosine conjugation (3): 4-phenyl-3*H*-1,2,4-triazole-3,5(4*H*)-dione (PTAD). In 2009, Barbas and co-workers have established an efficient click-like tyrosine ligation with cyclic diazodicarboxamide derivatives, 4-phenyl-3*H*-1,2,4-triazole-3,5(4*H*)-dione (PTAD) in mild aqueous media.[170] In sodium phosphate buffer, pH 7/acetonitrile (1 : 1), 2.5 equivalents of PTAD was reacted with a tripeptide containing Tyr within 30 min at room temperature to provide the conjugate in 85% yield. It was shown that aqueous conditions played a critical role, and that the reaction could not proceed in pure organic solvent. In the chemoselectivity study, PTAD was shown to react with trytophan and lysine as well. However, unlike tyrosine, tryptophan reacted with PTAD equally sluggish in organic solvent or in mixed aqueous media.

PTAD labelling was further studied with chymotrypsinogen A, bovine serum albumin (BSA) and horse heart myoglobin, in pH 7.4 phosphate buffer with a minimal amount (1–5%) of DMF. The conjugation efficiency (yield) was dependent on the protein type, and the electronic properties of the PTAD reagent.

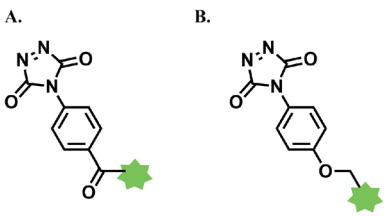

Fig. 12 PTAD reagents substituted with (a) electronically poor moieties; (b) electronically rich moieties.

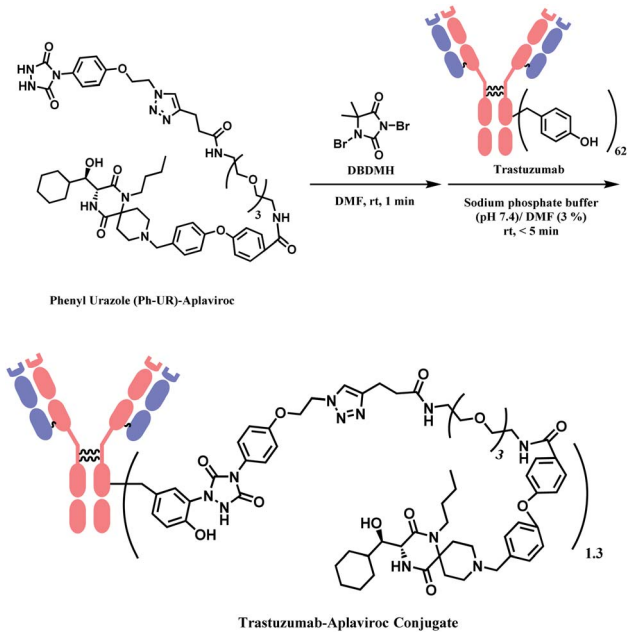

Scheme 43 Generation of trastuzumab–aplaviroc conjugate with the DAR of 1.3.

With an electron withdrawing group adjacent to the phenyl ring in PTAD (Fig. 12A), 60% of chymotrypsinogen A, 68% of BSA, and 16% of myoglobin were labelled. With the –OR group substituted PTAD (Fig. 12B), 81% of chymotrypsinogen A, 96% of BSA, 6–8% of myoglobin were labelled with the payload. In the substrate scope expansion done by the same research group suggested that an electron donating substitution on the phenyl ring in PTAD provides stability in water without compromising electrophilicity towards the phenol group of tyrosine.[171] In the further study, the research group selectively PEGylated tyrosine residues in chymotrypsinogen with 10 equiv. of PTAD-PEG within 30 min at room temperature, in pH 7.4 buffer. There are 4 tyrosine residues present in chymotrypsinogen, and mono-PEG adducts were produced predominantly.

Tyrosine click reaction with PTAD was further expanded to the synthesis of ADC of trastuzumab and aplaviroc (Scheme 43). An excess of phenyl urazole (Ph-Ur)-aplaviroc was oxidised by 1,3-dibromo-5,5-dimethylimidazolidine-2,4-dione (DBDMH) to produce the PTAD moiety, then immediately reacted with tyrosine residues of trastuzumab in 0.1 M phosphate buffer (pH 7) at room temperature, for less than 5 min. A trastuzumab mAb has 62 tyrosine residues in solvent-accessible regions, and the average DAR of the resulting trastuzumab–aplaviroc conjugate was 1.3. The neutralization activity and IC_{50} value of this conjugate were very similar to those of aplaviroc alone.

There are limitations of this conjugation method. Firstly, PTAD was shown to be stable in acetonitrile but to easily decompose in water to form isocyanate, an active electrophile (Scheme 44).[172] The resulting isocyanate undergoes undesired side reactions with lysine residues and the N-terminus. Berti and co-workers at Novartis used the PTAD reagent to selectively label tyrosine residues on CRM_{197}, a protein carrier in vaccines, and observed that 38% of CRM_{197} was unmodified, 33% was a phenyl isocyanate–lysine conjugate, and only a trace amount was a desired, PTAD-tyrosine conjugated product.[173]

Barbas and co-workers attempted to resolve this issue by using *tris*-(hydroxymethyl) aminomethane (Tris) buffer (0.1 M). The primary amine of the Tris buffer scavenges the isocyanate. However, using even high concentrations of the Tris buffer was not always fully effective and amine groups modifications were still observed.[158] It should be noted that the decomposition itself lowers the reaction's atom economy, even if the undesired isocyanate can be removed. Using acetonitrile as a co-solvent to stabilize PTAD limits the expansion of this reaction to protein conjugations; adding acetonitrile to an aqueous solvent is reported to enhance the peptide–peptide hydrogen bonds, leading to the denaturation of proteins.[174,175]

In order to overcome these limitations, Gouin and co-workers devised a strategy to electrochemically activate Ph-Ur species in the presence of proteins (Scheme 45), rather than oxidising them by DBDMH.[176]

In this 'e-Y-Click' reaction, Ph-Ur undergoes anodic oxidation at 0.36 V (*versus* saturated calomel electrode as the reference electrode) in pure phosphate buffer without the isocyanate scavenger, and PTAD is gradually produced in the reaction system. Because the PTAD generated by anode oxidation reacts with tyrosine instantaneously, side reactions with nucleophilic residues and N-terminus *via* isocyanate formation can be suppressed. A relatively low potential 0.36 V allowed peptides and proteins to be labelled without severe oxidative damage. Using glucose oxidase enzyme (GOx) as the substrate, they confirmed that the enzymatic activity of GOx was not affected by tyrosine

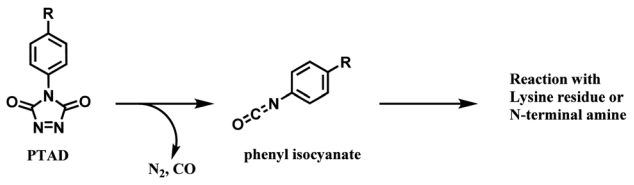

Scheme 44 Side reaction with amine groups *via* isocyanate generation.

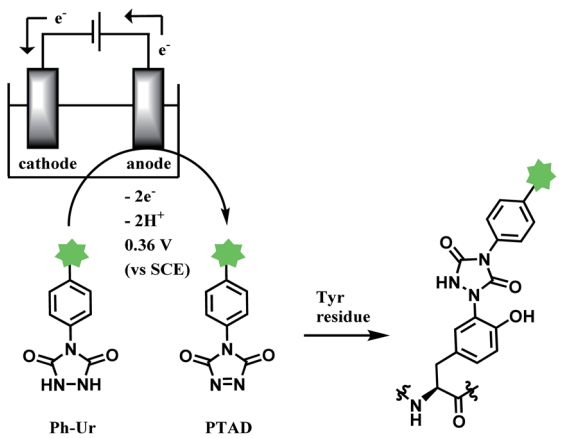

Scheme 45 e-Y-Click reaction.

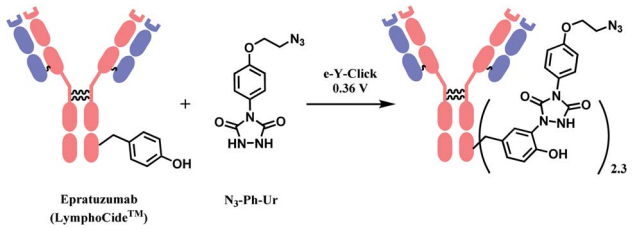

Scheme 46 Tyrosine conjugation of epratuzumab with N_3-Ph-Ur.

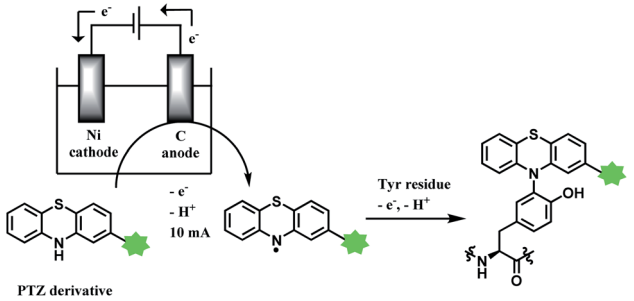

Scheme 47 Tyrosine-selective conjugation by PTZ derivatives.

labelling through the e-Y-Click reaction. This method was also applied in the antibody conjugation; 11.2 equiv. of N_3-Ph-Ur was reacted with epratuzumab (LymphoCide™), a humanized anti-CD22 mAb for the treatment of inflammatory autoimmune disease,[177] giving the conversion yield 95% within 2 h. The average Ph-Ur molecule loading per mAb was 2.3 (Scheme 46).

2.4.4. Tyrosine conjugation (4): phenothiazine. In 2019, Lei and co-workers identified a novel electrochemical anodic oxidation synthetic technique, that is metal- and additive-free, to enable the coupling of aromatic tyrosine amino acid residues with phenothiazine (PTZ) derivatives.[178]

The mechanism was proposed to proceed with an initial single-electron oxidation (SET) of PTZ, generating a nitrogen radical, and a subsequent site-selective addition of this radical to the *ortho*-position of the phenol ring on tyrosine residues (Scheme 47). As the *ortho*-positions are more electron rich as compared to the remaining *para*- and *meta*-positions, this favours the radical addition onto the *ortho*-position with excellent selectivity. With the optimized reaction conditions utilizing a graphite anode rod and a nickel cathode plate at a constant current of 10 mA for 75 min in Na_2SO_4 electrolyte and CH_3CN/H_2O (6.0 : 4.0 v/v ratio) at room temperature, protected tyrosine (1 equiv.) and an unsubstituted phenothiazine (1 equiv.) gave the product in an 85% yield. The solvent system with >50% CH_3CN was necessary.

In a further study, the group investigated the effects of various electron-withdrawing and electron-donating substituted phenothiazine and it was concluded that they were all decent substrates but relatively lower yields of 33–48% were obtained. Although the PTZ reagent is unreactive towards other aromatic amino acid residues, namely Trp, His and Phe, it is still able to react with cysteine residues probably due to it being able to be easily oxidized.

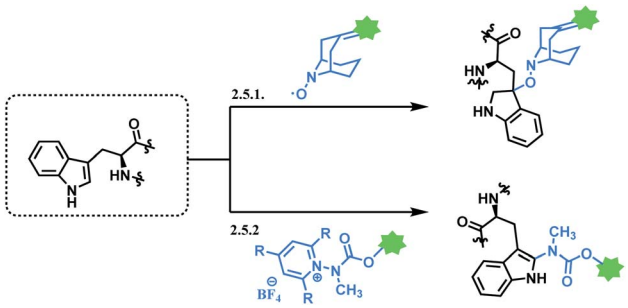

Scheme 48 Tryptophan conjugation methods.

The study also included the synthesis of PTZ-modified unprotected polypeptides from 5-mers to 29-mers Tyr-containing polypeptides, such as RGD peptide, acyclic pentapeptide and other endogenous peptides with biological activity. With the above optimized reaction conditions but in CH_3CN/PBS (1 : 1 v/v ratio), it was observed that phenothiazine chemoselectively conjugated to Tyr in 30 min at room temperature, even in the presence of other amino acid residues. Moreover, the research was extended to include insulin and myoglobin proteins and the results indicate a successful tagging of PTZ onto the Tyr residues.

2.5. Tryptophan functionalisation

There are only two reported methods which achieve tryptophan functionalisation without metal catalysts, in aqueous medium. They are summarised in Scheme 48.

2.5.1. Tryptophan conjugation (1): 9-azabicyclo [3.3.1] nonane-3-one-*N*-oxyl (keto-ABNO). In 2016, Kanai and co-workers have reported that a stable organoradical 9-azabicyclo [3.3.1]nonane-3-one-*N*-oxyl (keto-ABNO) selectively conjugates

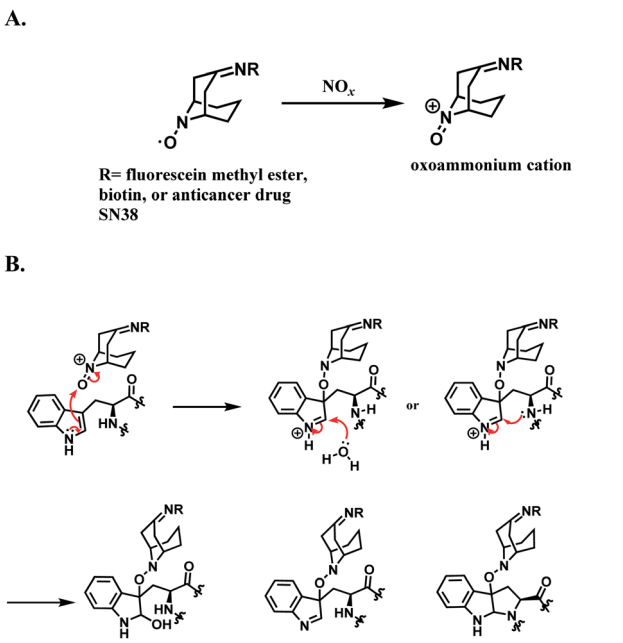

Scheme 49 (A) Oxidation of keto-ABNO by NO_x to generate oxoammonium electrophile; (B) proposed mechanism tryptophan conjugation with keto-ABNO.

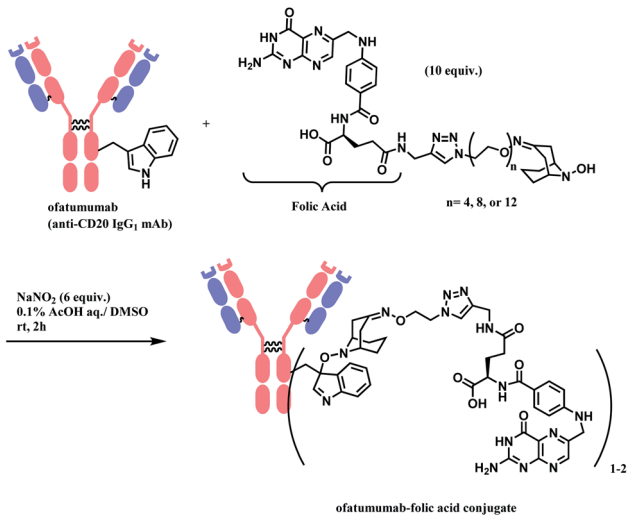

Scheme 50 Formation of ofatumumab-folic acid conjugate.

to tryptophan in the aqueous medium containing 0.1% acetic acid and $NaNO_2$. The conjugation was accomplished within 30 min.

Initially, keto-ABNO is oxidised to oxoammonium cation *via* disproportionation and oxidation by NO_x, which is generated from $NaNO_2$ and acetic acid (Scheme 49A). The enamine nucleophile in the indole ring of a Trp residue then attacks the oxoammonium, followed by the attack of H_2O or an adjacent nitrogen in the amide bond towards the resulting imine. This generates heterogenous products as shown in Scheme 49B.

The conjugation strategy was also applied to produce a conjugate of *anti-*$A\beta_{1-16}$ antibody (6E10) and fluorescein. Dot-blot assay showed that the binding ability of the antibody towards $A\beta$ was retained after ABNO labelling, demonstrating the method's high applicability in the ADC construction.

The research group expanded the scope of this tryptophan modification strategy by building an ofatumumab-folic acid conjugate with the keto-ABNO linker.[179] Folic acid is a ligand for cancer cells and ofatumumab is a CD20-targeting mAb. The resulting conjugate showed an antibody-dependent cellular cytotoxicity (ADCC) and induced an enhanced cytotoxic activity of natural killer (NK) cells against folic receptor-α positive cancer cells. 10 equiv. of ABNO-PEG-folic acid reagent in the presence of $NaNO_2$ and acetic acid yielded the degree of labelling of folic acid of 1–2 (Scheme 50).

2.5.2. Tryptophan conjugation (2): N-substituted pyridinium salts. In 2020, Taylor and co-workers have reported the photoconjugation of Trp, within 30–75 min in pH 6.9 NH_4OAc buffer.[180] It occurs *via* a photoinduced electron transfer (PET) with pyridinium salt, a subsequent fragmentation of pyridinium N–N bond and a simultaneous transfer of the group to Trp. This technique provides precise modification of Trp residues with a myriad of useful functional groups. Photoconjugation offers a supportive strategy to catalytic methods, employing mild labelling conditions and short reaction times, while acquiring advantage over the other amino acids for competition over site selectivity.

Simultaneous PET coupling and Trp labelling can be achieved with the utility of a Katritsky-type N-substituted pyridinium salt that possesses a carbamate label. The pyridinium salt having a positively charged π-electron system enables reduction *via* single electron transfer, while varying the substituents on the pyridinium ring and the substituted N atom facilitates homolytic cleavage of the reactive N–N bond. As such, the aromaticity of the pyridinium ring will be restored, and the corresponding radical species produced are reactive for a subsequent formation of bond. N-substituted pyridinium salt triggered by the single electron reductant Trp forms an N-centred and a positively charged Trp radicals, which then both recombine to give a selectively labelled Trp.

This selective labelling process is kinetically feasible and at the same time, prevents photodegradation especially when done in the optimised conditions with NH_4OAc buffer, UV-B light and in 1 mM of glutathione (GSH) to yield a complete conversion >95% (mono/di label ratio > 20 : 1). GSH functions as a reactive oxygen species (ROS) scavenger to promote the reaction restrictedly on the Trp residue for modification, where both the labels are found on Trp. On the other hand, the 2,4,6-tri-methylated pyridinium ring helps to prevent nucleophilic addition and thus, more stable and less prone to decomposition. Furthermore, with the carbamate functional group present on the pyridinium salt, it allows the salt to be derivatisable with other useful functional groups and subsequently, easily transferred onto Trp. These factors contribute to the high conversion of selective Trp labelling in moderately photolabile proteins, the exclusive reactive site, even in the presence of other amino acids of contrasting topologies and redox/photoionization potentials.

However, in a more photolabile protein (14.3 kDa) with many redox active residues, the undesired cys-glutathionylated products are observed as a result of thiyl radical exchange or TCEP reduction of disulfides in close vicinity to [Trp]*. Nonetheless, intraprotein PET degradation can be avoided by ensuring that the donation of a radical from Trp to an excited pyridinium salt is the primary route, which is achieved with a phenyl-substituted pyridinium salt, to produce a >90% conversion of 6 : 1 mono/di labelled conjugation, and a higher GSH concentration for irradiation not surpassing 320 nm.

Overall, PET is the key mechanism propelling the reaction of Trp labelling forward based on observations and results. Complete deuteration experiments of Trp at C4-position indicate that initiation of the reaction is due to the photoexcitation of Trp and pyridinium salt, while the quantum yield indicates that the mechanism consists of [Trp]* as the electron source for transfer. Additionally, the NMR data proves that labelling does not involve the methyl group of the indole, but at the C2-position *via* a formation of C–N bond. Precomplexation and amination mechanisms for Trp selectivity were ruled out as such behaviours are also displayed in phenylalanine and tyrosine.

2.6. Methionine functionalisation

Protein conjugation methods traditionally rely on the nucleophilicity of amino acid residues. Thus, methionine has not been a popular target for conjugation, as the thioether (-S-CH_3) side

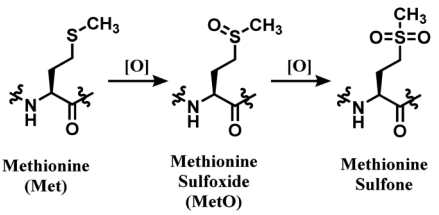

Scheme 51 Oxidation of methionine residue.

chain has a relatively weak nucleophilicity.[181] Moreover, with its hydrophobic side chain, methionine is mostly found buried in proteins, which makes it difficult to modify with labelling reagents.[182]

However, being an important cellular antioxidant, methionine is readily oxidised, rendering it susceptible to a modification *via* redox reactivity.[183] It should be noted, however, that the oxidation of methionine to methionine sulfoxide (MetO) is a major oxidative degradation pathway of IgG1 monoclonal antibodies.[184] When oxidised to MetO, the apolar chain transforms into a highly polar one, causing a disruptive change in the ternary structure of protein (Scheme 51). Thus, an important criterion for a methionine labelling agent is to be able to conjugate functional molecules to a methionine residue without forming MetO, while exploiting the redox reactivity.

An overall summary of reported methionine conjugation methods is shown in Scheme 52.

2.6.1. Methionine conjugation (1): oxaziridine. In 2017, Chang and co-workers have reported a strategy to use oxaziridine-based reagent for chemoselective methionine bioconjugation through redox reactivity.[185] The oxidation of thioethers with oxaziridine reagents provided the basis for bio-inspired strategy to form stable protein-bound sulfoximines under biocompatible conditions. This bioconjugation method, also known as redox activated chemical tagging (ReACT), was initially performed on sulfur imidation reactions with oxidant-mediated oxaziridine (Ox) reagents. Such reaction using a cosolvent system of CD_3OD/D_2O (1 : 1) involving a strained oxaridine molecule (Ox1) managed to provide a 95% conversion of the desired sulfimide product (NTP) and the undesired sulfoxide compound (OTP) in a 5 : 1 ratio, without the presence of any catalyst in a short time frame of 2.5 min, observed with ^{1}H NMR. The selectivity of the reaction can, however, be improved by replacing the carbamate moiety in Ox1 to a weaker electron withdrawing urea moiety in Ox2 yielded the products NTP : OTP in a 12 : 1 ratio with a similar conversion rate of 93%. Increasing the water content in the cosolvent system CD_3OD/D_2O to 1 : 19, the NTP : OTP selectivity improved significantly to 18 : 1. This could be accounted for by the better stabilization of the transition state of the NTP alkoxy anion intermediate due to better hydrogen bonding and thus, solvation.

This method of methionine functionalization with the ReACT reagent displayed exceptional selectivity over its sulfur analogues. Even though cysteine and selenocysteine were observed to be oxidised, no NTP product was formed. However, in a further study of oxaziridine probe functionalization with Ox4 and a whole proteome, HeLa cell lysate, it was verified with LC-MS/MS that not only 235 methionine residues were labelled, but an additional lysine residue was also conjugated. Similarly, the methionine bioconjugation strategy was shown to be successful with bovine serum albumin (BSA) protein. It was done with a two-step approach utilizing BSA (15 μM) was conjugated through ReACT with the Ox4 oxaziridine probe (100 μM) consisting of a bioorthogonal alkyne group, which can then undergo a second conjugation with Cy3-azide *via* a copper-catalyzed azide–alkyne cycloaddition (CuAAC) reaction. In-gel fluorescence imaging revealed a >95% yield and that the ReACT modification underwent completion in 1–2 min. In a separate ReACT modification of calmodulin (CaM, 100 μM) with various alkyne- and azide-containing oxaziridine probe molecules (1 mM), it demonstrated selective conjugation on the entire 9 methionine residues present on the CaM protein with good selectivity of NTP : OTP (25 : 1). Experiments on a variety of biomolecules such as biotin and polyethylene glycol (PEG) were also successful.

Moving on to the synthesis of ADCs, ReACT modification was performed on an antibody fragment to a green fluorescent protein (GFP-Fab). However, as the existing endogenuous methionine residues are inaccessible from the surface, they were unable to be conjugated unless additional methionine sites are engineered on the surface. Supporting evidence from experiments which involve the methionine-substituted antibody fragment at surface-accessible positions of heavy chain (HC)-A114 or light chain (LC)-V205 residues reported effective oxaziridine labelling with ReACT. Furthermore, in the attempt of methoinine conjugation through ReACT of an engineered Herceptin–Fab (Her–Fab) conjugate, enabled to possess one or two methionine residues on its light chain at the C terminus, the respective methionine labelled products generated exhibited an excellent DAR ratio with good purity. Notably, the ADC which was then produced from a subsequent conjugation reaction of the Her–Fab, installed with an azide or alkyne handle from methionine conjugation, and MMAE displayed five

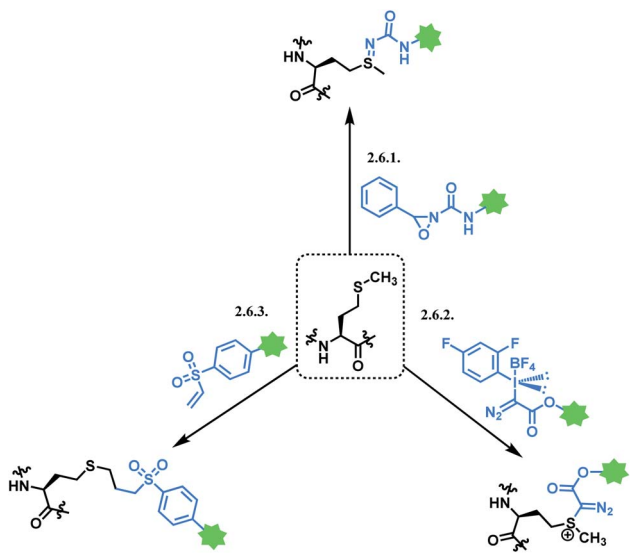

Scheme 52 Methionine conjugation methods.

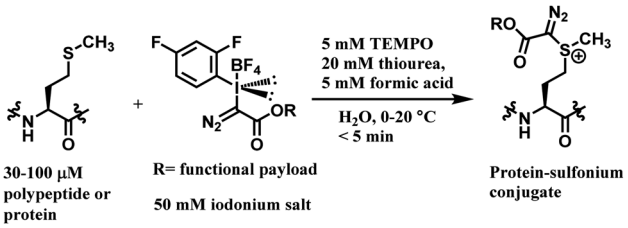

Scheme 53 Labelling methionine residue with hypervalent iodine reagent.

times more efficient toxicity to Her2-positive BT474 breast cancer cells, in contrast to the individual wild-type Her–Fab and free MMAE or when mixed.

2.6.2. Methionine conjugation (2): hypervalent iodine. Gaunt and co-workers have exploited the electrophilic reactivity of a hypervalent iodine to achieve a chemoselective labelling at methionine residues.[186] The conjugation was rapidly completed at a micromolar concentration of protein. The modification with the iodonium salt produces a high-energy conjugate equipped with reactive 'on-protein' groups that serve as a platform for post-functionalisation (Scheme 53).

The conjugation strategy was applied on exenatide (Byetta™), aviptadil, and tetracosactide, the therapeutic polypeptides with a single methionine residue. The addition of a low concentration of thiourea (20 mM) improved reaction kinetics, but it was accompanied by unselective modifications and oxidative by-products. 10 mM of TEMPO ((2,2,6,6-tetramethylpiperidin-1-yl) oxyl) and aqueous formic acid solution (5 mM, approximately pH 3) were required to minimise such side-reactions. The labelling happened almost instantaneously in water, with 500 equiv. to >1600 equiv. of the hypervalent iodine, at 0 to 20 °C.

Methionine residues on more complex protein systems such as teriparatide, α-lactalbulmin, aprotonin, and ubiquitin were also successfully labelled with the iodonium salt, with the conversion yields ranging from 84% to >95%. Teriparatide, containing two methionines, yielded a bis–sulfonium conjugate (di:mono-labelling ratio 12 : 1).

The resulting protein–sulfonium conjugate can undergo post-functionalisation *via* a photoredox radical cross-coupling with 2000 equiv. of *o*-tolyl Hantzsch ester. C-benzylation product is obtained with a good yield (Scheme 54). This radical–radical cross-coupling is orthogonal to native amino acids, and allows two distinct functionalities to be introduced sequentially at methionine residue. However, it must be noted that a transition metal catalyst (Ru(II)) was used for this secondary modification, which may deter the direct application in therapeutic protein modifications.

2.6.3. Methionine conjugation (3): lumiflavin-catalysis. Macmillan and co-workers have used lumiflavin (LF) photocatalyst under blue-light (Kessil, 440 nm) to achieve mild, selective and robust functionalisation of a methionine residue with various Michael acceptors.[187] The conjugation proceeds at 23 °C in PBS (pH 7.4)/DMF (19 : 1) at a micromolar concentration of proteins, and gives the conjugates with good conversion yields within 30 min. The 10 equiv. of lumiflavin and 200 equiv. of Michael acceptors relative to a protein system were required.

This method's selectivity towards methionine was tested with a wide range of peptides that do not contain methionine residues. The peptide substrates were recovered (>90%) with no conjugate product. However, thiol radicals generated from liberated cysteines readily underwent LF-catalysed Michael reactions.

It should be noted that iridium- and ruthenium-based complexes, the traditional metal-based photocatalysts, gave an undesired methionine sulfoxide (MetO), whereas lumiflavin did not, likely owing to its ability to act as a base in its radical anion form (LF^{-}). Followed by a single electron oxidation, the LF^{-} rapidly deprotonates the methyl group in sulfur radical cation

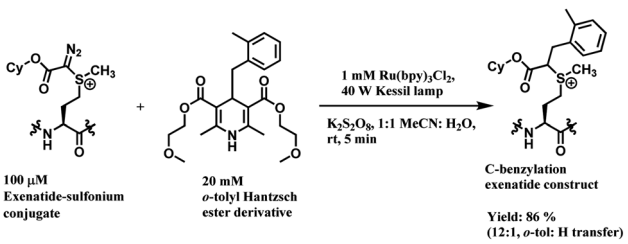

Scheme 54 Post-functionalisation *via* photoredox radical cross-coupling between the diazo sulfonium–protein conjugate and the C-4 substituted Hantzsch ester.

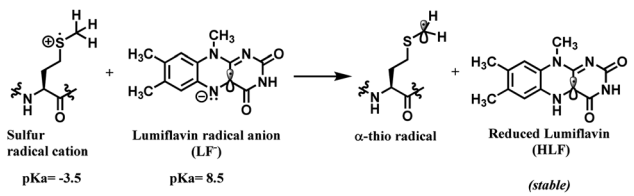

Scheme 55 Formation of α-thio radical from methionine radical cation *via* hydrogen abstraction by lumiflavin radical anion.

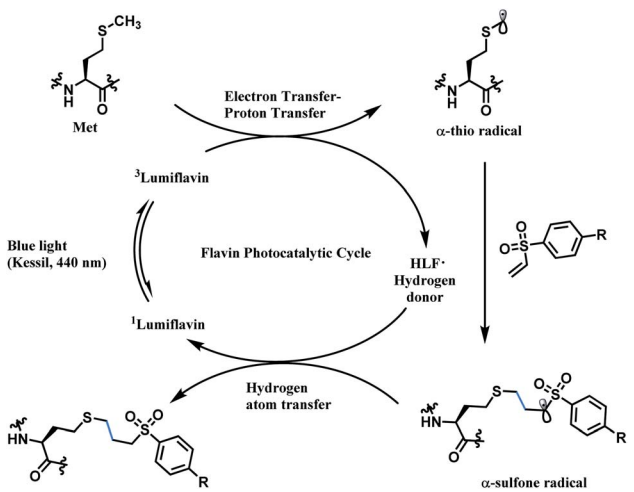

Scheme 56 Proposed mechanism of lumiflavin-catalysed methionine conjugation.

to generate α-thio radical, preventing the formation of MetO (Scheme 55).

The mechanism of lumiflavin-catalysed methionine conjugation is shown in Scheme 56. Lumiflavin, photoexcited to its triplet state ($E_{1/2}^{red}$ [^{3}LF/LF$^-$] = 1.5 V *vs.* SCE)[188] by blue-light, achieves a single-electron oxidation of the thioether. The α-thio radical then undergoes radical addition with the electrophilic alkene which has a high affinity towards SOMO, to generate α-sulfone radical. This radical intermediate is then reduced by HLF to give the methionine conjugate product, regenerating the ground state lumiflavin.

The conjugation strategy was applied on various functional proteins with different sizes, including aprotinin (6.5 kDa), α-lactalbumin (14.2 kDa), myloglobin (16.7 kDa) and enhanced green fluorescent protein. The fluorescence activity of enhanced green fluorescent protein (EGFP) was almost preserved (>95%) even after the methionine labelling, demonstrating this method's high applicability in biomolecule conjugation. No work on IgG monoclonal antibodies (~150 kDa)[189] was carried out.

Among many Michael acceptors, phenyl vinyl sulfones served particularly useful for post-functionalisation. A phenyl vinyl sulfone with an alkyne moiety in the R group was conjugated to EGFP with 45% conversion, and the conjugate subsequently undewent copper-catalysed alkyne–azide cycloaddition (CuAAC) with an azide-functionalised biotin or nonaarginine.

3. Summary and future outlook

In the era of immunotherapy, antibody–drug conjugate (ADC) is rising as a promising therapeutic modality. One attractive aspect of this modality is that a new linker leads to the registration of a new biologics entity in terms of intellectual property rights,[190] allowing a huge advantage in patent space and novelty.

Nanobodies,[191] non-Ig-Based protein scaffolds such as DARPins,[192] and peptide aptamers[193] are rising as alternatives to monoclonal antibodies with their competitive advantages (higher affinity binding, lower cost, and lower immunogenicity relative to mAbs). A wider toolbox of native amino acid conjugation methods which are orthogonal thus complementary to existing ones' synthetic scopes will open wider avenues to prepare biomolecule conjugates.

Orthodox bioconjugation methods are rooted in the nucleophilicity of substituents on amino acids and therefore, the functionalisation of non-nucleophilic amino acids, such as valine, leucine, or phenylalanine, remains a challenge. An extension of metal-free, rapid and aqueous synthetic methodologies in C–H activation will provide a wider pool of potential designs for antibody conjugation linkers.

While many reactions are reported for native amino acid functionalisation to produce antibody or protein–payload conjugate, only few has succeeded to do it in nearly 100% aqueous medium, within a short enough duration, without any potentially denaturing agents. Last but not least, atom-economy is highly important for the antibody conjugation efficiency. While disulfide rebridging linker is emerging as a promising approach to control Drug-to-Antibody Ratio (DAR), a recent preclinical study suggests that a strict control of DAR may not be the most critical factor in the therapeutic efficacy.[58] It seems that more thorough and detailed studies on different combinations of antibody, drug, linker's chemistry and conjugation site are required in order to better understand ADC's therapeutic profile. We envisage that antibody–payload conjugates will expand their indications beyond cancer, with the development of good linkers.

Author contributions

All of the authors participated in this review work. T. P. L. and M. S. K. proposed and designed the review. M. S. K., T. K., and J. K. prepared the draft. T. P. L. finally revised the review.

Conflicts of interest

The authors declare no competing financial interests.

Acknowledgements

We gratefully acknowledge the financial support from Distinguished University Professor grant, Nanyang Technological University, Singapore, and AcRF Tier 1 grants from the Ministry of Education of Singapore (RG11/20 and RT14/20). We thank Tianhu Li for his valuable insights and advice.

References

1 O. Koniev and A. Wagner, *Chem. Soc. Rev.*, 2015, **44**, 5495–5551.
2 P. Bross, J. Beitz, G. Chen, X. Chen, E. Duffy, L. Keiffer, S. Roy, R. Sridhara, A. Rahman, G. Williams and R. Pazdur, *Clin. Cancer Res.*, 2001, **7**, 1490–1496.
3 P. Hamann, L. Hinman, I. Hollander, C. Beyer, D. Lindh, R. Holcomb, W. Hallent, H. Tsou, J. Upeslacis, D. Shorchat, A. Mountain, D. Flowers and I. Bernstein, *Bioconjug. Chem.*, 2002, **13**, 47–58.
4 Y. N. Lamb, *Drugs*, 2017, **77**, 1603–1610.
5 R. A. de Claro, K. McGinn, V. Kwitkowski, J. Bullock, A. Khandelwal, B. Habtemariam, Y. Ouyang, H. Saber, K. Lee, K. Koti, M. Rothmann, M. Shapiro, F. Borrego, K. Clouse, X. H. Chen, J. Brown, L. Akinsanya, R. Kane, E. Kaminskas, A. Farrell and R. Pazdur, *Clin. Cancer Res.*, 2012, **18**, 5845–5849.
6 C. Deng, B. Pan and O. A. O'Connor, *Clin. Cancer Res.*, 2013, **19**, 22–27.
7 P. M. Challita-Eid, D. Satpayev, P. Yang, Z. An, K. Morrison, Y. Shostak, A. Raitano, R. Nadell, W. Liu, D. R. Lortie, L. Capo, A. Verlinsky, M. Leavitt, F. Malik, H. Aviña, C. I. Guevara, N. Dinh, S. Karki, B. S. Anand, D. S. Pereira, I. B. J. Joseph, F. Doñate, K. Morrison and D. R. Stover, *Cancer Res.*, 2016, **76**, 3003–3013.
8 D. P. Petrylak, A. V. Balar, P. H. O'Donnell, B. A. McGregor, E. I. Heath, E. Y. Yu, M. D. Galsky, N. M. Hahn, E. M. Gartner, J. Pinelli, A. Melhem-Bertrandt and J. E. Rosenberg, *J. Clin. Oncol.*, 2019, **37**, 4505.

9 E. D. Deeks, *Drugs*, 2019, **79**, 1467–1475.
10 L. Amiri-Kordestani, G. M. Blumenthal, Q. C. Xu, L. Zhang, S. W. Tang, L. Ha, W. C. Weinberg, B. Chi, R. Candau-Chacon, P. Hughes, A. M. Russell, S. P. Miksinski, X. H. Chen, W. D. McGuinn, T. Palmby, S. J. Schrieber, Q. Liu, J. Wang, P. Song, N. Mehrotra, L. Skarupa, K. Clouse, A. Al-Hakim, R. Sridhara, A. Ibrahim, R. Justice, R. Pazdur and P. Cortazar, *Clin. Cancer Res.*, 2014, **20**, 4436–4441.
11 J. M. Lambert and R. V. J. Chari, *J. Med. Chem.*, 2014, **57**, 6949–6964.
12 S. Modi, C. Saura, T. Yamashita, Y. H. Park, S. B. Kim, K. Tamura, F. Andre, H. Iwata, Y. Ito, J. Tsurutani, J. Sohn, N. Denduluri, C. Perrin, K. Aogi, E. Tokunaga, S. A. Im, K. S. Lee, S. A. Hurvitz, J. Cortes, C. Lee, S. Chen, L. Zhang, J. Shahidi, A. Yver and I. Krop, *N. Engl. J. Med.*, 2020, **382**, 610–621.
13 B. L. Staker, K. Hjerrild, M. D. Feese, C. A. Behnke, A. B. J. Burgin and L. Stewart, *Proc. Natl. Acad. Sci. U. S. A.*, 2002, **99**, 15387–15392.
14 Y. Y. Syed, *Drugs*, 2020, **80**, 1019–1025.
15 S. Lonial, H. C. Lee, A. Badros, S. Trudel, A. K. Nooka, A. Chari, A. O. Abdallah, N. Callander, N. Lendvai, D. Sborov, A. Suvannasankha, K. Weisel, L. Karlin, E. Libby, B. Arnulf, T. Facon, C. Hulin, K. M. Kortüm, P. Rodríguez-Otero, S. Z. Usmani, P. Hari, R. Baz, H. Quach, P. Moreau, P. M. Voorhees, I. Gupta, A. Hoos, E. Zhi, J. Baron, T. Piontek, E. Lewis, R. C. Jewell, E. J. Dettman, R. Popat, S. D. Esposti, J. Opalinska, P. Richardson and A. D. Cohen, *Lancet Oncol*, 2020, **21**, 207–221.
16 A. Lee, *Drugs*, 2021, **81**, 1229–1233.
17 T. Linke, M. T. Aspelund, C. Thompson, G. Xi, A. Fulton, M. Wendeler, T. M. Pabst, X. Wang, W. K. Wang, K. Ram and A. K. Hunter, *Biotechnol. Prog.*, 2014, **30**, 1380–1389.
18 R. J. Kreitman, *Hematology Am. Soc. Hematol. Educ. Program*, 2012, **2012**, 660–666.
19 S. Dhillon, *Drugs*, 2018, **78**, 1763–1767.
20 B. Leader, Q. J. Baca and D. E. Golan, *Nat. Rev. Drug Discovery*, 2008, **7**, 21–39.
21 R. M. Lu, Y. C. Hwang, I. J. Liu, C. C. Lee, H. Z. Tsai, H. J. Li and H. C. Wu, *J. Biomed. Sci.*, 2020, **27**, 1–30.
22 G. J. Weiner, *Immunol. Res.*, 2007, **39**, 271–278.
23 J. Christiansen and A. K. Rajasekaran, *Mol. Cancer Ther.*, 2004, **3**, 1493–1501.
24 J. M. Reichert, C. J. Rosensweig, L. B. Faden and M. C. Dewitz, *Nat. Biotechnol.*, 2005, **23**, 1073–1078.
25 H. M. Abdolahi, A. S. Asiabar, S. Azami-Aghdash, F. Pournaghi-Azar and A. Rezapour, *Asia-Pac. J. Oncol. Nurs.*, 2018, **5**, 57–67.
26 D. J. Craik, D. P. Fairlie, S. Liras and D. Price, *Chem. Biol. Drug Des.*, 2013, **81**, 136–147.
27 G. Von Minckwitz, C. S. Huang, M. S. Mano, S. Loibl, E. P. Mamounas, M. Untch, N. Wolmark, P. Rastogi, A. Schneeweiss, A. Redondo, H. H. Fischer, W. Jacot, A. K. Conlin, C. Arce-Salinas, I. L. Wapnir, C. Jackisch, M. P. DiGiovanna, P. A. Fasching, J. P. Crown, P. Wülfing, Z. Shao, E. R. Caremoli, H. Wu, L. H. Lam, D. Tesarowski, M. Smitt, H. Douthwaite, S. M. Singel and C. E. Geyer, *N. Engl. J. Med.*, 2019, **380**, 617–628.
28 J. D. Bargh, A. Isidro-Llobet, J. S. Parker and D. R. Spring, *Chem. Soc. Rev.*, 2019, **48**, 4361–4374.
29 Y. V. Kovtun, C. A. Audette, Y. Ye, H. Xie, M. F. Ruberti, S. J. Phinney, B. A. Leece, T. Chittenden, W. A. Blättler and V. S. Goldmacher, *Cancer Res.*, 2006, **66**, 3214–3221.
30 N. Jain, S. W. Smith, S. Ghone and B. Tomczuk, *Pharm. Res.*, 2015, **32**, 3526–3540.
31 G. K. Balendiran, R. Dabur and D. Fraser, *Cell Biochem. Funct.*, 2004, **22**, 343–352.
32 S.-J. Moon, S. V Govindan, T. M. Cardillo, C. A. D'Souza, H. J. Hansen and D. M. Goldenberg, *J. Med. Chem.*, 2008, **51**, 6916–6926.
33 D. M. Goldenberg, T. M. Cardillo, S. V Govindan, E. A. Rossi and R. M. Sharkey, *Oncotarget*, 2015, **6**, 22496–22512.
34 T. M. Cardillo, S. V. Govindan, R. M. Sharkey, P. Trisal and D. M. Goldenberg, *Clin. Cancer Res.*, 2011, **17**, 3157–3169.
35 H. Ruan, S. Hao, P. Young and H. Zhang, *Horizons cancer Res*, 2015, **56**, 23–40.
36 T. Tedeschini, B. Campara, A. Grigoletto, M. Bellini, M. Salvalaio, Y. Matsuno, A. Suzuki, H. Yoshioka and G. Pasut, *J. Control. Release*, 2021, **337**, 431–447.
37 F. M. H. De Groot, W. J. Loos, R. Koekkoek, L. W. A. Van Berkom, G. F. Busscher, A. E. Seelen, C. Albrecht, P. De Bruijn and H. W. Scheeren, *J. Org. Chem.*, 2001, **66**, 8815–8830.
38 Y. Ogitani, T. Aida, K. Hagihara, J. Yamaguchi, C. Ishii, N. Harada, M. Soma, H. Okamoto, M. Oitate, S. Arakawa, T. Hirai, R. Atsumi, T. Nakada, I. Hayakawa, Y. Abe and T. Agatsuma, *Clin. Cancer Res.*, 2016, **22**, 5097–5108.
39 Z. K. Glover, L. Basa, B. Moore, J. S. Laurence and A. Sreedhara, *MAbs*, 2015, **7**, 901–911.
40 M. J. Tamás, S. K. Sharma, S. Ibstedt, T. Jacobson and P. Christen, *Biomolecules*, 2014, **4**, 252–267.
41 S. Kiese, A. Papppenberger, W. Friess and H.-C. Mahler, *J. Pharm. Sci.*, 2008, **97**, 4347–4366.
42 A. Lahlou, B. Blanchet, M. Carvalho, M. Paul and A. Astier, *Ann. Pharm. Françaises*, 2009, **67**, 340–352.
43 E. Y. Chi, S. Krishnan, T. W. Randolph and J. F. Carpenter, *Pharm. Res.*, 2003, **20**, 1325–1336.
44 Y. Le Basle, P. Chennell, N. Tokhadze, A. Astier and V. Sautou, *J. Pharm. Sci.*, 2020, **109**, 169–190.
45 J. L. Spidel, B. Vaessen, E. F. Albone, X. Cheng, A. Verdi and J. B. Kline, *Bioconjug. Chem.*, 2017, **28**, 2471–2484.
46 J. P. M. Nunes, V. Vassileva, E. Robinson, M. Morais, M. E. B. Smith, R. B. Pedley, S. Caddick, J. R. Baker and V. Chudasama, *RSC Adv.*, 2017, **7**, 24828–24832.
47 S. J. Walsh, J. D. Bargh, F. M. Dannheim, A. R. Hanby, H. Seki, A. J. Counsell, X. Ou, E. Fowler, N. Ashman, Y. Takada, A. Isidro-Llobet, J. S. Parker, J. S. Carroll and D. R. Spring, *Chem. Soc. Rev.*, 2021, **50**, 1305–1353.
48 Q. Zhou, *Biomedicines*, 2017, **5**, 64.
49 S. Smolskaya and Y. A. Andreev, *Biomolecules*, 2019, **9**, 255.
50 B. Q. Shen, K. Xu, L. Liu, H. Raab, S. Bhakta, M. Kenrick, K. L. Parsons-Reponte, J. Tien, S. F. Yu, E. Mai, D. Li,

J. Tibbitts, J. Baudys, O. M. Saad, S. J. Scales, P. J. McDonald, P. E. Hass, C. Eigenbrot, T. Nguyen, W. A. Solis, R. N. Fuji, K. M. Flagella, D. Patel, S. D. Spencer, L. A. Khawli, A. Ebens, W. L. Wong, R. Vandlen, S. Kaur, M. X. Sliwkowski, R. H. Scheller, P. Polakis and J. R. Junutula, *Nat. Biotechnol.*, 2012, **30**, 184–189.

51 P. M. LoRusso, D. Weiss, E. Guardino, S. Girish and M. X. Sliwkowski, *Clin. Cancer Res.*, 2011, **17**, 6437–6447.

52 H. Kantarjian, E. Vandendries and A. Advani, *N. Engl. J. Med.*, 2016, **375**, 2100–2101.

53 V. Chudasama, A. Maruani and S. Caddick, *Nat. Chem.*, 2016, **8**, 114–119.

54 X. Hu, E. Bortell, F. W. Kotch, A. Xu, B. Arve and S. Freese, *Org. Process Res. Dev.*, 2017, **21**, 601–610.

55 Q. Jiang, B. Patel, X. Jin, D. Di Grandi, E. Bortell, B. Czapkowski, T. F. Lerch, D. Meyer, S. Patel, J. Pegg, A. Arbuckle, J. Lagliva, V. Sriskanda, L. Letendre, H. Li, E. Thomas and D. Nadkarni, *ACS Omega*, 2019, **4**, 6468–6475.

56 C. Selby, L. R. Yacko and A. E. Glode, *J. Adv. Pract. Oncol.*, 2019, **10**, 68–82.

57 M. T. Kim, Y. Chen, J. Marhoul and F. Jacobson, *Bioconjug. Chem.*, 2014, **25**, 1223–1232.

58 N. C. Yoder, C. Bai, D. Tavares, W. C. Widdison, K. R. Whiteman, A. Wilhelm, S. D. Wilhelm, M. A. McShea, E. K. Maloney, O. Ab, L. Wang, S. Jin, H. K. Erickson, T. A. Keating and J. M. Lambert, *Mol. Pharm.*, 2019, **16**, 3926–3937.

59 S. Choi, S. Connelly, N. Reixach, I. A. Wilson and J. W. Kelly, *Nat. Chem. Biol.*, 2010, **6**, 133–139.

60 G. W. Anderson, J. E. Zimmerman and F. M. Callahan, *J. Am. Chem. Soc.*, 1964, **86**, 1839–1842.

61 D. E. Ames and T. F. Grey, *J. Chem. Soc.*, 1955, 631–636.

62 M. Mentinova and S. A. McLuckey, *J. Am. Chem. Soc.*, 2010, **132**, 18248–18257.

63 S. Dou, J. Virostko, D. L. Greiner, A. C. Powers and G. Liu, *Nucleosides, Nucleotides Nucleic Acids*, 2015, **34**, 69–78.

64 A. D. Ricart, *Clin. Cancer Res.*, 2011, **17**, 6417–6427.

65 K. Ulbrich and V. Subr, *Adv. Drug Deliv. Rev.*, 2004, **56**, 1023–1050.

66 J. F. DiJoseph, K. Khandke, M. M. Dougher, D. Y. Evans, D. C. Armellino, P. R. Hamann and N. K. Damle, *Haematol. Meet. Reports*, 2008, **2**, 74–77.

67 V. H. J. van der Velden, J. G. te Marvelde, P. G. Hoogeveen, I. D. Bernstein, A. B. Houtsmuller, M. S. Berger and J. J. M. van Dongen, *Blood*, 2001, **97**, 3197–3204.

68 E. R. Boghaert, K. M. Khandke, L. Sridharan, M. Dougher, J. F. Dijoseph, A. Kunz, P. R. Hamann, J. Moran, I. Chaudhary and N. K. Damle, *Cancer Chemother. Pharmacol.*, 2008, **61**, 1027–1035.

69 S. Kalkhof and A. Sinz, *Anal. Bioanal. Chem.*, 2008, **392**, 305–312.

70 X. Chen, K. Muthoosamy, A. Pfisterer, B. Neumann and T. Weil, *Bioconjug. Chem.*, 2012, **23**, 500–508.

71 K. Yamada, N. Shikida, K. Shimbo, Y. Ito, Z. Khedri, Y. Matsuda and B. A. Mendelsohn, *Angew. Chem., Int. Ed.*, 2019, **58**, 5592–5597.

72 Y. Matsuda, K. Yamada, T. Okuzumi and B. A. Mendelsohn, *Org. Process Res. Dev.*, 2019, **23**, 2647–2654.

73 R. G. Arnold, J. A. Nelson and J. J. Verbanc, *Chem. Rev.*, 1957, **57**, 47–76.

74 A. V Wisnewski, R. Srivastava, C. Herick, L. Xu, R. Lemus, H. Cain, N. M. Magoski, M. H. Karol, K. Bottomly and C. A. Redlich, *Am. J. Respir. Crit. Care Med.*, 2000, **162**, 2330–2336.

75 G. R. Stark, *Biochemistry*, 1965, **4**, 1030–1036.

76 J. M. Hettick, T. B. Ruwona and P. D. Siegel, *J. Am. Soc. Mass Spectrom.*, 2009, **20**, 1567–1575.

77 M. S. Rolph, A. L. J. Markowska, C. N. Warriner and R. K. O'Reilly, *Polym. Chem.*, 2016, **7**, 7351–7364.

78 T.-T. Liu and T.-S. Yang, *J. Food Sci.*, 2010, **75**, C445–C451.

79 T. Nakamura, Y. Kawai, N. Kitamoto, T. Osawa and Y. Kato, *Chem. Res. Toxicol.*, 2009, **22**, 536–542.

80 D. S. Wilbur, M. K. Chyan, H. Nakamae, Y. Chen, D. K. Hamlin, E. B. Santos, B. T. Kornblit and B. M. Sandmaier, *Bioconjug. Chem.*, 2012, **23**, 409–420.

81 L. Petri, P. A. Szijj, Á. Kelemen, T. Imre, Á. Gömöry, M. T. W. Lee, K. Hegedus, P. Ábrányi-Balogh, V. Chudasama and G. M. Keseru, *RSC Adv.*, 2020, **10**, 14928–14936.

82 I. Dovgan, S. Ursuegui, S. Erb, C. Michel, S. Kolodych, S. Cianférani and A. Wagner, *Bioconjug. Chem.*, 2017, **28**, 1452–1457.

83 J. I. Gavrilyuk, U. Wuellner and C. F. Barbas, *Bioorganic Med. Chem. Lett.*, 2009, **19**, 1421–1424.

84 M. Hayakawa, N. Toda, N. Carrillo, N. J. Thornburg, J. E. Crowe Jr. and C. F. Barbas III, *ChemBioChem*, 2012, **13**, 2191–2195.

85 A. R. Nanna, X. Li, E. Walseng, L. Pedzisa, R. S. Goydel, D. Hymel, T. R. Burke Jr., W. R. Roush and C. Rader, *Nat. Commun.*, 2017, **8**, 1112.

86 D. Hwang and C. Rader, *Biomolecules*, 2020, **10**, 764.

87 D. Hwang, N. Nilchan, A. R. Nanna, X. Li, M. D. Cameron, W. R. Roush, H. J. Park and C. Rader, *Cell Chem. Biol.*, 2019, **26**, 1229–1239.e9.

88 J. Qi, K. Tsuji, D. Hymel, T. R. Burke, M. Hudecek, C. Rader and H. Peng, *Angew. Chem., Int. Ed.*, 2020, **59**, 12178–12185.

89 A. R. Nanna, A. V. Kel'in, C. Theile, J. M. Pierson, Z. X. Voo, A. Garg, J. K. Nair, M. A. Maier, K. Fitzgerald and C. Rader, *Nucleic Acids Res.*, 2020, **48**, 5281–5293.

90 M. Chilamari, N. Kalra, S. Shukla and V. Rai, *Chem. Commun.*, 2018, **54**, 7302–7305.

91 S. Asano, J. T. Patterson, T. Gaj and C. F. Barbas, *Angew. Chem., Int. Ed.*, 2014, **53**, 11783–11786.

92 J. T. Patterson, H. D. Wilson, S. Asano, N. Nilchan, R. P. Fuller, W. R. Roush, C. Rader and C. F. Barbas, *Bioconjug. Chem.*, 2016, **27**, 2271–2275.

93 M. J. Matos, B. L. Oliveira, N. Martínez-Sáez, A. Guerreiro, P. M. S. D. Cal, J. Bertoldo, M. Maneiro, E. Perkins, J. Howard, M. J. Deery, J. M. Chalker, F. Corzana,

G. Jiménez-Osés and G. J. L. Bernardes, *J. Am. Chem. Soc.*, 2018, **140**, 4004–4017.
94 R. G. Pearson, *J. Am. Chem. Soc.*, 1963, **85**, 3533–3539.
95 M. M. C. Sun, K. S. Beam, C. G. Cerveny, K. J. Hamblett, R. S. Blackmore, M. Y. Torgov, F. G. M. Handley, N. C. Ihle, P. D. Senter and S. C. Alley, *Bioconjug. Chem.*, 2005, **16**, 1282–1290.
96 H. Liu and K. May, *MAbs*, 2012, **4**, 17–23.
97 T. Wang, Y. D. Liu, B. Cai, G. Huang and G. C. Flynn, *J. Pharm. Biomed. Anal.*, 2015, **102**, 519–528.
98 D. V. Nadkarni, Q. Jiang, O. Friese, N. Bazhina, H. Meng, J. Guo, R. Kutlik and J. Borgmeyer, *Org. Process Res. Dev.*, 2018, **22**, 286–295.
99 R. P. Lyon, D. L. Meyer, J. R. Setter and P. D. Senter, *Methods Enzymol.*, 2012, **502**, 123–138.
100 D. G. Smyth, O. O. Blumenfeld and W. Konigsberg, *Biochem. J.*, 1964, **91**, 589–595.
101 T. Kuninori and J. Nishiyama, *Agric. Biol. Chem.*, 1985, **49**, 2453–2454.
102 S. C. Alley, D. R. Benjamin, S. C. Jeffrey, N. M. Okeley, D. L. Meyer, R. J. Sanderson and P. D. Senter, *Bioconjug. Chem.*, 2008, **19**, 759–765.
103 M. R. Lewis and J. E. Shively, *Bioconjug. Chem.*, 1998, **9**, 72–86.
104 C. Wei, G. Zhang, T. Clark, F. Barletta, L. N. Tumey, B. Rago, S. Hansel and X. Han, *Anal. Chem.*, 2016, **88**, 4979–4986.
105 A. D. Baldwin and K. L. Kiick, *Bioconjug. Chem.*, 2011, **22**, 1946–1953.
106 R. P. Lyon, J. R. Setter, T. D. Bovee, S. O. Doronina, J. H. Hunter, M. E. Anderson, C. L. Balasubramanian, S. M. Duniho, C. I. Leiske, F. Li and P. D. Senter, *Nat. Biotechnol.*, 2014, **32**, 1059–1062.
107 D. G. Smyth, A. Nagamatsu and J. S. Fruton, *J. Am. Chem. Soc.*, 1960, **82**, 4600–4604.
108 T. Kantner and A. G. Watts, *Bioconjug. Chem.*, 2016, **27**, 2400–2406.
109 H. Y. Shiu, T. C. Chan, C. M. Ho, Y. Liu, M. K. Wong and C. M. Che, *Chem. - Eur. J.*, 2009, **15**, 3839–3850.
110 E. Petit, L. Bosch, A. M. Costa and J. Vilarrasa, *J. Org. Chem.*, 2019, **84**, 11170–11176.
111 Y. Zhang, X. Zhou, Y. Xie, M. M. Greenberg, Z. Xi and C. Zhou, *J. Am. Chem. Soc.*, 2017, **139**, 6146–6151.
112 Y. Zhang, C. Zang, G. An, M. Shang, Z. Cui, G. Chen, Z. Xi and C. Zhou, *Nat. Commun.*, 2020, **11**, 1–10.
113 G. L. Ellman, *Arch. Biochem. Biophys.*, 1959, **82**, 70–77.
114 G. J. L. Bernardes, G. Casi, S. Trüssel, I. Hartmann, K. Schwager, J. Scheuermann and D. Neri, *Angew. Chem., Int. Ed.*, 2012, **51**, 941–944.
115 T. List, G. Casi and D. Neri, *Mol. Cancer Ther.*, 2014, **13**, 2641–2652.
116 D. Zhang, N. O. Devarie-Baez, Q. Li, J. R. Lancaster and M. Xian, *Org. Lett.*, 2012, **14**, 3396–3399.
117 N. Toda, S. Asano and C. F. Barbas, *Angew. Chem., Int. Ed.*, 2013, **52**, 12592–12596.
118 M. Davydova, G. D. Le Roi, P. Adumeau and B. M. Zeglis, *J. Vis. Exp.*, 2019, e59063.
119 R. van Geel, G. J. M. Pruijn, F. L. van Delft and W. C. Boelens, *Bioconjug. Chem.*, 2012, **23**, 392–398.
120 C. Zhang, P. Dai, A. A. Vinogradov, Z. P. Gates and B. L. Pentelute, *Angew. Chem., Int. Ed.*, 2018, **57**, 6459–6463.
121 M. A. Kasper, M. Glanz, A. Stengl, M. Penkert, S. Klenk, T. Sauer, D. Schumacher, J. Helma, E. Krause, M. C. Cardoso, H. Leonhardt and C. P. R. Hackenberger, *Angew. Chem., Int. Ed.*, 2019, **58**, 11625–11630.
122 M. A. Kasper, A. Stengl, P. Ochtrop, M. Gerlach, T. Stoschek, D. Schumacher, J. Helma, M. Penkert, E. Krause, H. Leonhardt and C. P. R. Hackenberger, *Angew. Chem., Int. Ed.*, 2019, **58**, 11631–11636.
123 O. Koniev, G. Leriche, M. Nothisen, J. S. Remy, J. M. Strub, C. Schaeffer-Reiss, A. Van Dorsselaer, R. Baati and A. Wagner, *Bioconjug. Chem.*, 2014, **25**, 202–206.
124 S. Kolodych, O. Koniev, Z. Baatarkhuu, J. Y. Bonnefoy, F. Debaene, S. Cianférani, A. Van Dorsselaer and A. Wagner, *Bioconjug. Chem.*, 2015, **26**, 197–200.
125 A. M. Spokoyny, Y. Zou, J. J. Ling, H. Yu, Y. S. Lin and B. L. Pentelute, *J. Am. Chem. Soc.*, 2013, **135**, 5946–5949.
126 C. Zhang, A. M. Spokoyny, Y. Zou, M. D. Simon and B. L. Pentelute, *Angew. Chem., Int. Ed.*, 2013, **52**, 14001–14005.
127 C. Zhang, M. Welborn, T. Zhu, N. J. Yang, M. S. Santos, T. Van Voorhis and B. L. Pentelute, *Nat. Chem.*, 2016, **8**, 120–128.
128 R. Tessier, R. K. Nandi, B. G. Dwyer, D. Abegg, C. Sornay, J. Ceballos, S. Erb, S. Cianférani, A. Wagner, G. Chaubet, A. Adibekian and J. Waser, *Angew. Chem., Int. Ed.*, 2020, **59**, 10961–10970.
129 N. Shindo, A. Ojida, K. Tokunaga, M. Sato, K. Kuwata, C. Miura, H. Fuchida, N. Matsunaga, S. Koyanagi and S. Ohdo, *J. Am. Chem. Soc.*, 2020, **142**, 18522–18531.
130 P. R. Khoury, J. D. Goddard and W. Tam, *Tetrahedron*, 2004, **60**, 8103–8112.
131 C. Schneider, K. Niisuke, W. E. Boeglin, M. Voehler, D. F. Stec, N. A. Porter and A. R. Brash, *Proc. Natl. Acad. Sci.*, 2007, **104**, 18941–18945.
132 A. Abbas, B. Xing and T. P. Loh, *Angew. Chem., Int. Ed.*, 2014, **53**, 7491–7494.
133 T. N. Tiambeng, D. S. Roberts, K. A. Brown, Y. Zhu, S. D. Mitchell, T. M. Guardado-alvarez, S. Jin and Y. Ge, *Nat. Commun.*, 2020, **11**, 3903.
134 A. J. Cameron, P. W. R. Harris and M. A. Brimble, *Angew. Chem., Int. Ed.*, 2020, **59**, 18054–18061.
135 M. R. Jafari, J. Lakusta, R. J. Lundgren and R. Derda, *Bioconjug. Chem.*, 2016, **27**, 509–514.
136 L. Pedzisa, X. Li, C. Rader and W. R. Roush, *Org. Biomol. Chem.*, 2016, **14**, 5141–5147.
137 A. M. Tsimberidou, J. A. Ajani, P. Hsu, I.-J. Chen and T. E. Pearce, *J. Clin. Oncol.*, 2020, **38**, TPS3657.
138 M.-C. Yang, Y.-J. Chen, C.-S. Shia, H.-W. Chang, W.-F. Li, C.-D. T. Yu and I.-J. Chen, *Cancer Res.*, 2019, **79**, 4815.
139 G. Badescu, P. Bryant, M. Bird, K. Henseleit, J. Swierkosz, V. Parekh, R. Tommasi, E. Pawlisz, K. Jurlewicz, M. Farys, N. Camper, X. Sheng, M. Fisher, R. Grygorash, A. Kyle,

A. Abhilash, M. Frigerio, J. Edwards and A. Godwin, *Bioconjug. Chem.*, 2014, **25**, 1124–1136.
140 S. Balan, J. Choi, A. Godwin, I. Teo, C. M. Laborde, S. Heidelberger, M. Zloh, S. Shaunak and S. Brocchini, *Bioconjug. Chem.*, 2007, **18**, 61–76.
141 S. J. Walsh, S. Omarjee, W. R. J. D. Galloway, T. T. L. Kwan, H. F. Sore, J. S. Parker, M. Hyvönen, J. S. Carroll and D. R. Spring, *Chem. Sci.*, 2019, **10**, 694–700.
142 V. Hong, S. I. Presolski, C. Ma and M. G. Finn, *Angew. Chemie Int. Ed.*, 2009, **48**, 9879–9883.
143 O. Koniev, I. Dovgan, B. Renoux, A. Ehkirch, J. Eberova, S. Cianférani, S. Kolodych, S. Papot and A. Wagner, *Medchemcomm*, 2018, **9**, 827–830.
144 N. Martínez-Sáez, S. Sun, D. Oldrini, P. Sormanni, O. Boutureira, F. Carboni, I. Compañón, M. J. Deery, M. Vendruscolo, F. Corzana, R. Adamo and G. J. L. Bernardes, *Angew. Chem., Int. Ed.*, 2017, **56**, 14963–14967.
145 J. A. Burkhard, G. Wuitschik, M. Rogers-Evans, K. Müller and E. M. Carreira, *Angew. Chem., Int. Ed.*, 2010, **49**, 9052–9067.
146 U. Hennrich and K. Kopka, *Pharmaceuticals*, 2019, **12**, 114.
147 P. Grass, P. Marbach, C. Bruns and I. Lancranjan, *Metabolism*, 1996, **45**, 27–30.
148 V. Vingtdeux, H. Zhao, P. Chandakkar, C. M. Acker, P. Davies and P. Marambaud, *Mol. Med.*, 2016, **22**, 841–849.
149 R. Guermazi, L. Royer, L. Galmiche, G. Clavier, P. Audebert and A. Hedhli, *J. Fluoresc.*, 2016, **26**, 1349–1356.
150 C. Canovas, M. Moreau, C. Bernhard, A. Oudot, M. Guillemin, F. Denat and V. Goncalves, *Angew. Chem., Int. Ed.*, 2018, **57**, 10646–10650.
151 R. Hoogenboom, *Angew. Chemie Int. Ed.*, 2010, **49**, 3415–3417.
152 N. Griebenow, S. Bräse and A. M. Dilmac, *RSC Adv.*, 2015, **5**, 54301–54303.
153 Y. Chen, W. Yang, J. Wu, W. Sun, T. P. Loh and Y. Jiang, *Org. Lett.*, 2020, **22**, 2038–2043.
154 L. H. Wu, S. Zhou, Q. F. Luo, J. S. Tian and T. P. Loh, *Org. Lett.*, 2020, **22**, 8193–8197.
155 A. Hung, M. Mager, M. Hembury, F. Stellacci, M. M. Stevens and I. Yarovsky, *Chem. Sci.*, 2013, **4**, 928–937.
156 K. J. Hamblett, P. D. Senter, D. F. Chace, M. M. C. Sun, J. Lenox, C. G. Cerveny, K. M. Kissler, S. X. Bernhardt, A. K. Kopcha, R. F. Zabinski, D. L. Meyer and J. A. Francisco, *Clin. Cancer Res.*, 2004, **10**, 7063–7070.
157 S. D. Tilley and M. B. Francis, *J. Am. Chem. Soc.*, 2006, **128**, 1080–1081.
158 S. Sato, K. Nakamura and H. Nakamura, *ACS Chem. Biol.*, 2015, **10**, 2633–2640.
159 S. Sato, K. Nakamura and H. Nakamura, *ChemBioChem*, 2017, **18**, 475–478.
160 S. Sato, K. Nakane and H. Nakamura, *Org. Biomol. Chem.*, 2020, **18**, 3664–3668.
161 N. S. Joshi, L. R. Whitaker and M. B. Francis, *J. Am. Chem. Soc.*, 2004, **126**, 15942–15943.
162 J. M. McFarland, N. S. Joshi and M. B. Francis, *J. Am. Chem. Soc.*, 2008, **130**, 7639–7644.
163 D. W. Romanini and M. B. Francis, *Bioconjug. Chem.*, 2008, **19**, 153–157.
164 J. M. Hooker, E. W. Kovacs and M. B. Francis, *J. Am. Chem. Soc.*, 2004, **126**, 3718–3719.
165 T. L. Schlick, Z. Ding, E. W. Kovacs and M. B. Francis, *J. Am. Chem. Soc.*, 2005, **127**, 3718–3723.
166 M. W. Jones, G. Mantovani, C. A. Blindauer, S. M. Ryan, X. Wang, D. J. Brayden and D. M. Haddleton, *J. Am. Chem. Soc.*, 2012, **134**(17), 7406–7413.
167 J. Gavrilyuk, H. Ban, M. Nagano, W. Hakamata and C. F. Barbas, *Bioconjug. Chem.*, 2012, **23**, 2321–2328.
168 J. Gavrilyuk, H. Ban, H. Uehara, S. J. Sirk, K. Saye-Francisco, A. Cuevas, E. Zablowsky, A. Oza, M. S. Seaman, D. R. Burton and C. F. Barbas, *J. Virol.*, 2013, **87**, 4985–4993.
169 H. Nakata, K. Maeda, T. Miyakawa, S. Shibayama, M. Matsuo, Y. Takaoka, M. Ito, Y. Koyanagi and H. Mitsuya, *J. Virol.*, 2005, **79**, 2087–2096.
170 H. Ban, J. Gavrilyuk and C. F. Barbas, *J. Am. Chem. Soc.*, 2010, **132**, 1523–1525.
171 H. Ban, M. Nagano, J. Gavrilyuk, W. Hakamata, T. Inokuma and C. F. Barbas, *Bioconjug. Chem.*, 2013, **24**, 520–532.
172 H. Wamhoff and K. Wald, *Chem. Ber.*, 1977, **110**, 1699–1715.
173 Q. Y. Hu, M. Allan, R. Adamo, D. Quinn, H. Zhai, G. Wu, K. Clark, J. Zhou, S. Ortiz, B. Wang, E. Danieli, S. Crotti, M. Tontini, G. Brogioni and F. Berti, *Chem. Sci.*, 2013, **4**, 3827–3832.
174 E. L. Kovrigin and S. A. Potekhin, *Biophys. Chem.*, 2000, **83**, 45–59.
175 K. Gekko, E. Ohmae, K. Kameyama and T. Takagi, *Biochim. Biophys. Acta*, 1998, **1387**, 195–205.
176 D. Alvarez-Dorta, C. Thobie-Gautier, M. Croyal, M. Bouzelha, M. Mével, D. Deniaud, M. Boujtita and S. G. Gouin, *J. Am. Chem. Soc.*, 2018, **140**, 17120–17126.
177 T. Dörner and D. M. Goldenberg, *Ther. Clin. Risk Manag.*, 2007, **3**, 953–959.
178 C. Song, K. Liu, Z. Wang, B. Ding, S. Wang, Y. Weng, C. W. Chiang and A. Lei, *Chem. Sci.*, 2019, **10**, 7982–7987.
179 H. Tagawa, K. Maruyama, K. Sasaki, N. Konoue, A. Kishimura, M. Kanai, T. Mori, K. Oisaki and Y. Katayama, *RSC Adv.*, 2020, **10**, 16727–16731.
180 S. J. Tower, W. J. Hetcher, T. E. Myers, N. J. Kuehl and M. T. Taylor, *J. Am. Chem. Soc.*, 2020, **142**, 9112–9118.
181 J. R. Kramer and T. J. Deming, *Chem. Commun.*, 2013, **49**, 5144–5146.
182 C. Zhu, Y. Gao, H. Li, S. Meng, L. Li, J. S. Francisco and X. C. Zeng, *Proc. Natl. Acad. Sci.*, 2016, **113**, 12946–12951.
183 J. C. Aledo, *Protein Sci.*, 2019, **28**, 1785–1796.
184 E. Folzer, K. Diepold, K. Bomans, C. Finkler, R. Schmidt, P. Bulau, J. Huwyler, H.-C. Mahler and A. Koulov, *J. Pharm. Sci.*, 2015, **104**, 2824–2831.
185 S. Lin, X. Yang, S. Jia, A. M. Weeks, M. Hornsby, P. S. Lee, R. V. Nichiporuk, A. T. Iavarone, J. A. Wells, F. D. Toste and C. J. Chang, *Science*, 2017, **355**, 597–602.
186 M. T. Taylor, J. E. Nelson, M. G. Suero and M. J. Gaunt, *Nature*, 2018, **562**, 563–568.

187 J. Kim, B. X. Li, R. Y. C. Huang, J. X. Qiao, W. R. Ewing and D. W. C. Macmillan, *J. Am. Chem. Soc.*, 2020, **142**, 21260–21266.
188 C. Lu, W. Lin, W. Wang, Z. Han, S. Yao and N. Lin, *Phys. Chem. Chem. Phys.*, 2000, **2**, 329–334.
189 J. T. Ryman and B. Meibohm, *CPT pharmacometrics Syst. Pharmacol.*, 2017, **6**, 576–588.
190 U. Storz, *MAbs*, 2015, **7**, 989–1009.
191 E. Y. Yang and K. Shah, *Front. Oncol.*, 2020, **10**, 1182.
192 O. N. Shilova and S. M. Deyev, *Acta Naturae*, 2019, **11**, 42–53.
193 R. Seigneuric, J. Gobbo, P. Colas and C. Garrido, *Oncotarget*, 2011, **2**, 557–561.